Engineered Cardiac Tissues for Delivery of Cells to the Injured Myocardium

A DISSERTATION

SUBMITTED TO THE FACULTY OF

UNIVERSITY OF MINNESOTA

BY

Jacqueline S Wendel

IN PARTIAL FULFILLMENT OF THE REQUIREMENTS

FOR THE DEGREE OF

DOCTOR OF PHILOSOPHY

Jianyi (Jay) Zhang, Adviser

Robert T. Tranquillo, Adviser

July 2015

Acknowledgements

It is nearly impossible to reach this point in a graduate career without assistance, and as I am certainly no exception to this rule, I would like to take some time to thank those who have helped and guided me along the way.

I would first like to thank my advisors, Bob and Jay, for going on a co-advisement adventure and taking on a student who had never worked with cells or tissues before for a project to construct and transplant cell-laden engineered tissues. Thank you for your confidence, mentorship and support throughout these past several years.

That being said, there was a sizeable initial learning curve and continually new things to learn along the way as my project developed. I owe many thanks to all of my current and former lab mates for their assistance in acquiring new skills and techniques, borrowing theirs, or to provide a fresh set of eyes and ears when problems presented themselves. I would like to especially thank Lei Ye for his incomparable surgical skills and collaboration over the years, Susan Saunders for sectioning and staining of more hearts than I can remember- I would still be sectioning today without her assistance, and Jeremy Schaefer and Sonja Riemenschneider always lending an extra hand when needed and their expertise at every bump along the way. I would also like to thank our collaborators in the UW-Madison lab of Dr. Tim Kamp for providing stem-cell derived cardiomyocytes for me use, allowing me to more efficiently use my time. I have additionally had the opportunity to work with a number of talented undergraduate volunteers, notably Michael Tradewell and Jackson Baril. Thank you for all your hard work and contributions to the research outlined in this dissertation.

As always, the work detailed in this dissertation would not be possible without considerable financial support, and I was fortunate to have funding form a number of different sources along the way. Many thanks to the Department of Education for a one-year fellowship, the department of Biomedical Engineering for providing teaching assistant positions, and the National Institute of Health for their support through research grants and one year of funding though a training grant.

Last, but not least, I have to thank my family for their continual support and encouragement throughout my life. Thank you for always asking how my either my cells or ‘patients’ are doing, and for trying to read through my first paper. To my parents, I cannot thank you enough for making me the only kid in school growing up who had Legos and Tonka trucks without also having older brothers, for putting in all those hours helping me with my homework, for encouraging my interest in math and all of the sciences even when it wasn’t easy, and for instilling in me the work ethic, perseverance and values it took to make me who I am today. Also, thanks to my sister Lindsay for her enthusiasm and always being willing to discuss science, grad school, or just about anything else.

Abstract

With the high incidence of heart failure in the developing world and the inherent risks and limited availability of donor hearts, cell-based solutions have become an attractive solution. However, current methods to deliver cells to the heart have resulted in limited long term cell retention and consequently minimal therapeutic efficacy. In this work, we aim to use engineered tissues as a means to deliver cells to the injured myocardium post- infarction with increased cell retention. The results detailed in this dissertation indicate that engineered tissues can be constructed from both primary rodent cardiomyocytes and human pluripotent stem cell derived cardiomyocytes, and that these tissues not only engraft post-infarction with high cell retention , but in some instances also result in improved cardiac function and limitation of left ventricular remodeling post-infarction.

Table of Contents

List of Tables

List of Figures

Chapter 1: Introduction

1.1 Introduction

Heart failure has many causes, but the most prevalent initiator is a myocardial infarction, in which myocardial tissue is deprived of oxygen for an extended period of time, usually through a blockage of one of the coronary arteries. In the ischemia induced by an infarction, up to one-quarter of the 4 billion cells in the left ventricle can be lost[1]. With this level of cell death, heart failure can develop as a result of the limited capacity of the injured myocardial tissue to recover or regenerate, leading to fibrosis and scar formation of the damaged myocardium, left ventricular dilation and thinning due to a resulting pressure and volume overload, and the inhibition of proper action potential propagation. Current treatments, whether they are pharmaceutical or medical device-based, act merely as palliative measures and the only effective long term treatment to date is to replace the damaged myocardium via total heart transplantation[2].

With the limited number of donors and the inherent risks of surgery and immunogenicity, cellular therapy has become an attractive solution to the high incidence of heart failure post-infarction. However, direct injection of cells into the myocardium has shown limited efficacy due to poor grafting efficiency[3]. Low rates of retention may be a product of cell loss due to inability to create focal adhesions with neighboring cells, the inflammatory response to myocardial injury,

or the hypoxic environment of the infarct zone. Thus, the use of engineered cardiac tissues has been a topic of increasing interest. Tissue engineering is not only provides a platform for the delivery of a large number of cells to the injured myocardium, it provides a means to replace damaged myocardium. Tissue engineering allows for in vitro development of cellular organization, intracellular communication and ECM deposition while also isolating the cells from the inflammatory infarct environment when implanted *in vivo*.

In this chapter, we will review the currently used methods used to create engineered cardiac tissues, or “cardiac patches”, and their efficacy when delivered *in vivo*. We will begin by surveying the cells, scaffold and in vitro conditioning used to create these patches, and then move on to how they are characterized, and finally their efficacy to limit left ventricular remodeling post-infarction.

1.2 Cells for Cardiac Tissue Engineering

1.2.1 Neonatal Rat Cardiomyocytes

Until functional cardiomyocytes were able to be differentiated from human pluripotent stem cell sources, primary isolates of neonatal rat cardiomyocytes were the standard cell source for the development of cardiac patches[4-6]. These cells have been well characterized *in vitro* and can be obtained in large numbers, making them a useful tool for developing cardiac patches and interrogating the effects of in vitro conditioning on these tissues.

1.2.2 Pluripotent Stem Cell Derived Cardiomyocytes

Stem cells, whether taken from an embryo or reprogrammed from an adult cell, have enormous therapeutic potential due to their ability to be expanded in an undifferentiated state, and differentiated into cells of any lineage found in the body. In their undifferentiated state, pluripotent stem cells cannot be transplanted into patients as they can form teratomas. However, as the ability to not only differentiate pluripotent stem cells into functional cardiomyocytes but also in numbers large enough to be used therapeutically has become available, these cells have become the new standard cell source for creating cardiac patches.

1.2.2.1 Embryonic Stem Cell Derived Cardiomyocytes

Spontaneous differentiation of embryonic stem cells (ESCs) to cardiogenic cells was first observed in mouse ESCs in 1981 when these cells were cultured in 3D aggregates, called embryoid bodies[7]. Human ESCs were first obtained from a blastocyst in 1998,[8] but it wasn't shown until 2001 that they could successfully be differentiated into functional cardiomyocytes that exhibited contractile force generation and recordable action potentials[9]. Human ESC-CMs are now commonly used as a cell source for cardiac tissue engineering [10, 11].

1.2.2.2 Induced Pluripotent Stem Cell Derived Cardiomyocytes

In 2006 it was discovered that the introduction of four transcription factors (Oct3/4, Sox2, c-Myc, and Klf4) into adult murine fibroblasts reprogrammed these cells into an embryonic state, called induced pluripotent stem cells (iPSCs).[12]

This was a landmark discovery, as the reprogramming of adult cells into an embryonic state not only alleviates the ethical concerns of using embryonic cardiomyocytes but also allows for potentially autologous cell transplantation, eliminating the immunogenicity obstacle of allogeneic transplantation. Human iPSCs were reported in 2007 using the same factors or a new combination of Oct4, NANOG, LIN28, and SOX2,[13, 14] and differentiated into functional cardiomyocytes in 2009. [15] They have been used in parallel with hESC-CMs for tissue engineering applications, and will likely become the preferred cell source for cardiac patches for the foreseeable future. [10]

1.2.2.3 Differentiation Methods

Initially, pluripotent stem cell derived cardiomyocytes were differentiated via the embryoid body method, where undifferentiated pluripotent stem cells are cultured in 3D aggregates on top of irradiated mouse embryonic fibroblast feeder cells and allowed to spontaneously differentiate into cells from all three embryonic germ layers, among them being cardiomyocytes. However, as can be expected, this method results in low percentages and yields of cardiomyocytes and requires purification steps in order to obtain high percentages of cardiomyocytes. In efforts to efficiently obtain high yields of cardiomyocytes from stem cell differentiation, Zhang et al developed a new method in which cells are cultured between two layers of matrigel,[16] resulting in a significant increase in differentiation efficiency to cardiomyocytes. Recently, small molecule methods of

reprogramming and differentiation under defined conditions have been developed to eliminate the need for viral vectors and to increase reprogramming efficiency. [17]

1.2.3 Cardiac Progenitor Cells

The heart has a limited capacity to regenerate via the presence of sparsely distributed resident cardiac progenitor cells (CPCs) and cardiac side population (SP) cells within the myocardium, approximately one CPC for every 30,000-40,000 cells in the myocardium.[18] These cells have been isolated based on their expression of a number of cell surface markers and gene expression, including c-kit,[19] Sca-1, [20] and islet-1 [21] as well as from their migration of progenitor cells out of excised cardiac tissue when cultured in vitro.[22] Cells selected through these methods display the capacity to self-renew and differentiate into cardiomyocyte as well as endothelial phenotypes and can be used to create cardiac patches. [11, 23]

1.2.4 Non-Cardiomyocyte Cells and Co-Culture of Cells for Cardiac Patches

Cardiomyocytes are not the only cell type used to create engineered tissues for cardiac repair. Non-cardiomyocyte cells are required for the creation of cardiac patches that utilize compacting biopolymer hydrogels, as cardiomyocytes do not contract collagen and fibrin hydrogels. Despite improvements in differentiation techniques, pluripotent stem cell-derived CM

populations are only 60-90% pure CMs, with the remaining 10-40% of cells primarily being fibroblast-like cells, though those cells remain poorly characterized. Neonatal rat cell isolates also contain between 50-60% of a heterogeneous population of non-CM cells, consisting primarily of fibroblasts, but also containing smooth muscle cells and endothelial cells from the vasculature and other interstitial cells from the myocardium[24]. The addition or inclusion of non-CM cells into cardiac patches has proven beneficial. Co-culture of hESC and hiPSc-derived cardiomyocytes with endothelial cells with or without mesenchymal stromal cells has resulted in an increase in contractile force generation by the resulting cardiac patches,[10] and the force generated per cardiomyocyte has shown to be higher with less pure populations of hESC-CMs. [25] Other non-CM cells used in cardiac tissue engineering include blood outgrowth endothelial cells (BOECs)[26], human umbilical endothelial cells (HUVECs),[27] pericytes (PCs)[28], and human dermal fibroblasts (HDFs).[29] These cells are used either in combination with cardiomyocytes or by themselves in engineered tissues, all with the goal of rescuing the injured myocardium post-infarction.

1.3 Scaffolds for Cardiac Tissue Engineering

Cardiac patches are typically formed by the in vitro seeding and culturing cells in 3-dimensional scaffolds. The choice of scaffold influences cell survival, phenotype, and function through its physical and chemical properties, including stiffness, microstructure, and surface chemistry. Two general classes of scaffolds

are utilized to create cardiac patches: prefabricated scaffolds, in which cells are seeded onto a pre-existing scaffold structure; and biopolymer scaffolds, in which cells are present during scaffold polymerization and become entrapped in a fibrous network.

1.3.1 Prefabricated Scaffolds

Synthetic biodegradable, elastomeric polymers including polycaprolactone (PCL),[30] poly(glycerol-sebacate) (PGS)[31], and poly(lactide-co-glycolide) (PLGA)[32] copolymers and natural materials such as collagen I,[33] alginate,[34] and gelatin[35] are materials that have been used to create prefabricated foam or nanofiber scaffolds. Foam scaffolds allow for control of pore size and structure through the use of different material processing techniques. Highly porous scaffolds have proven successful in creating cardiac patches with high cell viability, but they are often isotropic and do not result in cellular alignment. Nanofiber scaffolds can be created through electrospinning [36], in which fiber diameter and orientation can be controlled, mimicking organization of collagen fibers in the native myocardium. These scaffolds can be fabricated in advance and can incorporate surface modifications to enhance cell adhesion and activity, such as the conjugation of RGD peptides.[23]

1.3.2 Biopolymer Scaffolds

Biopolymers are another class of scaffolds used in cardiac tissue engineering. These are native protein fibril networks in hydrogel form made from

either collagen I or fibrin [5, 37, 38]. Rather than being seeded onto pre-formed scaffolds, cells are suspended in a gel-forming solution and fibrillogenesis occurs around the cells, entrapping them in a hydrated, fibrillar network. Initially, collagen and fibrin gels are extremely soft andisotropic. Over time, entrapped non-CM cells compact the gel, resulting in a denser fibril network. Eventually, the entrapped cells not only compact the gel, but begin to degrade the fibrils (in the case of fibrin gels) and replace them with cell-produced matrix. By constraining the compaction of the gel, fibrillar and cellular alignment can be induced in these gels. Induction of alignment allows the native architecture of the myocardium to be mimicked and has been shown to result in an increase in both contractile force generation by entrapped cardiomyocytes and the presence of gap junctions between cardiomyocytes.[5] Collagen and fibrin biopolymer scaffolds can be altered by the addition of Matrigel. [10, 25, 39] Other biopolymer scaffold materials include alginate, which can be 3D printed into various geometries [23].

1.3.3 Tissue-Based Scaffolds

Decellularized heart tissue has been used as a scaffold to culture cardiac cells. Heart tissues are decellularized by perfusion with SDS followed by Triton-X to remove cells while leaving most of the heart ECM content and structure intact.[40] Cells can then be reperfused into the heart,[40] or entrapped in an ECM-hydrogel matrix to create cardiac patches. [41]

1.3.4 Scaffold-Free Tissues

Scaffold-free approaches have been used to create cardiac patches in the form of cell sheets [42] and cell aggregate patches [43]. Cell sheets are created by seeding cells onto temperature-responsive membranes, allowing them to deposit cell-produced ECM and form cellular connections, and releasing them from the culture surfaces through temperature reduction. Cell sheets can then be stacked to create thin 3D tissues or layered with cell sheets of endothelial cells to facilitate rapid vascularization upon implantation [42]. Cell aggregate patches are prepared by culturing cells on a low-attachment plate placed on an orbital shaker, allowing for large numbers of cells to aggregate in solution and form tissues.

1.4 *In vitro* Cellular Conditioning

In addition to seeding cells onto or into scaffolds, external stimulation of the cells is often required to induce them to convert the scaffold into a functional cardiac tissue. This may be achieved through mechanical, electrical, or pharmacological stimulation.

1.4.1 Mechanical Stimulation

Cardiomyocytes in the native myocardium experience cyclic mechanical stretch as part of the cardiac cycle. Taking inspiration from this, *in vitro* mechanical stimulation has been widely used to stimulate alignment, hypertrophy, and maturation of cardiomyocytes in engineered tissues. Stimulation through cyclic stretching has been achieved for ring-shaped cardiac patches using two methods: looping the patch around one fixed post and another

coupled to a motorized stretching device,[44] or through pneumatically-controlled distension of a latex mandrel on which the patch is mounted[37]. In both instances, cyclic stretching resulted in over a two-fold increase in contractile force generation.

1.4.2 Electrical Stimulation

Ventricular cardiomyocytes in the heart beat under the continuous regulation of their electrical activity through the cardiac conduction system originating at the sinoatrial node. *In vitro*, cardiomyocytes in cardiac patches beat spontaneously, but often at an irregular and variable rate, and not in synchrony with cardiomyocytes in other regions of the patch. Electrical stimulation of cardiac patches throughout culture has resulted in increases in the maximum frequency at which these patches can be stimulated and elicit a contractile response synchronous with pacing, a reduction in the voltage threshold at which cardiomyocytes contract, increased contractile force and also stimulated cardiomyocyte hypertrophy.[45]

1.4.3 *In vitro* Perfusion

Due to the high metabolic demand of cardiomyocytes, diffusion limitations hamper the ability to make the large thickness cardiac patches that are necessary to achieve clinical relevance. To increase oxygen and nutrient availability to cells, different methods of in *vitro* perfusion have been utilized in cardiac patches. Pulsatile perfusion of cell culture medium through porous pre-

formed scaffolds has proven effective in increasing cell viability and myofibril assembly through media flow[6] and activates the ERK 1/2 signaling pathway[46]. In biopolymer hydrogels, microchannels have been included in the gel,[47] and perfusable microvessels have been created within the gel to allow for medium flow through the gel during culture[48-50]. Though promising, this latter approach has yet to be combined with cardiomyocyte culture *in vitro*.

1.4.4 Medium Supplementation

Supplementation of culture medium with pharmacological agents can also be used to stimulate development of cardiac patches. The addition of platelet-derived growth factor BB (PDGF-BB) to cultures of collagen/matrigel scaffolds containing neonatal rat cardiomyocytes protected cells from apoptotic death, thus increasing the final contractile performance of the patch.[51] Insulin and ascorbic acid have been used to promote matrix deposition by entrapped non-CM cells.[37]

1.4.5: Combination Treatments

In addition to exposing cardiac patches to one form of in vitro conditioning, combinations of the above mentioned techniques have been used in combination to further condition tissues. Electrical stimulation has been used in concert with perfusion and resulted in an increase in cell elongation, enhanced expression of gap junction protein connexin-43, increase in cell number, and an increase in contractile performance.[52, 53] However, the combination of stretch and β-adrenergic stimulation resulted in no additional benefit.[53]

1.5: Characterization of Cardiac Patch Function

One additional benefit of using engineered tissues to treat heart failure post-infarction is that these engineered tissues and the cells entrapped in them can be functionally characterized in vitro, allowing for quality control and a more thorough understanding of the benefits of cell transplantation. Functional performance of patches is primarily assessed through contractile force measurements and optical mapping of electrical conductivity.

1.5.1: Contractile Force Measurements

Cardiac patches should, once developed, function as a piece of cardiac muscle tissue and generate contractile stresses close to physiological values. Quantification of this contractile activity is widely used to assess the quality of a cardiac patch. Contractile activity can be assessed through the magnitude of patch contraction both spontaneously and in response to pacing, the maximum frequency by which a patch can be paced and still elicit a contractile response in phase with the electrical stimulus, the force-frequency relationship of contractile amplitude with increasing pacing frequency, and the contractile response of the patch to exposure to pharmacological agents. Such agents include β-adgrenergic agonists, gap junction blocker 1-Heptanol,[54] or cholinergic agonist carbacol,[39]

1.5.2 Optical Mapping

Electrical activity of cardiac patches can be assessed through optical mapping. To do this, tissues are submerged in medium containing a voltage

sensitive dye, such as Di-4ANEPPS or ANNINE-6. The tissues are then point-stimulated and the action potential propagation is recorded by a high speed camera. This data can be analyzed to assess both conduction velocity (the rate at which action potentials propagate across the tissue), and action potential duration (the time it takes for a cell to re polarize to either 50 or 90% of its resting potential). This data can be used to obtain the conduction velocities of action potentials across the patch, as well as the action potential duration.. These values can then be compared to physiological values to assess the functional quality of the cardiac patch [55]. Additionally, calcium transients can be similarly imaged with a calcium sensitive dye. [56]

1.6 *In vivo* Assessments of Cardiac Patches

Although cardiac can be fully characterized in vitro and can be conditioned in vitro to obtain functional values close to that of the native myocardium, cardiac patches can only truly be effective if their implantation results in the restoration of cardiac function post-infarction. Some studies have made progress towards achieving this goal, utilizing both small and large animal models, and acute or delayed implantation. The timing of patch implantation is a crucial aspect of in vivo assessments as a way to help determine the mechanisms by which any benefits provided by the patch occur. Acute transplantation is transplantation of the patch immediately after infarction, delivering it during the initial inflammatory phase before fibrosis begins to occur. Chronic, or delayed transplantation,

requires a second surgery and applies the patch after the inflammatory phase has passed and either before or after mature scar formation, depending on the time of implantation.

1.6.1 Rodent Models

Rodent models of myocardial infarction treatments are commonly used as the first initial model due to the smaller size of patch required for treatment. Acute placement of a cardiac patch using fibrin as the scaffold and syngeneic neonatal rat cardiac cells, with*in vitro* stretch conditioning of the patch prior to implantation, resulted in minimal scar formation and restoration of cardiac function 4 weeks post-infarct, with 36% cardiomyocyte retention. [37] A similar patch made with a collagen/Matrigel scaffold rather than fibrin and implanted two weeks post-infarction limited further scar formation and preserved cardiac function from the time of implantation. [4] Transplantation of a layered neonatal rat cell sheet patch into a nude rat infarct model 14 days post-infarction resulted in significant improvements in cardiac function, though cell retention was minimal after 4 weeks.[57] Few studies to date have been published assessing the functional consequences of a human stem cell derived cardiac patch in an infarcted rat model. Acute transplantation into non-infarcted rats of scaffold-free tissue patches utilizing hESC-CMs and HUVECs resulted in rapid vascularization of the patches in vivo. Patches containing only an enriched CM population resulted in poor CM retention. [58]

1.6.2: Large Animal Models

The use of large animal models of myocardial infarction is a necessary step towards bringing cardiac patches to clinical relevance Few studies to date have been able to generate the large numbers of human stem cell derived cardiomyocytes required to create cardiac patches large enough to be implemented in large animal models. Human ESC-CMs in cell sheet form were transplanted into a porcine ischemia-reperfusion model 4 weeks after ligation in a feasibility and safety study, and it was found that the cell sheet treatment resulted in a reduction in LV dilation and an improvement in cardiac function both 4 and 8 weeks post-transplantation.[59]

1.7 Current Deficiencies and Obstacles

Despite the many advances in cardiac tissue engineering, there remain deficiencies in the field and many obstacles still to be overcome. Contractile force generation and cellularity of cardiac patches average far below physiological values of 44 mN/mm^2 and 20-40M cells/gram for human ventricular myocardium and 56.4 N/mm^2 rat ventricular myocardium.[60] Diffusional limitations may contribute to this, and may be overcome by the development of a microvascular network- withing the patch during its fabrication. As mentioned earlier, progress has been made, but microvascular network have yet to be created and perfused in the presence of a cardiomyocyte-containing patch of size relevant to even a rat infarct. Other issues that will be addressed in the coming years are maturation

mismatch of donor cells to recipient hearts. Currently used stem cell-derived cardiomyocytes are a mixture of atrial, ventricular, and pacemaker phenotypes, and all exhibit a fetal or neonatal phenotype. Immature phenotypes also have different electrophysiological, metabolic, and contractile properties than adult CMs. It has yet to be determined if transplantation of immature cells will elicit arrhythmic events, or if cells need to be differentiated to maturity prior to transplantation. However, more mature cells may not survive transplantation with the same efficiency as less mature cells.

Chapter 2: Creation and Optimization of a Tissue-Engineered Cardiac Patch Utilizing Neonatal Rat Cardiac Cells

2.1 Introduction

The creation of a tissue-engineered cardiac patch to replace damaged tissue or deliver cells to the injured myocardium has become an attractive solution to the shortcomings of direct cell injections to the heart. An ideal cardiac patch would contain high densities of elongated cardiomyocytes that are electrically coupled, generate contractile stresses near physiological values (44 mN/mm^2 for rat, 56.4 mN/mm^2 for human)[60], and remain viable after transplantation, coupling to the host myocardium and supplementing left ventricular contractility. To determine the ideal material and culture conditions for the creation of a cardiac patch, neonatal rat cardiomyocytes were used in the following initial studies, as they have been well characterized in the literature[4-6] and can be isolated from hearts with high viability and little to no loss of resultant CM function, something which is not feasible with cardiomyocytes isolated from adult hearts[61]. The following studies outline the creation and optimization of a neonatal rat cell-based cardiac patch using fibrin as a biomaterial scaffold.

2.2 Methods

2.2.1 Primary Cell Isolation of Neonatal Rat Cardiac Cells

Neonatal rat cardiac cells were isolated from 48-72h neonatal Sprague-Dawley rats (HSD, Harlan Sprague Dawley) as previously described[5] by a serial

collagenase digestion. Briefly, pups were anesthetized via hypothermia and euthanized via decapitation. The chest was swabbed with iodine, the sternum was opened with a scalpel and the heart was removed and rinsed in a solution of cold 3.96 g/L D-glucose (PBS-glucose) in phosphate-buffered saline (PBS) and 1% penicillin/streptomycin. The ventricles were then excised from the hearts and minced into < 1 mm^2 pieces. Minced ventricles were placed into tubes containing a solution of 37°C PBS-glucose containing 300U/ mL collagenase and incubated for 7 minutes on a shaker at 37°C. The tissue-collagenase mixture was agitated to knock free loose cells, and the supernatant was removed and the collagenase was quenched with a solution containing 10% serum. The sedimented tissue pieces were re-incubated in collagenase solution and this process was repeated 7 times, until most all tissue had been digested. Quenched supernatant was strained through 70 μm cell sieves, centrifuged, and washed twice in basal media before being prepared for creation of cardiac patches.

2.2.2 Fibrin Patches With Cell –Induced Alignment

Aligned patches were constructed by combining a mixed population of neonatal rat cardiac cells at a concentration of $4x10^6$ cells/mL with a fibrin-forming solution consisting of bovine fibrinogen (5 mg/mL, Sigma), bovine thrombin (2 U/mL, Sigma), and 2 μM $CaCl_2$ in a 4:1:1 ratio to create a final fibrin concentration of 3.3 mg/mL. The fibrin forming solution containing cells was injected into 13 mm long, 1.25 mL tubular molds consisting of an 8mm outer

diameter Teflon mandrel coated in 2% agarose to allow for cell-induced gel compaction and alignment in the circumferential direction or on solid Teflon mandrels to prevent lateral compaction and result in planar isotropic patches as previously described[5] and depicted in Figure 2.1. The cell-containing solutions were incubated for 15min at 37°C to allow the fibrin gel to form. Once formed, the molds were ejected from their casings and placed into culture medium (Dubecco's modified eagle medium, 10% heat-inactivated horse serum (to limit fibroblast proliferation), 1% fetal bovine serum, 1% penicillin-streptomycin, 2mg/mL aminocaproic acid (to limit fibrinolysis), with 2 μg/mL insulin and 50 μg/mL ascorbic acid (to promote extracellular matrix (ECM) production).

2.2.3 Modulation of Cell Preparation and Gel Formulation to Maximize Contractile Force Generation

To optimize the cell content of patches to maximize contractile force generation,

two different parameters were investigated: the ratio of cardiomyocytes to non-cardiomyocytes and the fibrin concentration in the initial gel.

2.2.2.1 Fibrinogen Concentration

To assess the influence of matrix structure on cardiomyocyte survival and force generation, subsets of patches were constructed with fibrin concentrations of 2 mg/mL, 3.3 mg/mL and 4 mg/mL. The ratio of fibrinogen/thrombin in the initial solutions was kept the same in all conditions and patches were constructed

with the same cell number and cultured statically for 14 days before being harvested for contraction force testing and histology.

2.2.2.2 Cardiomyocyte Purity

Studies previously initiated in the Tranquillo lab utilized Percoll, colloidal silica particles coated in polyvinylpyrrolidone (PVP), to enrich cell populations for cardiomyocytes[62]. Isolated cardiac cells were placed on top of a single layer gradient consisting of 40% Percoll diluted in Hank's Buffered Saline Solution (HBSS) and spun at 2200 rpm for 20 minutes. The cells that transited the gradient and formed a pellet at the bottom was collected and used to fabricate patches at a cell concentration of $5x10^6$ cells/gel, similar to that of non-enriched cell populations. Patches were cultured statically for 14 days prior to being harvested for contraction force testing and histology. Cardiomyocyte percentages were determined after casting histologically through immunostaining of freshly constructed fibrin gels.

2.2.4 Uniaxial mechanical Testing

To assess the overall mechanical properties of the patches, tissue strips consisting of one-half the length of a patch were tested for tensile properties in the circumferential direction. Tissue thickness was measured using a 50g force probe coupled to a displacement transducer and then strips were placed in grips attached to the actuator arm and load cell of a uniaxial tensile testing system (MTS systems), straightened, and preconditioned by 6 cycles of 0–10% strain at

2 mm/min. The tissues were then stretched to failure at the same rate. Young's modulus (E) was determined by linear regression of the linear region of the stress-strain curve, and ultimate tensile strength (UTS) was determined by the stress at failure.

2.2.5 Contraction Force Testing

To assess the macroscopic contractile activity of patches at the end of culture, patches a custom built force transducer setup was used. Ring-shaped patches were placed in a 37ºC media bath consisting of basal media, 2 mM Ca^{++}, and 50 µg/mL ascorbic acid, and looped between two posts, one adjustable and coupled to a force transducer (Figure 2.2a). Patches were pre-tensioned to 1 gram force and exposed to field stimulation of 1-8 Hz square wave pulses, 10ms duration, 8V amplitude from two carbon electrodes located on either side of the posts. Data was acquired using a LabView data acquisition program and analyzed offline in using a custom Matlab script. Contraction force was measured as peak force obtained during pacing or spontaneous activity minus baseline tension before stimulus (Figure 2.2b). Patches were allowed to reach steady state for 5 seconds at each frequency before recording data for analysis.

2.2.6 Stretch Conditioning of Patches

To investigate the effect of cyclic stretching on patch contractile force generation, a pre-existing cyclic distension system was utilized[63] (Figure 2.3a).

Patches were statically cultured 7 days and then transferred to 8 mm outer diameter distensible thin latex tubes, with 2-3 patches per tube (Figure 2.3b). Tubes were capped at one end with polycarbonate plugs, and attached to a pressurized air source on the other end. Airflow was controlled externally via a pressure regulator and downstream solenoid valve. Mounted patches were placed inside sealed, vented jars containing 50 mL of cardiomyocyte (DMEM, 10% heat-inactivated horse serum, 1% fetal bovine serum, 2 mg/mL ε-aminocaproic acid, 2 μg/mL insulin, 50 μg/mL ascorbic acid, 100 U/mL penicillin and 100 μg/mL streptomycin) medium. Distension of the tubes (and consequently the patches) was regulated by a control set located outside the incubator, consisting of a pressure regulator, timing circuit, and a three-way solenoid valve, allowing for independent control of the frequency, duty cycle, and amplitude of pressurization of the latex mandrels. After being transferred to the cyclic distension system, patches were cultured while exposed to cyclic stretching at a frequency of 1Hz and duty cycle of 66.7%, for a total of 14 days culture, the same as for statically-cultured samples. Three stretch ratios of 5%, 7.5%, and 10% were investigated for the optimal stretch conditions. Stretch ratios were established via a pressure-diameter correlation of the latex tubing. Non-stretched constructs on latex tubing were cultured side by side with stretched constructs and those statically cultured on agarose and Teflon mandrels. To further investigate the influence of stretch parameters on contractility of patches,

patches were stretched at 5% stretch ratio for varying duration, 5, 7, or 9 days. Total culture time remained 14 days.

2.2.7 Histology

For histological analysis, patches were cut into pieces and fixed in 4% paraformaldehyde for 1 hour on ice, frozen in embedding medium (Tissue-Tek OCT), cut with a cryostat into 5 μm-9 μm sections at -18°C and placed onto Superfrost Plus Microscope slides (ThermoFisher Scientific) for histological analysis. Cyrosections were labeled with fluorescent antibodies and subsequently imaged to assess the cellularity, cell composition, and cell morphology. A subset of patch pieces were not frozen after fixation and used for whole-mount tissue staining.

For immunofluorescence staining of sections on slides, sections were permeabilized with 0.01% Triton-X-100 (Sigma), blocked in 5% Normal Donkey Serum (Jackson Immunoresearch), incubated overnight at 4°C in primary antibody followed by a 60 minute incubation in secondary antibody at room temperature and a 10 minute incubation in Hoescht 3332 (LifeTech). Slides were mounted in fluorescent mounting medium (Dako) and imaged within 24 hours. For immunofluorescence staining of whole tissue pieces, a similar process was followed, but with extended incubation times to allow for antibody and reagent diffusion into the tissue thickness. Additional histology methods and information can be found in the protocols contained in appendices 3 and 4.

2.2.8 Protein Extraction and Western Blotting

To assess the effect of stretch on gap junction formation between adjacent CMs, portions of both statically cultured and stretch-conditioned patches were frozen after contraction force testing and stored at -80ºC for protein analysis. For analysis, patches were thawed and lysed using a sonicator (QSonica Q125) at 4°C in a NP-40 lysis buffer consisting of 0.5% Nonidet P-40, 5% glycerol, 25 mM Tris (pH 7.4), 25 mM NaF, 225 mM NaCl, 0.025% sodium deoxycholate, 1 mM EDTA, 2 mM $NaVO_4$, and 1 mg/mL each of aprotinin, pepstatin, and leupeptin (Sigma-Aldrich). Total protein was assessed using a BCA protein assay (Pierce Biotechnology). 10µg of protein was loaded into the lanes of a 4-20% Mini-Protean TGX 10-well gel (BioRad) for protein separation and transfer. Western blot was conducted by assessing using primary antibodies for the proteins connexin-43 and β-actin, blocked in 5% blocking grade buffer (BioRad) with 0.1% Tween (Sigma-Aldrich), horseradish-peroxidase conjugated secondary antibodies (GE Healthcare Life Science) and chemiluminescence agent (Millipore). Expression intensity was analyzed using ImageJ software.

2.2.9 Statistics

All data are presented as mean +/- standard deviation. When applicable, results were compared using student's t-test or a one-way analysis of variance (ANOVA) in conjunction with a Tukey HSD post-hoc testing. p-values <0.05 were considered significant.

2.3 Results

2.3.1 Maximal Force Generation with Non-Enriched Cell Populations and 3.3 mg/mL Fibrin Gels

After it was established that aligned patches could be constructed, the optimal ratio of cardiomyocytes to non-cardiomyocytes was ascertained. Patches created with enriched CM populations exhibited an increase in axial length (width) compared their non-enriched counterparts, but were otherwise similar in appearance (Figure 2.4a). More importantly, enriched cardiomyocyte population patches had reduced measured contraction forces than those created with the native cell population (Figure 2.4 b). Thus, it was determined that the native ratio of fibroblasts to cardiomyocytes was optimal for patch creation, concurrent with other published results that show that high purities of cardiomyocytes result in decreased contractile force generation when using neonatal rat cardiomyocytes.[6, 64]

To further validate the use of a native cell isolate, cardiomyocyte preparations gathered using Percoll gradients gave highly variable CM purities, ranging from 42-67% CMs, with an average CM fraction of 53.5% based on histological staining of fibrin gels immediately after casting, no different than the average 45% CM fraction of the native cell isolate. The use of percoll was additionally associated with decreased cell yields, indicating a negative effect of Percoll on cell viability.

2.3.2 Increased Contractile Force Generation with Cyclic Stretching

2.3.2.1 Dependence upon Stretch Amplitude

It was found that 5% stretch ratio amplitude was optimal based on measurements of twitch force generation, with a 2.12±0.51 fold increase over statically cultured samples (Figure 2.5a). Neither a 7.5% or 10% stretch ratio led to an increase in twitch force generation of patches (0.99±0.40 and 1.35±0.55 fold change compared to static, respectively). Although there was an increase in contractile force generation with 5% stretch, the exact mechanism by which this improvement is achieved is unknown. Previous work has shown an increase in the contractile force generation was associated with an increase in the presence of gap junction protein connexin 43 (CX43) in patches that featured aligned matrix fibers and cells rather versus isotropic[5], but no further increase was seen when aligned patches were cyclically stretched (Figure 2.6). Upon histological interrogation, no increase in cell density or cardiomyocyte size was observed (Figure 2.7), indicating minimal or negligible effects of cell survival, proliferation, or significant hypertrophy.

2.3.2.2 Independence from Stretch Duration

At 5% stretch ratio, there was found to be no dependence upon the duration of stretching (Figure 2.5b) in terms of force generation by patches. This would imply that the increase in contractile force generation is more likely a stimulus response than a sustained response.

2.4 Discussion

This work was a continuation of the work completed by Black and Myers, et al[5], which created aligned patches containing neonatal rat cardiac cells in a fibrin scaffold, and found that aligned patches generated more contractile force than isotropic patches through an increase in the presence of CX43. Here we further optimized these patches to maximize contractile force generation. We found that neither modulation of the initial matrix density nor enrichment for CMs resulted in increased force generation. However, patches that were bioreactor conditioned with exposure to cyclic mechanical stretch displayed over a 2-fold increase in contractile force generation, although the exact mechanisms of this increase remain unknown. Other reports have shown evidence of physiological CM hypertrophy when engineered cardiac tissues have been exposed to cyclic stretching[10, 44], but CM hypertrophy was not clear in this study with the methods used to characterize these patches. Future work to elucidate the mechanism of this increase in contractile force generation would protein analysis to evaluate the presence and relative presence of contractile proteins, and DNA synthesis markers to assess hypertrophy. Rather than fully investigate the effect of cyclic stretching on neonatal rat cardiomyocytes in these patches, we elected to assess the functional benefits these patches have when transplanted into an acute rat infarct model and pursue the cyclic stretching studies in a more clinically relevant, human iPSC-CM model.

2.5 Figures

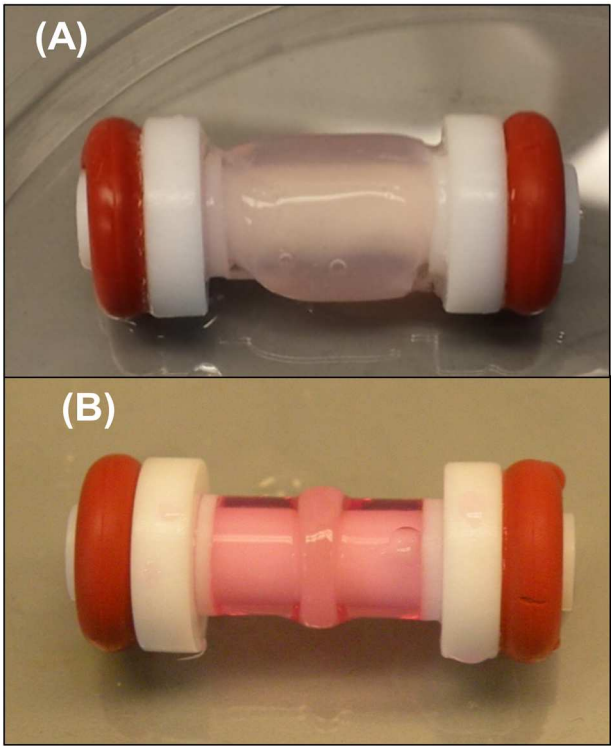

Figure 2.1: Aligned patch immediately after gel formation (A) and after 14 days static culture (B). Fiber alignment is in the circumferential direction around the agarose-coated mandrel.

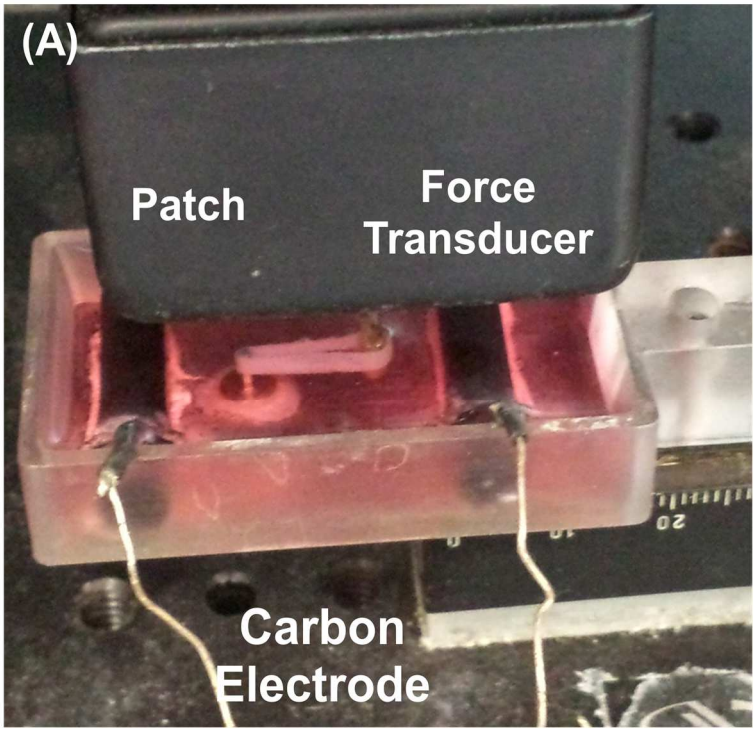

Twitch Force Measurements

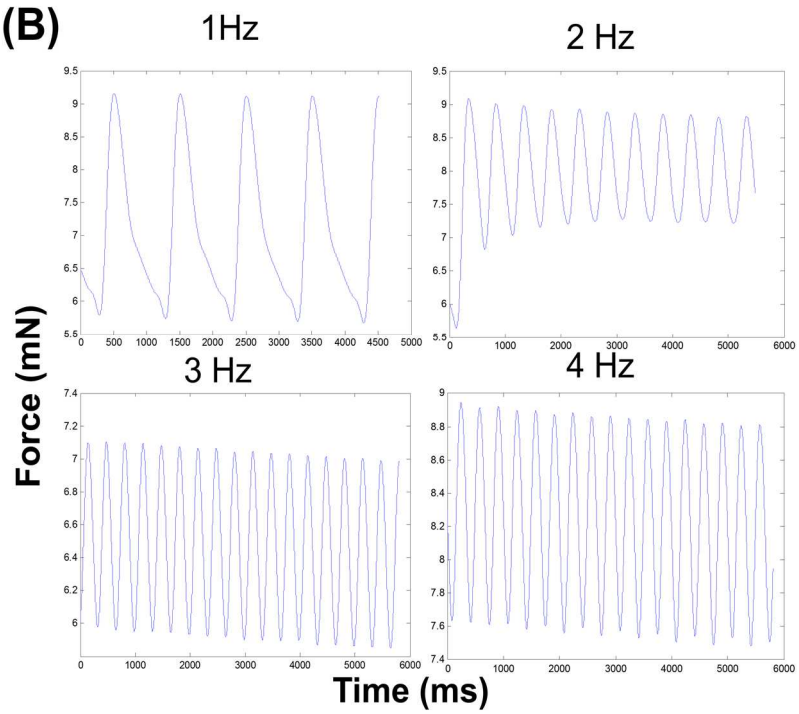

Figure 2.2: Contraction force measurement setup (A) and representative images of force generation recordings at varying frequencies (B).

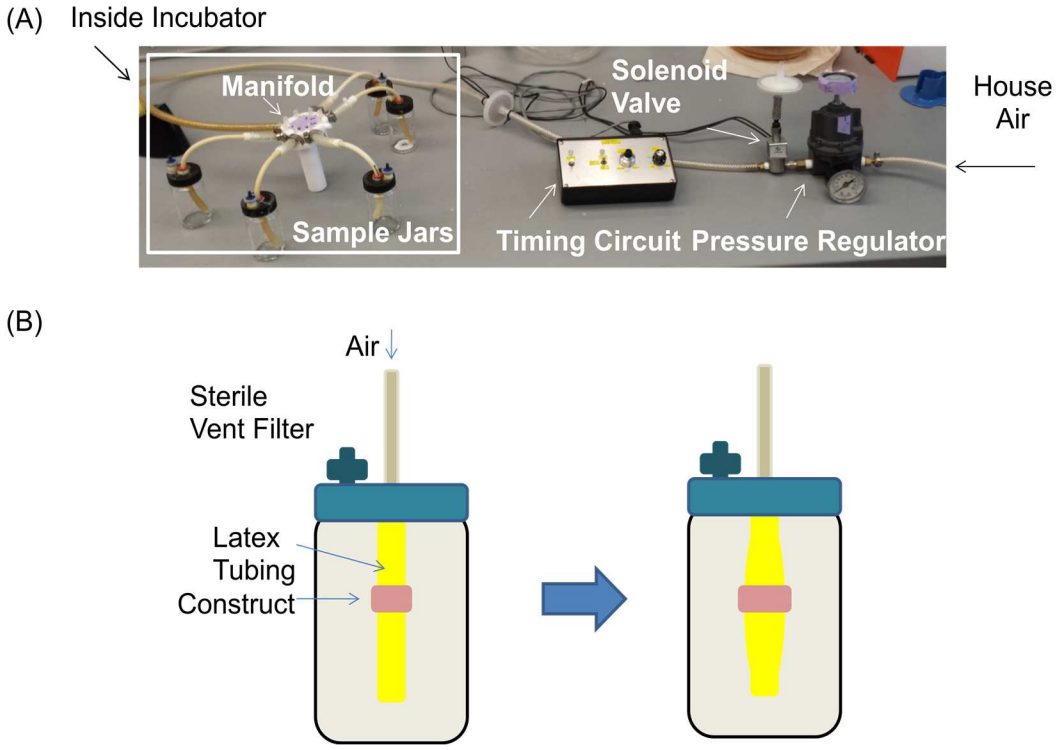

Figure 2.3: Setup of cyclic distension bioreactor (A) and schematic of bioreactor jar[37] (B).

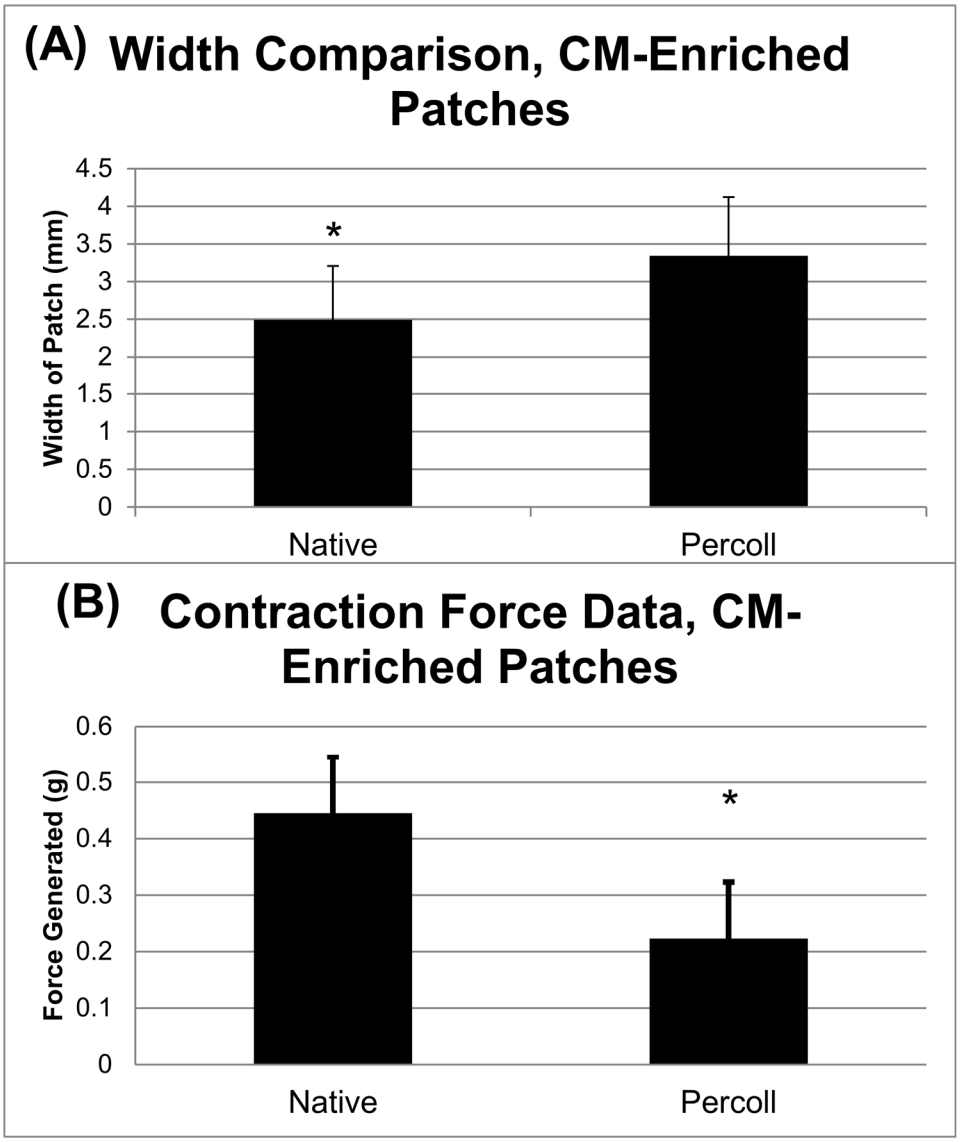

Figure 2.4: Size (A) and contractile force generation (B) of patched created using an enriched (Percoll) and non-enriched (Native) CM preparation. Percoll-enriched CM cell population patches generated lower average contractile force than patches made with the native cell population.

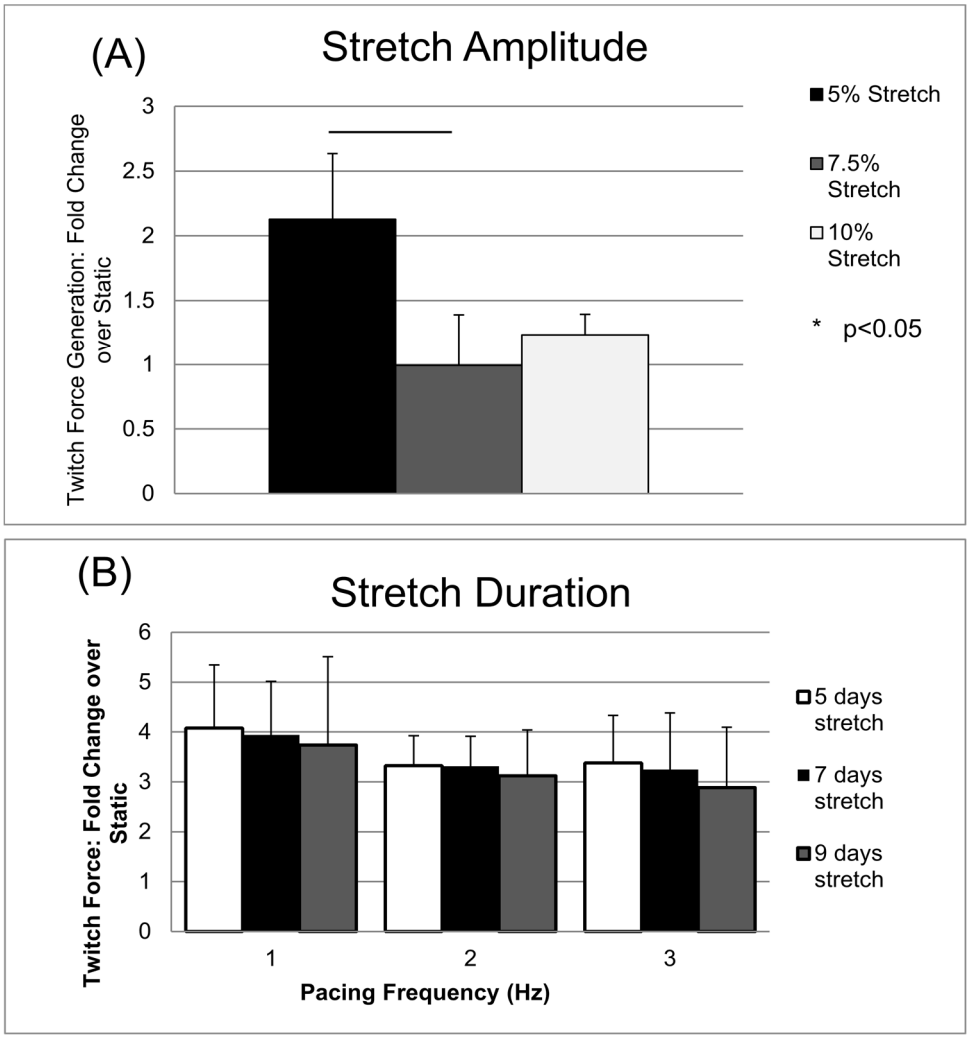

Figure 2.5: Contractile force generation of stretch conditioned patches. A 2-fold increase over statically cultured sampled was observed with a 5% stretch amplitude. The duration of stretch had no effect on force generation. [37]

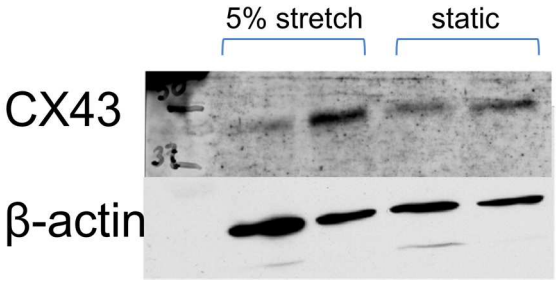

Figure 2.6: Western Blot for gap junction protein connexin-43 (CX43) of stretched and statically cultured samples. Stretched samples were stretched at 5% strain for 7 days at 1 Hz

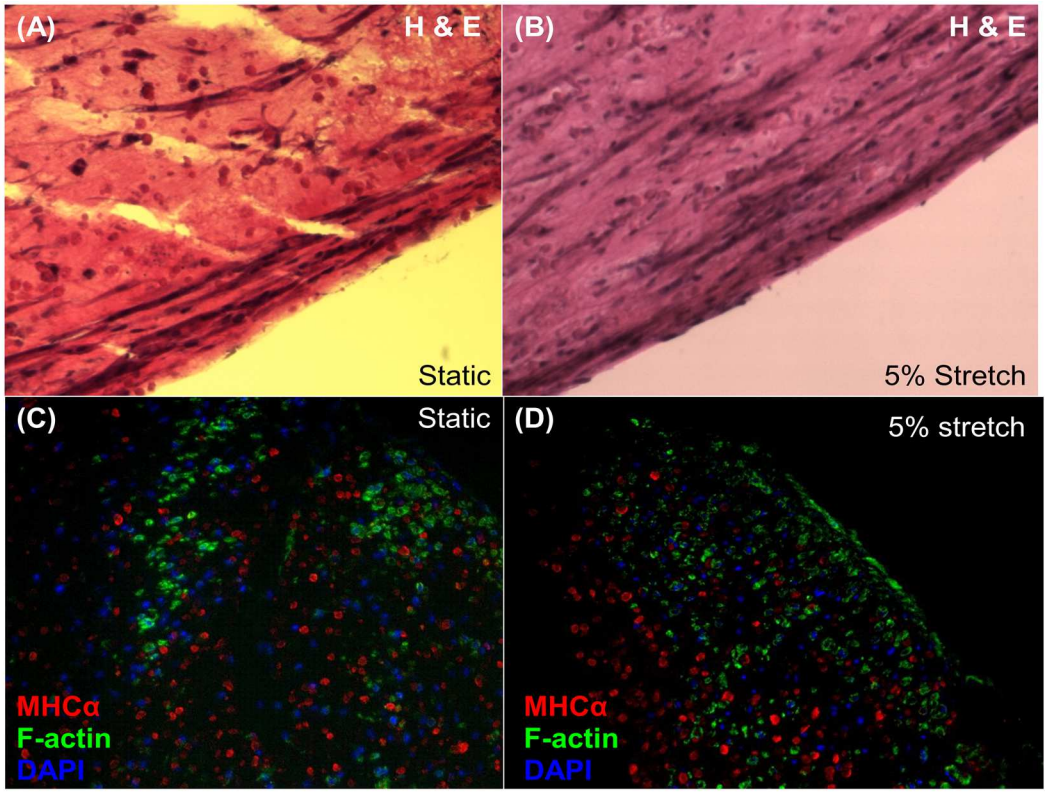

Figure 2.7: Histological comparison of statically cultured (A, C) and stretch conditioned (B, D) patches. No qualitative increase in cell number or cell size was observed with stretch conditioning

Chapter 3: Functional Consequences of a Tissue-Engineered Myocardial Patch for Cardiac Repair in a Rat Infarct Model

The material discussed in this Chapter is adapted from the following:

Wendel et al, Functional Consequences of a Tissue-Engineered Myocardial Patch for Cardiac Repair in a Rat Infarct Model. Tissue Engineering Part A. 2014[37]

3.1 Introduction

Though cell-based therapies hold much promise to limit left ventricular remodeling post-infarction, the mechanisms responsible for the improvements observed largely unknown. The transplanted cells may limit LV remodeling and infarct expansion by fusing directly with native tissues, stimulating the growth of new blood vessels that subsequently increase perfusion to the infarcted area[65], releasing cytokines that reduce cardiomyocyte apoptosis[3], to improve the passive mechanical properties of the ventricle.[66] However, in most studies utilizing directly injected cells as a method of delivery, very few transplanted cells are retained in the infarcted region, perhaps because they fail to create focal adhesions with neighboring cells, or because the inflammatory response to myocardial injury and the hypoxic environment of the infarct zone reduce cell survival.[67] Thus, the use of engineered tissues has become an attractive solution to deliver cells to the injured myocardium high retention.

In Chapter 2, we observed that cyclic stretching causes a 2-fold increase in contractile force generation of our cardiac patches. However, the end-goal of these patches is to limit left ventricular remodeling post-infarction, and the ability

of these optimized patches to improve cardiac function post-infarction had yet to be investigated.

While some studies have assessed the benefits of a cardiac patch in the acute phase using non-cardiac cells[68] or when administered 14 days post-infarction[4], of an engineered cardiac patch using a fibrin scaffold in the acute phase, post-infarction has yet to be investigated. Thus, for the experiments described in this report, we created engineered heart-tissue patches by seeding a fibrin gel with either the complete native population or a cardiomyocyte-depleted population of neonatal rat cardiac cells, and then stimulated cellular alignment and maturation by cyclically stretching the patches for seven days. A cardiomyocyte-depleted population was used to evaluate whether or not any benefits obtained from the patch originated from cardiomyocytes or from non-cardiomyocyte paracrine effects. The patches were evaluated in a rat acute myocardial injury model to determine whether fibrin-based engineered tissues could improve cardiac function and limit adverse cardiac remodeling one and four weeks after experimentally induced MI.

3.2 Methods

3.2.1 CM + and CM- Patch Construction

Two kinds of patches were made for this study. The first, further noted as CM+ patches, were constructed similar to the patches constructed in Chapter 2 using cardiac cells from syngeneic Fisher F344 (Harlan Sprague Dawley) rats

and cultured statically for 7 days before being stretch-conditioned at 5% stretch at 1Hz frequency for 7 days, as optimized in Section 2.3.2.

Secondly, to determine if any benefits seen from patch transplantation are attributed to active coupling of donor cardiomyocytes to the host or paracrine factors from the co-entrapped non-cardiac cardiac cells, patches containing only non-cardiomyocytes were constructed, further noted at CM- patches. Non-cardiomyocytes were selected through pre-plating of the cardiac cell isolates for 45 minutes on tissue culture plastic in complete medium (DMEM high glucose with 10% FBS and 1% penicillin/streptomycin) to remove slow-adhering cardiomyocytes. Adherent cells were cultured in 15% serum complete medium until confluent before harvesting for patch construction. Immunostaining for cTnT revealed the initial cell population had been reduced to 6.0 ± 2% CMs at the time of harvest. Non-cardiomyocyte (CM-) patches were fabricated at a cell concentration of $2.4x10^6$ cells/mL in order to match the approximate number of non-cardiomyocytes contained in CM+ patches made from the entire isolate, as the freshly isolated cardiac cell population was found to contain approximately 40-45% cardiomyocytes and 55-60% non-cardiomyocytes. The CM- patches were cultured otherwise identical to CM+ patches.

3.2.2 Quantitative Image Analysis to Assess Cell Distribution

To assess the cellularity and cell distribution of patches, a custom matlab algorithm was developed. Cross-sectional images of patch sections co-labeled

with DAPI (cell nuclei), f-actin, and either cardiomyocyte (cTnT), myofibroblast (smooth muscle actin), or endothelial (CD31) markers. Gray-scale images of each component stain were imported into matlab, normalized ofr intensity, thresholded, converted to binary, and overlaid on top of each other.

F-actin/DAPI co-labeling (Alexa Fluor 488 Phalloidin, Invotrogen) was used to quantify live cell % within cross-sections of the patches prior to implantation. This method was chosen due to the relatively large thickness (657-694 μm) and the non-uniform cell distribution through the thickness of the patches. F-actin was assumed to be present in all live cells, as after cell death F-actin dissociates into G-actin monomers, which is not labeled by Phalloidin. To verify this approach, a subset of patches were first subjected to live/dead staining via a 5 minute incubation in 10 μg/mL Hoescht 33342 (Invitrogen) and 10 μM Sytox Green nucleic acid stain (Molecular Probes)in Hank's Buffered Saline Solution (HBSS). Samples were next fixed in 4% PFA, frozen in OCT, and cut into 9 μm sections before imaging. Live cell% was quantified as the percentage of total cells DAPI+/Sytox-. This data was then compared to the percentage of cells co-labeling for F-actin and DAPI in sections from the same sample.

Cell types and locations were identified by the intersection of a cell nucleus (DAPI+ object) with f-actin and the desired cell label staining. Both global and local cell numbers and densities could be determined using this method. More detail can be found in Appendix 2

3.2.3 Implantation of a Cardiac Patch into an Acute Infarct Model

Procedures used in this study were reviewed and approved by the University of Minnesota Institutional Animal Care and Use Committee (IACUC) and the Research Animal Resources (RAR) Committee.

Female Fisher F344 syngeneic immune competent rats, weighing 175-199 g (Harlan Sprague Dawley), were used in these studies. Rats were anesthetized with 50 mg/kg Ketamine and 2 mg/kg Xylazine delivered intramuscularly, intubated, and the heart was exposed through a limited left lateral thoracotomy. To induce a myocardial infarction (MI), the pericardium was opened and the left anterior descending (LAD) coronary artery was permanently ligated with a 6-0 polypropylene suture. After a MI had been established, approximately 5-10 min post-ligation, a single patch was applied across the epicardial surface of the infarcted area of the left ventricle, approximately parallel with surface myocardial alignment. Patches, some of which were incubated with 1μg/mL DAPI overnight prior to implantation to label donor cells, were removed from their mandrels, cut into 3 individual 8 mm strips and sutured parallel to each other on the epicardial surface of the LV over the infarct area immediately below the ligation using 8-0 vicryl sutures. The epicardium was scratched in this process to allow for the patch to bond with the host myocardium. After patch placement, the chest was closed and the animal was allowed to recover. 5 mg/kg Ketoprofen supplemented with 0.05 mg/kg Buprenorphine, delivered subcutaneously, were used as analgesia for 72 hours post-operatively. 15 mg/kg enrofloxacin, delivered

subcutaneously, was administered for 5 days post-operatively to prevent infection. Animals were euthanized by an intracardiac injection of Potassium Chloride 3, 7, or 28 days post-operatively.

3.2.4 Functional Analysis

Cardiac function was evaluated via echocardiograph assessments of left ventricular fractional shortening (LVFS) and left-ventricular ejection fraction (LVEF), as previously described, [69] both 1 week and 4 weeks post-implant. Hearts were harvested at either the 1 week or 4 week time point for histological assessment.

3.2.5 Histology and Immunohistochemistry

Non-implanted patches were fixed in 4% paraformaldehyde on ice for 1 hour, frozen in embedding medium (Tissue-Tek OCT), cut with a cryostat into 5 µm- 9 µm sections at -18°C and placed onto Superfrost Plus Microscope slides (ThermoFisher Scientific) for histological analysis.

After harvest, the left ventricles of explanted hearts were sliced circumferentially into 2-4 mm slices and slices were either fresh frozen in embedding medium, cut into 5 µm slices at -18°C and fixed in 4% PFA, or fixed overnight in a 10% formalin solution, paraffin embedded, and cut into 4 µm slices and placed onto slides for histological analysis.

Cyrosections were labeled with fluorescent antibodies and subsequently imaged to assess the cellularity and cell composition of the patch prior to

implantation, and the patch-grafted area on the heart. Cell density and cellular composition of the patches were determined using a custom MATLAB program detailed in chapter 2.2.8. Live cell percentage was determined as the percentage of cells staining positive for both DAPI and f-actin.

Infarct size and wall thicknesses are reported as the average of measurements performed on Masson's trichrome-stained sections from each of three locations of the left ventricle: immediately below the ligation suture, mid-way between the ligation suture and the apex, and near the apex. Infarct sizes were calculated as the percentage of LV anterior wall surface area that was occupied by scar tissue, and wall thicknesses were measured across the infarcted portion of the wall.

3.2.5 Experimental Design

Four groups were investigated for this study: 1) Sham (n=5): No ligation, the chest and pericardium were opened and then closed. 2.) MI only (n=6): ligation of the LAD coronary artery and no treatment. 3.) CM- patches (n=5): patches made with a cardiomyocyte-depleted cell population, and 4.) CM+ patches (1 week, n=3, 4 weeks, n=7): patches made with cardiomyocytes + non-myocyte cardiac cells.

3.2.6 Statistical Analysis

Data are presented as means ± standard deviations. All results were compared using MiniTab statistical software. One-way analysis of variance

(ANOVA) in conjunction with Tukey HSD post-hoc testing was used to compare all groups. P-values <0.05 were considered significant.

3.3 Results

3.3.1 In vitro Characterization of Patches

As shown in Figure 3.1, the average cell viability for F-actin/DAPI staining was 87±10.0% and for live/dead staining was 83.4±7.7% (p=0.31).Thus F-actin/DAPI staining is sufficient in the patches used in this study to quantify live cell%.

Figure 3.2a shows stretch-conditioned patches prior to implantation. Both CM+ and CM- patches had compacted into short tubes, or rings, and were dimensionally similar with thicknesses of 657 ±41.3 μm and 694 ±70.9 μm, and axial lengths of 3.15±0.29 mm and 2.72 ±0.3 mm, respectively. Both samples had a circumferential length of 25.1mm, based on the mandrel outer diameter. Both patches had similar moduli (CM+: 86.0±3.8 kPa CM-: 135.5±46.7) and UTS (CM+: 75.7±11.5 kPa, CM-: 47.2±12.1 kPa) in the aligned (circumferential) direction in the rings, values near to what has been reported for myocardium (50-100kPa for both modulus and UTS).[31, 70, 71]

In order to assess the quality and consistency of implanted patches, a subset of samples intended for implantation were histologically and functionally evaluated after stretch conditioning to quantify their cellular composition and contractile response. These patches had approximate cell densities of 1540 ±631

cells/mm^2 for CM+ patches and 1030±219 cells/mm^2 for CM- patches based on immunoflourescent staining of 5 μm sample cross-sections (Table 3.1). However, cellularity was not homogenous throughout the patches.SMA+ cells being located primarily on the abluminal surface of CM- patches (Figure 3.2 i) and higher densities of cardiomyocytes were located near the outer surface and edges of the ring-shaped patches (Figure 3.2 e, f). SMA+ cells within the CM+ patches were primarily found in areas containing cardiomyocytes (not shown). Cells throughout the patches exhibited elongated morphologies aligned in the circumferential direction (Figure 3.2 d, g) and adjacent cardiomyocytes within the CM+ patches exhibited gap junctions as well (Figure 3.2 d). CM+ patches were found to contain 90.1 ±7.1 % live cells (f-actin+/DAPI+), 39.1±16.5% of which were cardiomyocytes (f-actin+/DAPI+/cTnT+) and 15.2±3.7% were positive for α-smooth muscle actin (f-actin+/DAPI+/SMA+), indicating they were either smooth muscle cells or myofibroblasts (Table 3.1). The final percentage of cardiomyocytes was similar to that of the initial cell population, which can be attributed to the use of horse serum, which limits fibroblast proliferation, in the culture medium. Only a few cells were found to be CD31+ endothelial cells in either group. Cells positive for neither cardiomyocyte markers, SMA or CD31 were assumed to be quiescent cardiac fibroblasts, which constituted 45.7±20.2% of the final cell population. CM- patches were found to contain 92.7±3.8 %live cells, 1.8%±1.0% cardiomyocytes, 11.5±14.1% SMA+ cells, and 80.4±15.2% quiescent fibroblasts.

In addition to histological interrogation of the patches to assess cellularity, extracellular matrix production by the entrapped cells was also evaluated. Trichrome staining (Figure 3.3 b) revealed that after 14 days in vitro culture, the content of the patch ECM remained primarily fibrin. However, collagen I and the basement membrane proteins laminin and collagen IV were deposited in the extracellular space surrounding all cells within the CM+ patches, and significantly less of collagen I and IV were produced in the CM- patches (Figure 3.3 a, c). Small amounts of collagen III and fibronectin were also present in the ECM of both patches (not shown).

CM+ patches exhibited visible, measurable contractions both spontaneously and synchronously in response to electrical pacing from 1-4Hz frequency (Figure 3.2 b-c). The maximum pacing frequency in which a twitch force could be measured occurring synchronous with stimulation averaged between 5-7 Hz, comparable to the heart rates of the rats used in these studies. The twitch force ranged from 1.3-2.7 mN over 1-4 Hz, values that were over three-fold higher than samples cultured statically for 14 days.

3.3.2 Functional Consequences of Patch Transplantation

3.3.2.1 Echocardiography

Echocardiography was conducted both 1 week and 4 weeks post operatively. One week post-implant, neither treatment group displayed a reduction in ejection fraction or fractional shortening of the LV wall compared to

the sham surgery, but there was a reduction in cardiac function in the animals receiving MI-only (data not shown). Four weeks post-implantation, both ejection fraction and fractional shortening were further reduced in animals receiving MI-only as compared to values 1 week post-ligation (Figure 3.4 a, b). Animals receiving the CM- patches showed no improvement in either ejection fraction or fractional shortening over MI-only. Hearts receiving CM+ patches had ejection fractions and fractional shortenings substantially higher than both MI-only and CM- patch groups, values which were not different than the sham operated group (Figure 3.4 b). This indicates that a patch containing the full complement of cardiac cells, cardiomyocytes included, yielded the best functional outcome.

3.3.2.2 Left Ventricular Remodeling

Animals receiving MI-only had large infarcts (Figure 3.5 a), comprising on average 61.3 ±7.9 % (range 53.7%-69.5%) of the LV anterior wall surface area, with significant wall thinning to 661.3 ± 37.4 μm, or ~25% of the thickness of the non-infarcted myocardium (Table 3.2). CM- patches resulted in significant reduction of infarct size (Figure 3.5 b) to 36.9 ±10.1% (range 30.9%-48.6%). Thinning of the LV anterior wall was also substantially reduced to 1058.2±136.4μm, or ~40% of the thickness of the non-infarcted myocardium. Concurring with the functional data, animals receiving the CM+ patch had very small infarcts (Figure 3.5 c) of 13.9±10.8% (range 5.4%-29.1%) of the LV anterior wall. Wall thinning was also substantially reduced over both MI-only and CM-

patch groups, to 2274.6±111.5 μm, a value not significantly different than that of the sham-operated myocardium (Table 3.2).

3.3.3 Patch Engraftment

At 1 week post-implant, CM+ patch recipients were found to have a large amount of adhesions and scar tissue surrounding the heart, rendering it difficult to remove the heart with the patch intact. After 4 weeks *in vivo*, the presence of adhesions was reduced, and hearts receiving either CM+ or CM- patches had a thin, pale film covering the epicardial surface of the LV anterior wall, consistent with a collagenous tissue film revealed with trichrome staining not seen on a sham-operated myocardium (Figure 3.6 b, c), extending across both the infarcted and non-infarcted area of the LV epicardial surface. This film was not seen in sham-operated hearts (Figure 3.6 a) or those receiving ligation only (not shown) and had an average thickness of 372.6 ±55.39 μm and 131.0 ±39.0 μm for CM+ patch and CM- patch recipients, respectively. Cyrosections of these hearts revealed that this film contained large numbers of DAPI+ cells (Figure 3.7), indicating that these cells were donor cells and that the film seen was the remodeled patch. DAPI+ cells were also found in the host myocardium in hearts that received CM+ patches, indicating that there was cell migration from the engrafted patch into the myocardium. Invading donor cells both 1 week and 4 weeks post-implantation (Figure 3.7 a. b), and donor cells were found associated with vascular structures within the host myocardium interspersed with host cells

(Figure 3.7 b). Invading donor cells located outside of vascular structures, presumably cardiac fibroblasts (cells both SMA- and CD31-), were found inside the host myocardium and in neo-tissue identifiable as the zone devoid of cardiomyocytes between the host myocardium and patch. At 1 week post-implant, bright DAPI+ cells were widely spread throughout the patch and the interface, and cells were seen in the myocardium as well. At 4 weeks post-implant, DAPI+ cells were much dimmer. This dimming may be attributed to dilution of the DAPI label through cell division.

The engrafted patches underwent near complete remodeling in vivo, with the ECM being converted from being primarily fibrin at implantation (Figure 3.3 b) to highly collagenous at explant (Figure 3.6 b, c). Elongated donor cardiomyocytes were found within the patches of animals that received CM+ patches (Figure 3.6 d, f), but not CM- patches (Figure 3.6 e). Both patches were vascularized *in vivo*, with ingrowth of host endothelial cells seen both 1 week and 4 weeks post-implantation (Figure 3.8 c, d). Vascular structures containing red blood cells found throughout the entire engrafted areas of both CM+ (Figure 3.8 a, b) and CM- (not shown) patches, with no difference in the vascular density within the patches between the two groups (not shown). The presence of red blood cells in these vessels indicates that the patches were perfused through angiogenesis from the host myocardium. In the engrafted CM+ patch, the percentage of cardiomyocytes present was reduced to 11.0 ± 10% after 4 weeks *in vivo*, with a very heterogeneous distribution. There was over an 18-fold

increase in the cell density in the engrafted patch compared to patches prior to implantation. This increase in cell density and reduction in cardiomyocyte percentage could be attributed to cell death due to ischemia post-implantation, proliferation of donor non-cardiomyocytes in vivo, and the infiltration of host cells into the patch. Factoring in the increase in cell density and the percentage of cardiomyocytes within the patches, it can be estimated that 36.5% of implanted cardiomyocytes survived transplantation. Gap junctions between donor cardiomyocytes were found within the patch (Figure 3.6 f); however, electrical coupling of donor cardiomyocytes to the host myocardium was not possible due to the presence of a 101± 40 μm non-cardiomyocyte neo-tissue zone between the CM+ patch and the host myocardium. This area consisted primarily of fibroblast-like cells of both donor (DAPI+) and host origin, but also contained numerous microvessels spanning the zone. Additionally, alignment of the patch with the host myocardium was not completely maintained. Regional alignment of donor cardiomyocytes within the CM+ patches was seen, but this alignment did not consistently match the alignment of the host cardiomyocytes along the epicardial surface of the heart. This misalignment may be attributed to movement or misplacement of the patch during or shortly after implantation, but before patch attachment to the host engraftment.

3.4 Discussion

The main finding of this study is that engraftment of the CM+ patch occurred by 4 weeks after implantation, accompanied by a remarkable amelioration of left ventricular remodeling underneath the patch (Figures 3.5, 3.6) in the form of a reduction in both LV scar size and wall thinning accompanied by a substantial improvement of LV contractile function (Figure 3.4). A surprise and novel finding of this study is that the administration of a CM- patch also resulted in a reduction of LV scar formation and thinning of the LV anterior wall, but to a lesser extent than the CM+ patch (Figure 3.5, Table 3.2) and without improvements in contractile function, suggesting the benefits observed with this treatment require cardiomyocytes.

3.4.1 Fibrin Patch Transplantation

The creation of an in vitro myocardial patch is an area that has seen significant and increasing interest for many years, leading to a number of studies utilizing a variety of different cell sources and fabrication methods. The objective of restoring LV contraction by transplantation of a patch that generates physiological contractile stress to the injury site of the LV has been largely unsuccessful.[66, 72-78] Rather than trying to replace the damaged myocardium, the present study evaluated the capacity of a patch, with or without donor cardiomyocytes present, to restore LV contraction. Fibrin was chosen as the scaffold due to its biocompatibility and capacity to be remodeled both in vitro[79, 80] and in vivo. [81] Fibrin possesses many of the properties of collagen that are

advantageous for tissue engineering[82], such as being a native substrate for cell adhesion and the capacity for the protein fibrils to become aligned when cell induced gel compaction is mechanically constrained.[83] This cell induced alignment has been shown to be associated with an increase in the contractile force generation of engineered myocardial tissues.[5] Fibrin gels have also been seeded with human embryonic stem cell-derived cardiomyocytes[84], murine cardiovascular progenitor cells or with both mESC-derived CM and non-myocyte supporting cells to generate engineered cardiac tissues. These tissues contained aligned, highly differentiated and electromechanically coupled CMs that exhibited rapid conduction velocities (22-25 cm/s) and contractile forces of up to 2 mN in static culture.[11]

3.4.2 Patch-Induced Myocardial Protection

One of the major objectives of the present study was to evaluate the efficacy by which a fibrin-based, stretch conditioned myocardial patch can limit left ventricular remodeling and infarct expansion. It was a surprise finding that the patch implantation caused a dramatic reduction of infarct size (Figure 3.5). In addition, the beneficial effects were remarkably more prominent in hearts receiving a CM+ patch compared to a CM- patch (51 % reduction in CM- and 77 % reduction for CM, $p<0.05$, Figure 3.5, Table 3.2). Although the transplantation of a non-cardiomyocyte patch was associated with reduction in infarct size and LV wall thinning, these beneficial effects were improved and cardiac function was

completely restored in hearts receiving a patch containing both cardiomyocytes and non-cardiomyocytes (Figures 3.4, 3.5). Although a large fraction of the donor cardiomyoctes (36%) were estimated to survive 4 weeks implantation within the CM+ patches, these remarkable effects were not caused by their electrical coupling to the host myocardium as the presence of a physical barrier in the form of a non-cardiomyocyte neo-tissue zone separating donor cardiomyocytes from the host myocardium and preventing electrical coupling between them. This zone could be scar formation as a result of the patch implantation or the patch remodeling and engraftment process itself. Due to the thin size, low stiffness properties and modest twitch force generation of the CM+ patch when implanted, these effects were also not likely a result of passive or active force inhibition of LV scar formation and dilation, but rather through cytokine support provided by donor cardiomyocytes. The affixed patch on the surface of the infarcted region prevented host cardiomyocyte death immediately after infarction. Two physical effects occur as a consequence of this cytokine support. First, a reduction in host cardiomyocyte death in the infarct zone prevents overstretching of neighboring host ventricular cardiomyocytes, thus blocking the detrimental signaling pathways initiated by cardiomyocyte overstretch.[85] Second, the regional left ventricular wall stress, and therefore the energy demand of the host myocardium is decreased which in turn prevents LV bulging.[86, 87] Consequently, ischemic cardiomyocytes that would otherwise progress towards apoptosis are spared until perfusion can be re-established. The

end result of these two events is a significant reduction in LV scar size and a subsequent reduction in LV dilation.

Since we employed a permanent LAD occlusion model, the level of reduction of coronary flow at initiation of occlusion was identical among the hearts with or without patch implantation. Therefore, the reduction of infarct size that resulted from the patches was a result of either sparing the ischemia threatened cardiomyocytes that otherwise would go on to the apoptosis pathways, as noted above, or from the mobilization of the endogenous cardiac progenitors to the injury site to facilitate regeneration. Survival of donor cardiomyocytes within the patch (Fig 3.7 c, e, f) was not surprising, as neonatal rat cardiomyocytes have been shown to be hypoxia-resistant due to their ability to rely on glycolysis until a vascular network has been established.

3.4.3 Cytokine Effects

Invasion of donor cells from the CM+ patch into host myocardium was seen both 1 week and 4 weeks post-ligation (Figure 3.7), suggesting the important paracrine effect of the patch requires communication between cardiomyocyte and non-cardiomyocyte cardiac cells. Cytokine-driven cardiac repair has been hypothesized to be mediated primarily by non-cardiomyocytes, [88, 89] and yet apparent cytokine benefits in this study were seen to a much higher degree in the CM+ patch compared to the CM- patch. Thus, cardiomyocytes played an indirect, yet crucial role in this system. While there are a wealth of

studies investigating the role non-cardiomyocytes have on cardiomyocytes in culture and during development,[10, 11, 88-91] the influence cardiomyocytes exert on non-cardiomyocytes has been less thoroughly investigated. When exposed to stretch, cardiac fibroblasts have been shown to increase ECM production, but only in the presence of cardiomyocytes or cardiomyocyte-conditioned media through cardiomyocyte-produced TGF-β1.[92, 93] This result is consistent with the CM+ patches used in this study, with an increase in both collagen I and collagen IV compared to CM- patches (Figure 3.3 c).

Previous work has shown that cell-based therapies can improve cardiac function post-infarction through paracrine factors or neovascularization.[86, 87] It was also shown that stretch-conditioned engineered patches constructed from neonatal rat cells entrapped in a collagen gel limit further LV remodeling and electrically couple to the host myocardium when implanted 14 days post-infarction, with improvements in cardiac function in cases of severe infarctions.[4] However, these functional improvements were limited, and no invasion of donor cells into the host myocardium was reported. The patch to heart size ratio was larger compared to this study, perhaps resulting in benefits through passive or active mechanical affects not seen in this study. Interestingly, no beneficial effects were reported with the administration of collagen-based non-cardiomyocyte patch, whereas a decreased size of infarct and a reduction in LV anterior wall thinning occurred in this study for the fibrin-based CM- patches.

These differences may be attributed to either the patch itself or the timing of treatment.

3.5 Figures and Tables

All figures and tables are adapted from Wendel et al, Tissue Engineering Part A 2014[37]

Table 3.1: Cell Composition in Patches Pre-Implantation

Patch	Cell density (cells/mm^2)	% Live	% CMs	SMA +	CD31+
CM+	1540 ±631	90.1±7.1%	39.1±16.5%	15.2±3.7%	<0.5%
CM-	1030±219	92.7±3.8%	1.8%±1.0%	11.5±14.1%	<0.5%

Table 3.2: Infarct Size and LV Thickness of 4-week implants

Group	Infarct Size	LV anterior wall thickness
Sham (no ligation)	-	2618.9± 221.4μm * #
MI only	61.3 ±7.9 %	661.3 ± 37.4μm
MI + CM- patch	36.9 ±10.2% *	1058.2±135.4μm*
MI + CM+ patch	13.9±10.8% * #	2274.6±37.4μm * #

* p< 0.05 vs. MI only, # p< 0.05 vs CM- patch

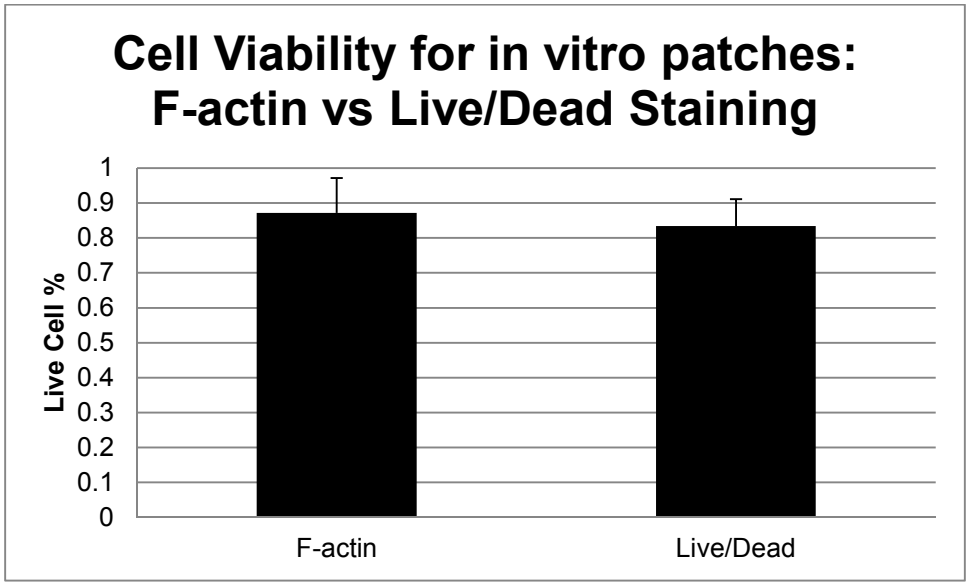

Figure 3.1: Validation of the use of f-actin as a marker for live cells

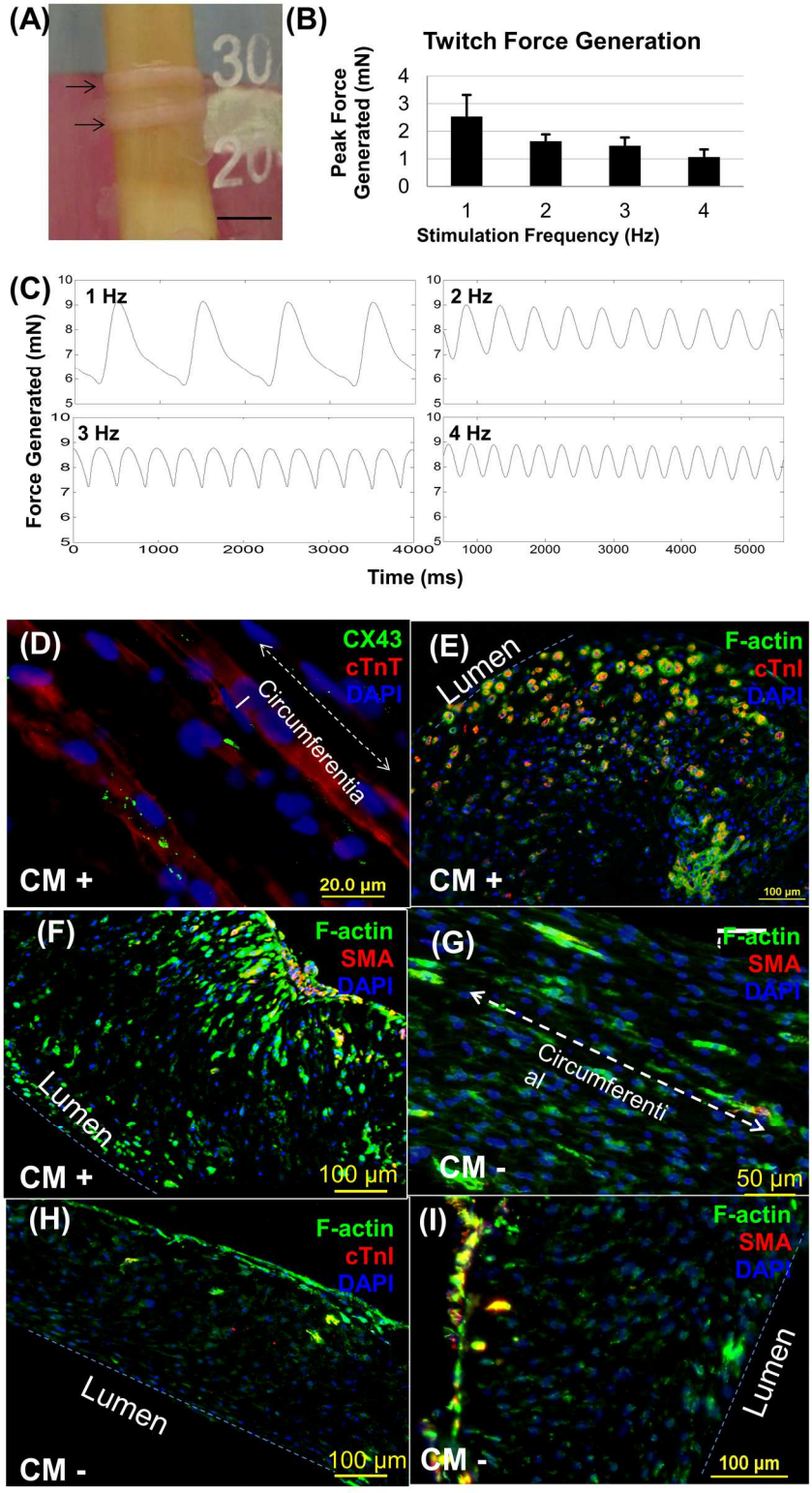
(A)
(B)
Twitch Force Generation
Peak Force Generated (mN)
Stimulation Frequency (Hz)
(C)
1 Hz
2 Hz
3 Hz
4 Hz
Force Generated (mN)
Time (ms)
(D)
CX43
cTnT
DAPI
Circumferential
CM +
20.0 µm
(E)
Lumen
F-actin
cTnI
DAPI
CM +
100 µm
(F)
F-actin
SMA
DAPI
Lumen
CM +
100 µm
(G)
F-actin
SMA
DAPI
Circumferential
CM -
50 µm
(H)
F-actin
cTnI
DAPI
Lumen
CM -
100 µm
(I)
F-actin
SMA
DAPI
Lumen
CM -
100 µm

Figure 3.2: In vitro characterization of cardiac patches: twitch force and cellularity. Ring-shaped patches prior to cutting into strips for implantation were characterized. Top Panels: (A) Two patches on a distensible latex mandrel in the cyclic distension bioreactor. Scale= 5mm. (B-C) Twitch force generation of CM+ patches in response to electrical pacing of variable frequencies. Bottom Panels: Circumferential (D,G) and cross-sectional (EF), (H-I) views of CM+ and CM- patches, showing elongated, aligned cells in each patch (D,G) and cell distribution of both cTnT+ and SMA+ cells in each patch. Few cardiomyocytes were found in the CM- patch, and SMA+ cells were located close to the abluminal surface in both patches.

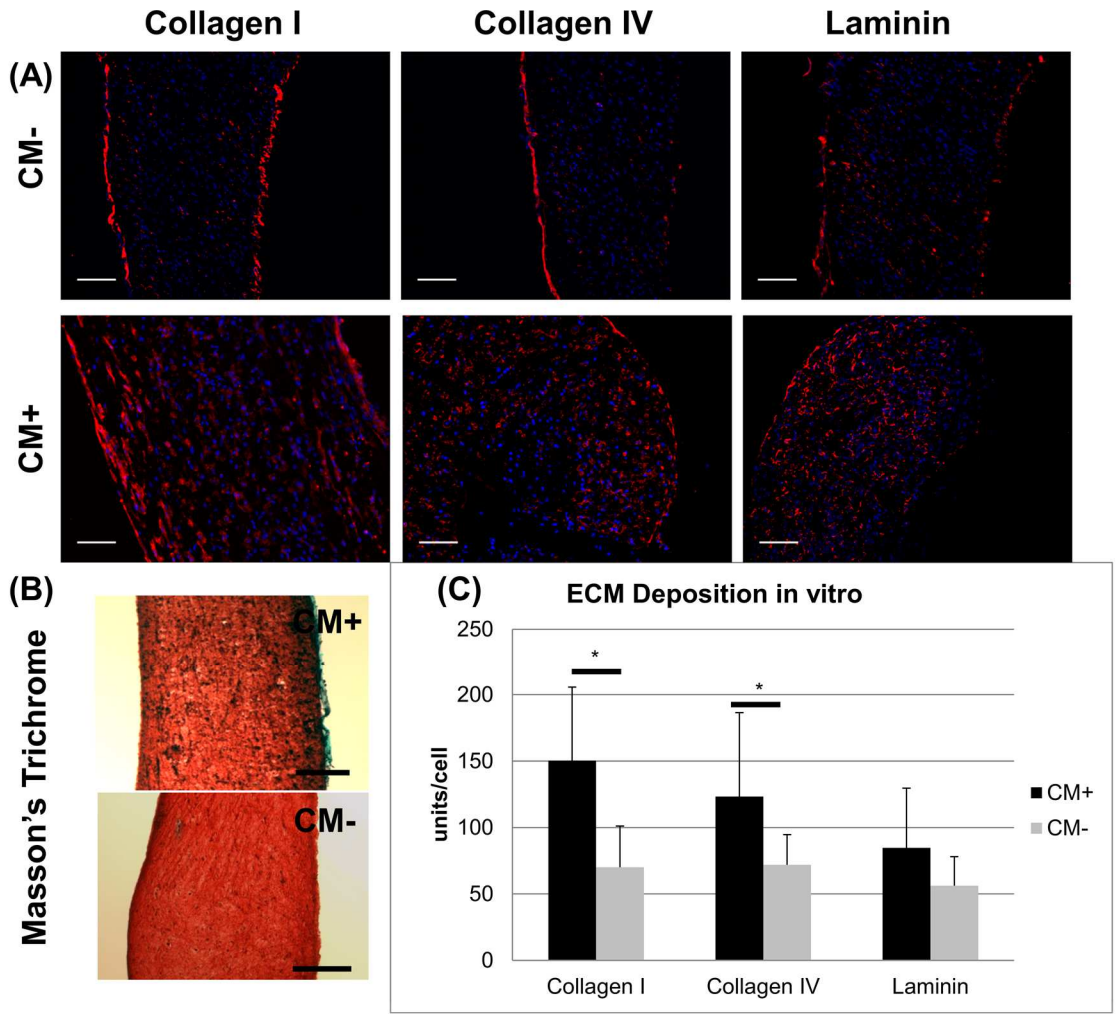

Figure 3.3: In vitro characterization of cardiac patches: ECM deposition. Cellular deposition of collagen I, IV, and laminin was evident after 14 days in vitro culture (A), even though the patch ECM still consisted primarily of fibrin, as seen in Masson's Trichrome images of CM+ and CM- patches (B). Increased deposition of collagen I and IV was found in CM+ patches compared to CM- patches (C), based on quantitative image analysis of staining intensity normalized to cell count. This is evident by the presence of matrix proteins distributed throughout

CM+ patches while ECM deposition in CM- patches was largely limited to the exterior of the patch. *p<0.05.

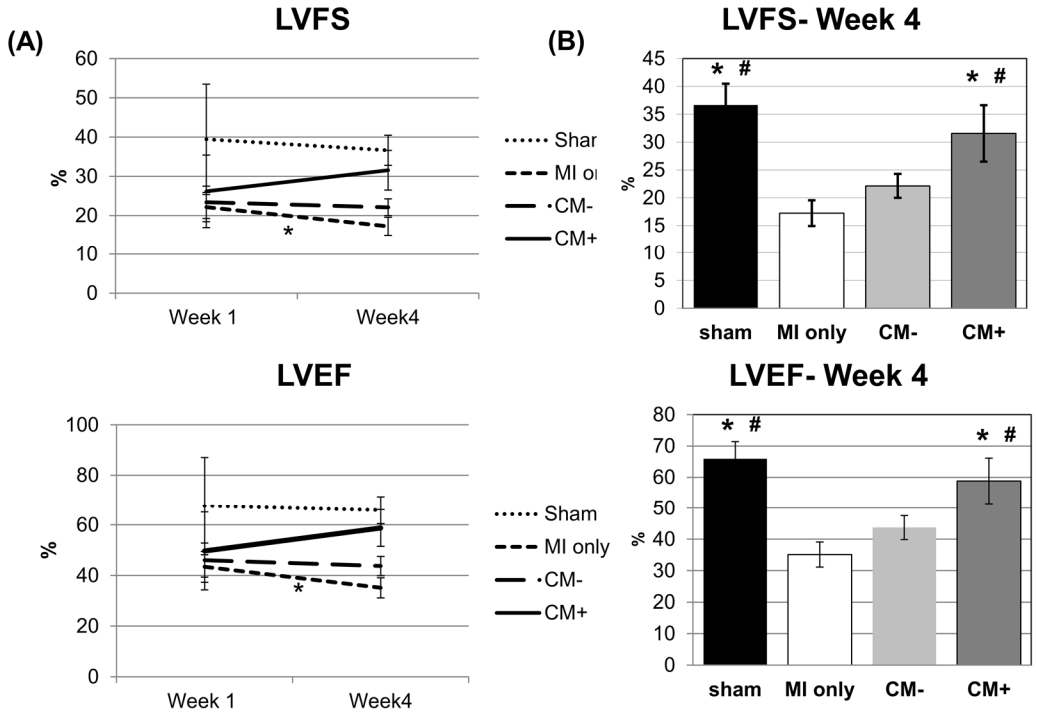

Figure 3.4: Echocardiography results 1 week and 4 weeks post-implantation. A significant reduction in both LVEF and LVFS from 1 week to 4 weeks post-ligation was seen in animals receiving no treatment (A). *p<0.05 Week 4 vs. Week 1. However, substantial improvement over the MI only control and CM- graft in ejection fraction (EF) and fractional shortening (FS) resulted with the application of a CM+ patch by 4 weeks of implantation (B). * p<0.05 vs. MI only. # p<0.05 vs. CM- patch.

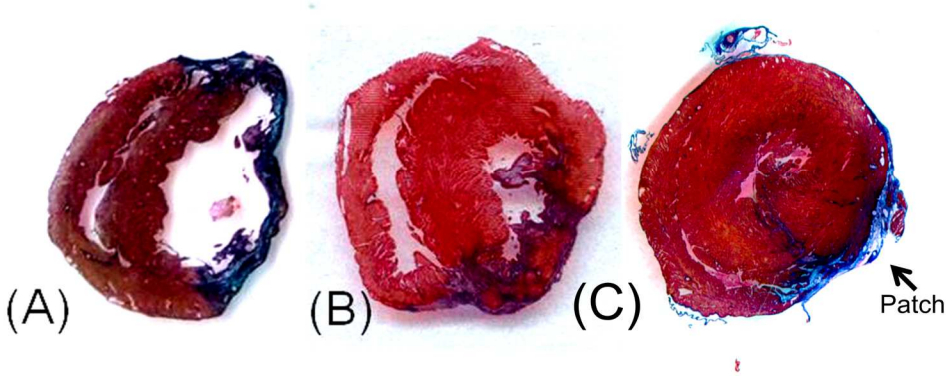

Figure 3.5: Infarct size and LV free wall thickness from coronal sections. Masson's Trichrome image of a MI-only heart (A), and hearts that received a CM- patch (B) and CM+ patch (C). The engrafted patch can be seen as the thin blue layer on the outside of the heart in (C). CM- patches were not easily distinguishable using Trichrome due to large infarct scars.

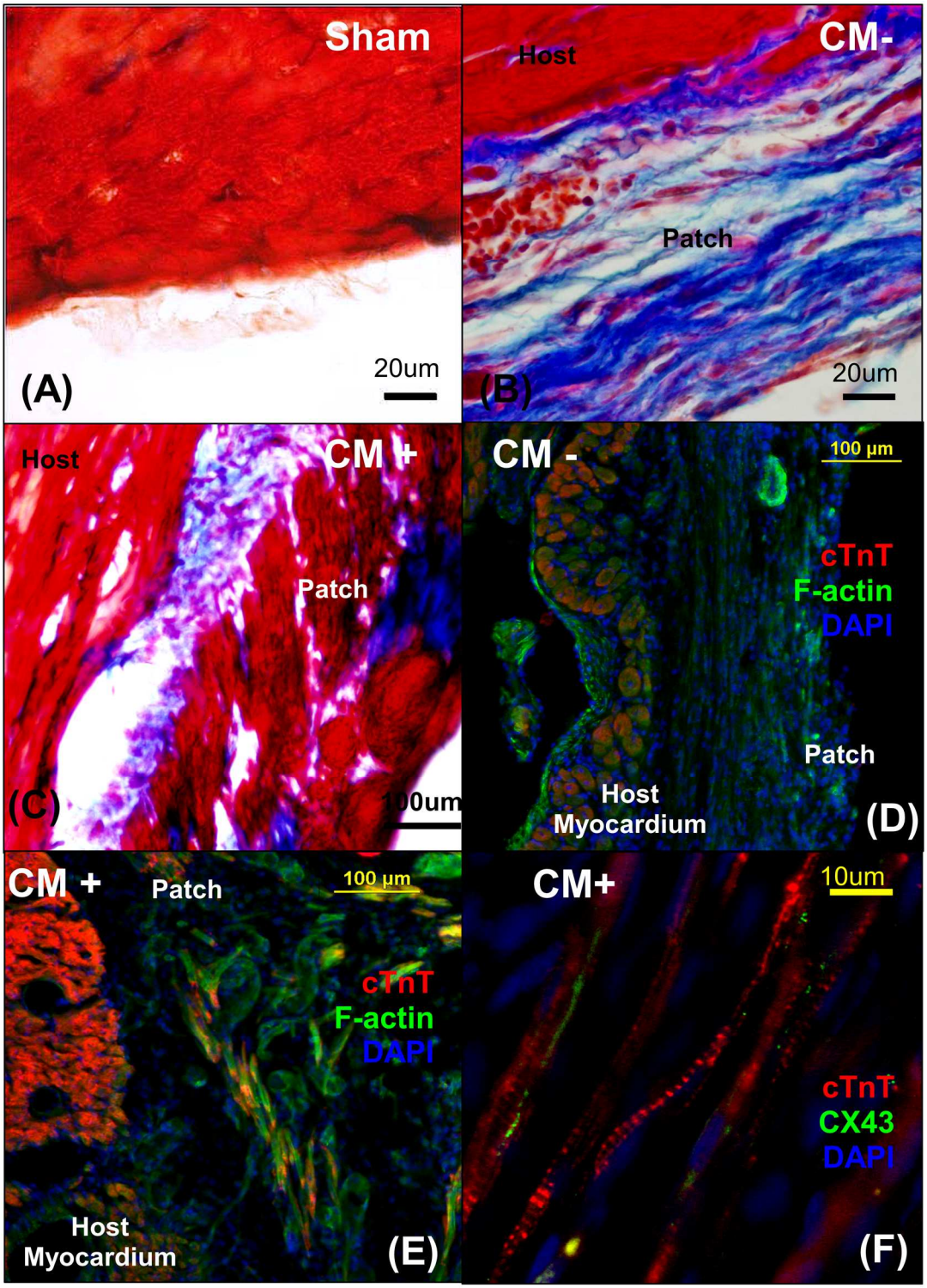

Figure 3.6: Patch Engraftment 4 weeks post-implant.

Massons's Trichrome stained sections of a sham-operated (A), CM- patch (B), and CM+ patch (C) recipient heart, indicating the presence of a remodeled patch affixed to the epicardium (. (D)-(F): Immunohistochemistry of patches. Cardiomyocytes (cTnT+ cells) are present in the engrafted CM+ patch (E), and an absence of cTnT+ cells are visible in the CM- patch (D), along with substantial thinning of the LV free wall. (F) Sarcomeric organization is visible in cardiomyocytes within the engrafted CM+ patch, along with evidence of gap junctions between adjacent CMs within the patch.

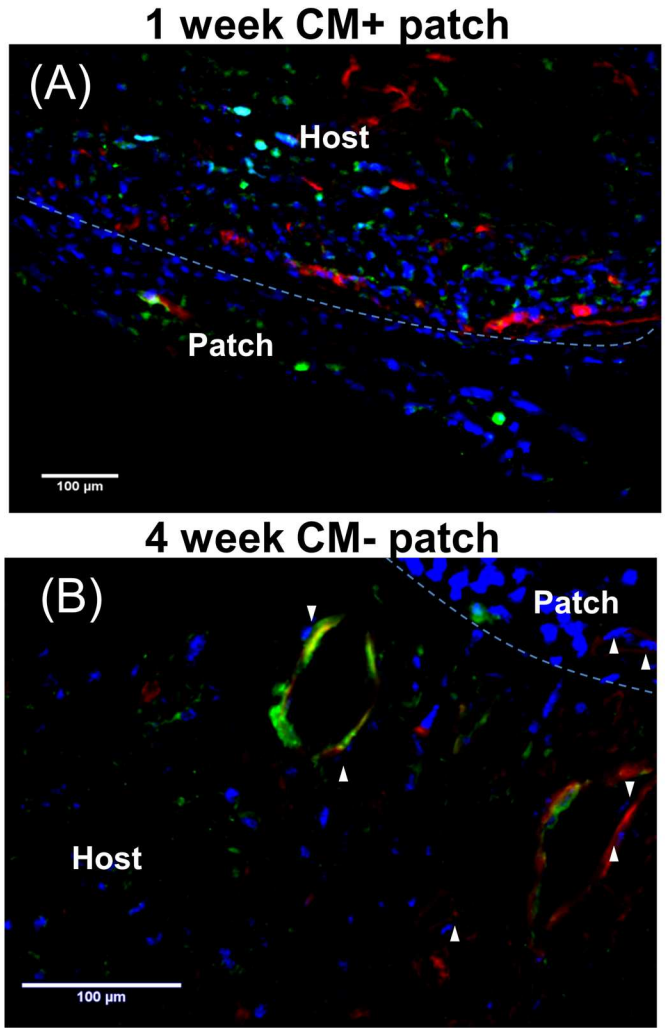

Figure 3.7: Invasion of DAPI pre-labeled cells into host myocardium

Blue = DAPI prelabeled donor cells. Cell invasion occurred for CM+ patches at 1 week (A) and 4 weeks (B) post-implantation. Some of the invading cells were associated with vascular structures within the host myocardium (white arrows).

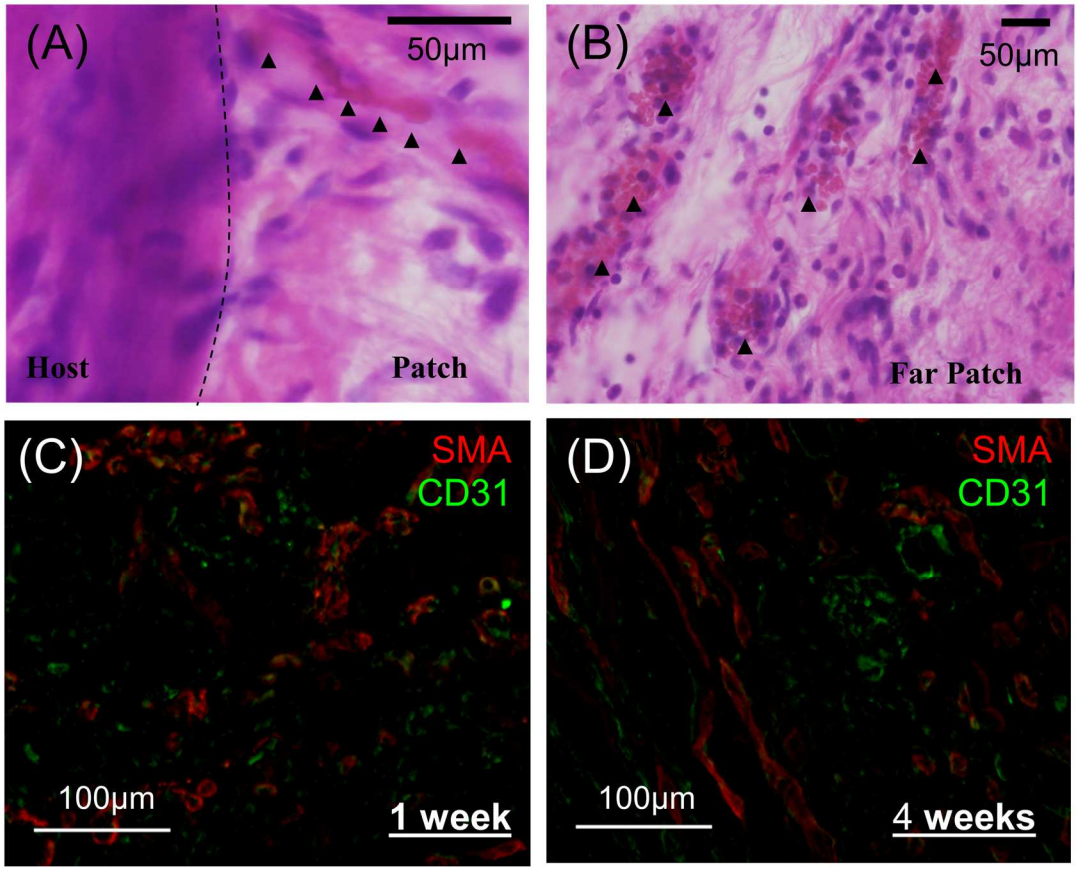

Figure 3.8: Vascularization of the CM+ patch.

Top Panels: H&E of an engrafted CM+ patch after 4 weeks in vivo. Red blood cells, noted by black arrows and indicating perfusion, are visible in the patch-host interface (A) and in the patch itself far (C) from the host myocardium. Bottom Panels: SMA/CD31 staining of engrafted patches both 1 (C) and 4 (D) weeks after implantation, showing both host endothelial cell migration into the patch and the establishment of vessels in the patch.

Chapter 4: The Creation and Optimization of a Tissue-Engineered Cardiac Patch from Human Induced Pluripotent Stem Cell-Derived Cardiomyocytes

Portions of the following chapter along with chapter 5 were adapted from: Wendel, et al*. Functional Effects of a Tissue-Engineered Cardiac Patch from Human Induced Pluripotent Stem Cell-Derived Cardiomyocytes in a Rat Infarct Model*. Stem Cells Translational Medicine. Accepted June 2015

4.1 Introduction

Cardiovascular diseases remain a leading cause of death in the developed world,[94] and despite advances in interventional and pharmacological therapies, these treatments remain largely palliative. In light of these shortcomings, cell-based therapies have become an attractive approach to prevent heart failure post-infarction. Cardiac tissue engineering, which aims to generate functional myocardium *in vitro*, provides a method to deliver cells to the injured myocardium with enhanced cell survival and large graft sizes, enhancing the ability of cells to regenerate myocardium *in vivo* and limit left ventricular remodeling post-infarction. With the discovery of induced pluripotent stem cells (iPSCs)[14] and the ability to differentiate human iPSCs into functional cardiomyocytes (hiPSC-CMs),[15, 95] these cells have become a prime candidate for use in cardiac tissue engineering. First differentiated to cardiomyocytes using the embryoid body method[15], hiPSCs are now differentiated by using a matrix sandwich method[16] or by small molecule methods modulating the Wnt/β-catenin

signaling pathway[17] to provide the high yields of hiPSC-CMs needed for use in engineered cardiac tissues (ECT). These methods have been able to achieve highly variable cardiomyocyte (CM) purities, but for enhanced therapeutic effect or to study the interactions of CMs with a defined population of non-CM cells, further purification may be necessary. Purification of CMs has been achieved through genetic methods utilizing puromycin resistance[96] and non genetic methods such as the use of CM-specific cell surface markers for fluorescence[97-99] and magnetic-activated cell sorting[100], microdissection[101], and targeting metabolic pathways as used in lactate-based purification[102].

While there are numerous studies reported for ECTs constructed using neonatal rat cells[4, 5, 37], there are far fewer made from human pluripotent stem cells. Human embryonic stem cell derived CMs (hESC-CMs) have been entrapped in fibrin-matrigel,[25] collagen-matrigel[10], and gelfoam scaffolds.[58] These studies have shown that the addition of non-CM cell types not only facilitate the compaction of biopolymer hydrogels, but result in improved contractile force generation and survival of entrapped cardiomyocytes.

4.2 Methods

4.2.1 Culture of Human iPSC-Derived Cardiomyocytes

Human iPSC-derived cardiomyocytes were prepared in the lab of Dr. Timothy Kamp at the University of Wisconsin-Madison. The hiPSC line DF19-9-11T[103] was used in this study for cardiomyocyte differentiation. Cells were

differentiated via the small molecule Wnt/GSK3 inhibition (GiWi) protocol,[17] and the purity of cardiomyocytes was measured by flow cytometry for $cTnT^+$ cells at 15 days differentiation. hiPSC-CMs with a purity of 70-95% cTnT+ cells were frozen into cryovials in 90%FBS, 10%DMSO at 10 $x10^6$ cells/vial before shipping. Cells were thawed into T75 flasks coated with 2.5 $\mu g/cm^2$ fibronectin (Sigma-Aldrich) at $10x10^6$ cells/flask. Adherent iPSC-CMs were cultured in EB20 medium (20% FBS, 1% penicillin/streptomycin (Gibco), 0.1 mM nonessential amino acids (NEAA, Gibco), 0.1 mM β-mercaptoethanol (Gibco) in DMEM/F12 Basal Media (Corning)) for 48 hours, and reduced to 2% serum media (EB2) for an additional 24 hours before harvesting for patch creation. Initial studies investigated the use of CMs for casting directly from thaw or cells that had been cultured as above prior to be used for gel creation.

4.2.2 Harvest of hiPSC-CMs for Use in Patch Construction

HiPSC-CMs were harvested for construct preparation by rinsing cells in the flask twice with phosphate-buffered saline (PBS) and then exposing cells to a solution of 0.25% Trypsin (Hyclone) with 2% Chicken Serum (Hyclone) at 37ºC for 5-10 minutes before quenching with EB20 medium. Cells were spun down at 200 x g for 5 minutes at room temperature prior to being counted and resuspended in EB20 medium for patch creation.

4.2.3 Hemispheres for Screening of hiPSC-CM Density and Matrix Formulations

As hiPSC-CMs are not available in the same quantities as neonatal rat cardiomyocytes, small hemispheres were created to screen multiple gel formulations and cell seeding densities while limiting the number of cells used. Hemispheres were created by melting a circular ring into a tissue culture plate using a heated tissue punch. Gel forming solution was dropped into the center of these circular stamps, and gels were allowed to polymerize for 6 minutes at room temperature before being transferred to a 37ºC, 5% CO2 incubator for 15 minutes. After polymerization was complete, EB20 media was added to each well to cover the gel and the gels were returned to the incubator. EB20 media was changed the next day and after 48 hours switched to 2% serum media for the remainder of culture. Hemispheres were cultured and observed daily for a total of 14 days before being fixed in 4% PFA for qualitative histological assessment. In these experiments, 4.5 mm and 6 mm diameter tissue punches were used to create 25 µL and 50 µL hemispheres, respectively, and the gel and cell seeding densities were assessed as displayed in Table 4.1. Media to cell ratios were kept constant to ensure that relative nutrient availability did not affect the results.

4.2.4 Construction and Culture of hiPSC-CM Patches

To quantitatively assess the cellularity and contraction force generation aligned patches containing hiPSC-CMs and to compare them to the previously constructed neonatal rat cell patches, aligned hiPSC-CM patches were constructed nearly identical to the patches constructed in **Chapter 2** by mixing

$2.2x10^6$ CMs with a fibrin-forming solution and injecting it into a 8mm-ID, 1.25 mL tubular mold as previously described[37] to create a final fibrin concentration of 3.3 mg/mL. The cell-containing, fibrin-forming solutions were incubated at 37°C for 15 min to allow formation of a fibrin gel. Gels were then removed from their casings and placed in EB20 culture medium supplemented with 2 mg/mL ACA for the first 48 hours of culture, followed by culture in 2% serum medium for the remaining 12 days culture, 14 days total static culture, with media changes 3 times weekly. $2.2x10^6$ CMs were chosen to put into these patches in order to match the input number of cardiomyocytes to that of the rat patches constructed in chapter 2 and chapter 3.

4.2.6 Purification of hiPSC-CMs

hiPSC-CMs used in these studies were received with CM fractions ranging from 70-95% cTnT+ cells. The remaining 5-30% of cells in these preparations is comprised of primarily fibroblast-like cells that remain poorly characterized to date. Little has been reported on the non-CMs in CM preparations from pluripotent stem cells, these cells have been reported to express one or multiple of the following proteins: VE-Cadherin, PDGFRb, Vimentin, VonWillebrand Factor, SM22α, and TRA-1-160, a marker for undifferentiated cells[25, 104]. Thus, for experimental consistency and quality control purposes, obtaining a cell population of cardiomyocytes with maximal purity is necessary.

4.2.6.1 CM Purification through Pre-plating

The use of pre-plating has been widely used with neonatal rat cells to select for cardiomyocytes. Pre-plating functions based on differential adhesion- the fact that some cell types (in this instance cardiomyocytes) take longer to settle and adhere to substrates than others (in this instance fibroblasts and other interstitial cardiac cells). Thus, allowing a cell suspension to settle and begin adhering for a short period of time before removing the supernatant and re-plating the cells into a new container will theoretically separate a large number of non-cardiomyocytes from the cardiomyocyte cell population. Two variables were assessed to optimize the pre-plating procedure for selection of hiPSC-CMs: length of time cells are allowed to adhere to the initial substrate prior to removing the supernatant, and the protein coating on the preplating substrate. Unlike neonatal rat cardiomyocytes, hiPSC-CMs require a protein coating to support cell adhesion to tissue culture plastic. The following combinations of variables were assessed:

Pre-plating incubation time:

- 20, 40, 60, 80, 120, 180, and 240 minutes

Protein Coating on pre-plating surface:

- Fibronectin, Gelatin Collagen I, and Tissue culture plastic

Cells were plated from thaw into either 6 or 24 well plates in EB20 media. Fibronectin wells were coated with 2.5 μg/cm^2 of fibronectin for 1 hour at room

temperature, and gelatin wells were coated with 1 mg/mL gelatin for 10 minutes at room temperature prior to seeding cells. Collagen-I coated wells were incubated overnight in 0.05mg/mL collagen I at 37ºC and then rinsed twice with Hank's Buffered Saline Solution (HBSS) prior to seeding cells. Cells were then allowed to adhere for the allotted amount of time before the supernatant was removed and placed into an adjacent well. Fresh EB20 was then added to the preplate wells and all cells were allowed to adhere and culture for 24 hours prior to being fixed in 4% paraformaldehyde (PFA) for histological assessment of CM purity.

CM purity was assessed by staining cells in all wells for DAPI, f-actin (all cells) , and cTnT (cardiomyocytes). A custom matlab code was then used to import images and count he numbers of the designated cell types in each image. At least 9 images were acquired for each condition and averaged to obtain an overall CM%. Additional information on the cell-counting matlab code can be found in Appendix 2.

4.2.6.2 CM Purification through the Targeting of Metabolic Pathways Utilizing Lactic Acid

As an alternative method to pre-plating, cardiomyocytes were purified using a lactate-based selection media targeting the differing metabolic pathways of fibroblast-like cells, which rely on glycolysis, and cardiomyocytes, which can utilize both glycolysis and oxidative phosphorylation for energy metabolism.

Based on previous work[102] and a protocol obtained from the Healy lab at the University of California-Berkley, the use of lactate-supplemented glucose-free media was investigated as a means to select for cardiomyocytes.

Prior to exposing hiPSC-CMs to the lactate selection media, the optimal conditions for eliminating non-cardiomyocytes were assessed by treating human pericytes (PCs), ovine dermal fibroblasts (ODFs), and neonatal human dermal fibroblasts (NHDFs) to various media compositions to ascertain the formulation that will eliminate non-cardiomyocytes while minimize the stress upon remaining cardiomyocytes. An initial experiment was conducted with ODFs and PCs and a follow up study was run with NHDFs. The following conditions were investigated in a lactate media consisting of glucose-free DMEM (Invitrogen), penicillin/streptomycin, NEAA, β-mercaptoethanol, and the following:

ODFs and PCs:

- 1mM or 4mM lactic acid (Sigma-Aldrich, stock diluted to 1M in HEPES)
- 0% or 2% FBS. Serum contains an undetermined amount of glucose, which may or may not provide enough nutrients to sustain non-cardiomyocytes in culture.

NHDFs:

- 1 mM or 4 mM lactic acid
- 0 mM or 1 mM NEAA

Cells were plated to be confluent and allowed to culture in their respective culture

medias 24h prior to exposure to the test medias. Cells were imaged daily with a phase contrast inverted microscope until significant cell death was observed or 7 days passed.

Once the media conditions were assessed with non-cardiomyocyte cells, the candidate media formulations were used with hiPSC-CMs. The candidate media formulation used in this experiment consisted of DMEM no glucose, 0% serum, 1 penicillin/streptomycin, 0.1mM NEAA, 0.1mM β-mercaptoethanol, and 4mM lactic acid. hiPSC-CMs were plated into 48 well plates coated in 2.5 ug/cm2, per the standard thaw and culture protocol in EB20 media. Cells were maintained in EB20 until day 3 of culture, at which they were switched to a 2% serum media for 24 hours before being switched to the treatment lactate media. Lactate media was changed every 2 days, and at every change cells were rinsed with PBS twice before adding new media. Cells were cultured in lactate media for 2, 4, 6, or 7 days before being fixed for immunofluorescent staining and imaging to assess CM% at each time point.

After the optimal media formulation and exposure time were obtained for maximum hiPSC-CM purity, a comparison of purified and unpurified hiPSC-CMs was conducted to assess any potential changes to the cell phenotype as a result of lactate treatment. For comparison of unpurified and purified hiPSC-CMs, cells were seeded directly from thaw into 24 well plates coated with 2.5μg/cm^2

fibronectin at a density of $1x10^5$ cells/cm^2. Adherent hiPSC-CMs were cultured in EB20 medium for 48 hours, and reduced to 2% serum media (EB2) for an additional 24 hours. On day 4 of culture, half of the cells were exposed to lactate media and the remaining wells were maintained in EB2 media. Cells were exposed to either lactate or EB2 media for 4 days, two total media changes, before being returned to EB2 media on day 8 of culture. Cells were cultured for an additional 3 days in EB2 media before being harvested for protein analysis.

4.2.6 Co- entrapment of Purified hiPSC-CMs with PCs

As cardiomyocytes have been shown to exhibit increased survival and contractile force generation when co-entrapped with non-cardiomyocyte support cells, and non-CMs are necessary to induce compaction of the fibrin gel, which is essential to concentrate and align CMs,[37] we investigated the use of utilizing pericytes (PCs) as a support cell for cardiomyocytes. PCs were chosen with respect to future strategies to include preformed microvessels created with PCs and endothelial cells in gels along with hiPSC-CMs.

GFP-labeled human brain pericytes were obtained from the lab of Dr. George Davis at the University of Missouri-Columbia, and were previously characterized to express nuclear GFP.[28] Pericytes were cultured for 10 days on gelatin coated flasks in culture media consisting of DMEM low-glucose (Gibco), supplemented with 10% FBS, 1% penicillin/streptomycin and 0.01mg/mL

gentamycin (Gibco). Pericytes were harvested by exposing cells to a solution of 0.05% Trypsin EDTA (Hyclone) for 5 minutes before quenching with FBS.

For initial experiments to validate whether or not hiPSC-CMs and PC can be co-entrapped together, 50 µL hemispheres similar to those constructed with hiPSC-CMs alone were created with 3.3mg/mL fibrinogen, the same seeding density of CMs ($2.2x10^6$ CMs/mL), and either 1.5, 1.0 or 0.5 $x10^6$ PCs/mL. Hemispheres were cultured in CM media (EB20, EB2) supplemented with ACA for 14 days static culture prior to harvest for histological assessment of cell morphology.

4.2.7 Statistical Analysis

Data are presented as means ± standard deviations. All results were analyzed using Microsoft Excel or MiniTab statistical software. Student's t-tests and one-way analysis of variance (ANOVA) in conjunction with Tukey HSD post hoc testing was used to compare all groups. p-values <0.05 were considered significant.

4.3 Results

4.3.1 Preferential CM morphology and Cell Distribution with Pre-Cultured CMs

Two methods of hiPSC-CM culture were used in preliminary studies entrapping hiPSC-CMs in fibrin: entrapping CMs directly after thaw or pre-

culturing CMs for 72-96 hours prior to harvesting for patch construction. At thaw, CMs had on average X% viability, but fewer than 20% of the cells remained viable in the long-term and successfully adhered to the fibronectin-coated T75 flasks. Although there was significant cell loss with pre-culture, patches these cells largely remained viable after entrapment in fibrin, exhibiting spread morphologies and resulting in patches that generated visible contractions. However, when patches were created with cells directly from thaw, the vast majority of the cells that survived entrapment retained small, rounded morphologies and resultant patches contained a large amount of cellular debris with minimal to no visible contractions. Thus, for all successive experiments, hiPSC-CMs were pre-cultured in flasks prior to use for patch construction.

4.3.2 hiPSC-CM Patches Exhibit Similar Cell Densities to Neonatal Rat Cell Patches But With Decreased Contractile Force Generation

hiPSC-CMs remained viable and exhibited elongated morphologies in all gel formulations and cell seeding densities investigated (data not shown). However, gels cast at low fibrinogen concentrations (1.5, 2.0 mg/mL) resulted in gels that were qualitatively less dense and more fragile than those fabricated with higher fibrinogen concentrations, limiting these tissues ability to be feasibly handled and sutured for transplantation. Due to these results and to best facilitate a comparison between the characteristics of hiPSC-CM and neonatal rat

cell patches, all future hiPSC-CM patches were fabricated at a fibrinogen concentration of 3.3 mg/mL.

Rings created using hiPSC-CMs compacted similarly to neonatal rat cell patches, resulting in a tissue approximately 3mm wide and 400 um thick, compared to the approximate dimensions of the neonatal rat cell patches of 3mm wide and 550 um thick. Cross-sectional CM densities after 14 days in vitro culture (cTnT+/DAPI+ cells) were not significantly different between hiPSC-CM and neonatal rat cell patches (Figure 4.1) and cells were elongated and aligned in the circumferential direction (Figure 4.2) in both cases. At higher magnification, it was observed that many hiPSC-CMs were either multi-nucleated and/or clumped together in long, elongated strands rather than existing as single elongated cardiomyocytes (Figure 4.3) As it was not easy to distinguish the boundaries between CMs, it cannot be determined to what degree these structures are multinucleated and multicellular. Interestingly, although there was a widely observed decrease in cell and CM density towards the center of patches and CM concentration in regions along the edges of patches made with neonatal rat cells (Figure 4.2, Figure 3.1 b, c), CM distribution was relatively uniform across all dimensions of hiPSC-CM patches, negating any further need for patch optimization to attain uniform cell density.

hiPSC-CM patches generated measurable forces both spontaneously and in response to pacing frequencies between 0.5 and 1.5 Hz, with a maximum

average force generation of 0.46 mN/ ring (0.2nN/ input CM) at 0.5 Hz pacing frequency (Figure 4.4). Patches were not able to respond synchronously to pacing above 1.5 Hz. These values are significantly lower than those obtained for neonatal rat cell patches, and could be due to the differing species and maturation states of these cells, as hiPSC-CMs are widely considered to be more immature than neonatal cell phenotypes[105]. More on cell maturity can be found in Chapter 6. This decrease in overall force generation may likely also be due to non-optimal gel and culture conditions for hiPSC-CMs, as these studies are all preliminary.

4.3.3 Efficient Purification of hiPSC-CMs is achieved With Lactate- Based Selection Media

Two methods of CM purification were investigated with hiPSC-CMs, differential adhesion via pre-plating and a lactic acid supplemented selection media. Through preplating, the combinations of different pre-plating incubation times and substrate protein coatings were utilized to optimize this process for maximal CM capture. The percentages of adhered CMs in all conditions can be found in Table 4.2. In summary, it was found that there is no difference in adhesion time for CMs and non-CMs in hiPSC-CM cell populations, and short-term adhesion was not altered by the presence of any protein coating. As expected, cells adhesion was substantially reduced after 24 hours in well that

had no protein coating (data not shown). Thus, pre-plating is not a reliable method to select for hiPSC-CMs.

In the optimization process for a lactate-based selection media, it was found that the concentration of lactic acid (1 mM vs. 4mM) had no effect on the cell death timeline of the non-cardiomyocyte cells evaluated (Table 4.3), but the addition of 2% serum with daily media changes provided enough glucose to sustain cells indefinitely. In the absence of serum, ODFs began to die after 5-6 days of glucose and serum deprivation; PCs began to die after 4 days and were completely eliminated by day 6 of exposure; and cell death was induced in NHDFs by day 2 of exposure and cells were completely eliminated by day 3-4. Additionally, the addition or withdrawal of NEAA had no effect on the results obtained with NHDFs.

Based on these results, two candidate selection mediums were chosen to use with hiPSC-CMs: both contained DMEM no glucose, NEAA, β-mercaptoethanol, and penicillin/streptomycin, and 4mM lactic acid. As the concentration of lactic acid had no effect on non-myocyte death, the higher concentration was used in hiPSC-CM studies. The only difference between treatment groups was the addition of supplemental L-glutamine and media changes every 2 days, based on an existing protocol form the lab of Kevin Healy at UC-Berkley, and a protocol based on the initial non-CM experiments without supplemental L-glutamine and daily media changes. After 2 days culture, Lactate

media with daily media changes has a significantly higher CM fraction than control cells (Figure 4.5, 4.6), and by day 4 both treatment groups contained ~95% CMs while control cells remained ~80% cTnT+. CM purity reached 97-98% after day 6-7 in culture, but significant cell loss of both CMs and non-CMs alike began after 5 days in lactate media. Interestingly, although the purification process was begun on day 4 of culture when CMs had not yet resumed beating after thaw, CMs began beating on average at day 2 of lactate treatment, approximately the same time point in which cells cultured in control media began to beat. Additionally, in later studies in which hiPSC-CMs were returned to their normal culture media after 4 days of lactate media, there appeared to be no overall loss in confluency or expected cell yield (~20% of cells that were thawed), indicating that CMs enlarged in culture to occupy the space left by eliminated non-CMs and may potentially have expanded to some degree, though no evidence has been found to support the latter hypothesis to date.

Thus, it was concluded that a lactic acid supplemented culture media was an effective and efficient method to purify hiPSC-CMs. Due to the similar results of both treatment groups, the lactate media with media changes every 2 days was chosen for use in future studies to maximize cell culture efficiency.

4.3.4 hiPSC-CMs Can Be Successfully Co-Entrapped With PCs in Fibrin Gels

Pericytes were chosen to replace the poorly characterized non-CM population eliminated from the hiPSC-CM population through purification, acting as a support cell type to CMs and as a contractile cell type to compact and align the fibrin into a tissue. PCs added at 0.5, 1.0, or 1.5 x 10^5 cells/mL to 50 µl hemispheres led to gel compaction in all cases, and did not qualitatively affect CM survival or morphology (Figure 4.7 a-c). All hemispheres contained hiPSC-CMs with spread morphologies and visible striations (Figure 4.7 d) and macroscopic beating was observed in all experimental groups (data not shown). These results indicate that not only can pericytes serve as a support cell type to contract the gel and facilitate CM beating, but that the hiPSC-CM purification process does not negatively affect the ability of hiPSC-CMs to survive and beat after entrapment.

4.4 Discussion

In this chapter, we established that pre-cultured hiPSC-CMs can be entrapped in a fibrin matrix and result in a compacted, aligned tissue that generates measurable contractile forces. Through this process, we found that when seeded at similar densities to the neonatal rat cell patches in Chapter 2, the final CM density in hiPSC-CM patches were similar to the CM densities in neonatal rat cell patches, but with reduced CM elongation and substantially reduced contractile force generation. This difference in CM morphology and force generation may likely due to the relatively immature phenotype of the hiPSC-

CMs used in this work[16], and further optimization of these patches is needed in the future to maximize force generation of these CM in their current maturation state, as the contractile forces generated in this work are not only lower than what has been achieved with our neonatal rat cell patches, but is also lower than similar patches made by other groups (Figure 4.8). Further optimization may be conducted to induce some degree of cell maturation *in vitro*, which may result in increased cell elongation and increased force generation, as physiological hypertrophy is an effect of cell maturation[105]. However, maturation of hiPSC-CMs *in vitro* has not proven to be an easy task, and is elaborated upon in Chapter 6.

It was additionally found that hiPSC-CMs can be efficiently and consistently purified to 95% cTnT+ cells after 4 days of exposure to glucose-free, serum-free media supplemented with 4mM lactic acid. Purification of hiPSC-CMs is necessary for experimental consistency, as different preparation of hiPSC-CMs have purities ranging from 70%-90% cTnT+ cells, as well as to limit potential variability and contributing effects of the poorly characterized non-CMs in the hiPSC-CM preps. These purified hiPSC-CMs were subsequentially co-entrapped with PCs, a cell type that has been characterized in the literature[28, 106-108], to enable patch compaction and act as a support cell to the hiPSC-CMs. Future work featured in Chapter 5 will assess the capacity of these purified hiPSC-CM + PC patches to engraft and survive *in vivo*, as well as their effect on left ventricular remodeling post-infarction.

4.5 Figures and Tables

Table 4.1: Experimental Design of Preliminary Hemisphere Experiments

	Fibrinogen Concentration (mg/mL)			
	1.5	2	3.3	4
hiPSC-CM Seeding Density (M/mL) 4	$2x10^5$ cells, 0.85 mL media	$2x10^5$ cells, 0.85 mL media	$2x10^5$ cells, 0.85mL media	$2x10^5$ cells, 0.85mL media
6	$3x10^5$ cells, 1.25mL media	$3x10^5$ cells, 1.25mL media	$3x10^5$ cells, 1.25mL media	$3x10^5$ cells, 1.25mL media
8	$4x10^5$ cells, 1.7 mL media	$4x10^5$ cells, 1.7 mL media	$4x10^5$ cells, 1.7 mL media	$4x10^5$ cells, 1.7 mL media

Table 4.2: CM fractions, Pre-Plating Experiments

Pre-Plate Wells

	Fibronectin						
	20 min	40 min	60 min	80 min	120 min	180 min	240 min
avg	0.66	0.73	0.68	0.76	0.66	0.69	0.69
stdev	0.05	0.04	0.02	0.03	0.04	0.08	0.06
	Gelatin						
	20 min	40 min	60 min	80 min	120 min	180 min	240 min
avg	0.74	0.82	0.79	0.82	-	-	-
stdev	0.11	0.01	0.03	0.01	-	-	-
	Collagen I						
	20 min	40 min	60 min	80 min	120 min	180 min	240 min
avg		0.76	0.73	0.77	-	-	-
stdev	0.01	0.10	0.16	0.07	-	-	-
	Tissue Culture Plastic						
	20 min	40 min	60 min	80 min	120 min	180 min	240 min

avg	0.67	0.65	0.70	0.71	-	-	-
stdev	0.07	0.07	0.04	0.05	-	-	-

Supernatant Wells

	Fibronectin						
	20 min	40 min	60 min	80 min	120 min	180 min	240 min
avg	0.65	0.34	0.42	0.45	0.20	0.45	0.39
stdev	0.13	0.16	0.30	0.25	0.55	0.50	0.18
	Gelatin						
	20 min	40 min	60 min	80 min	120 min	180 min	240 min
avg	0.44	0.23	0.23	0.20	-	-	-
stdev	0.17	0.15	0.10	0.19	-	-	-
	Collagen I						
	20 min	40 min	60 min	80 min	120 min	180 min	240 min
avg	0.53	0.24	0.43	0.36	-	-	-
stdev	0.04	-	0.20	0.11	-	-	-
	Tissue Culture Plastic						
	20 min	40 min	60 min	80 min	120 min	180 min	240 min
avg	0.58	0.45	0.30	0.31	-	-	-
stdev	0.07	0.10	0.15	0.08	-	-	-

Table 4.3: Time to Cell Death for non-CM Cell Types in Lactate (LA) Selection Media

	Time to Cell Death (Days)					
	ODF		PC		NHDF	
	start	complete	start	complete	start	complete
1mM LA, no serum	5	-	4	6	2	3
1mM LA, 2% Serum	n/a	n/a	n/a	n/a	n/a	n/a
4mM LA, no serum	6	-	4	6	3	4

4mM LA, 2% serum	n/a	n/a	n/a	n/a	n/a	n/a

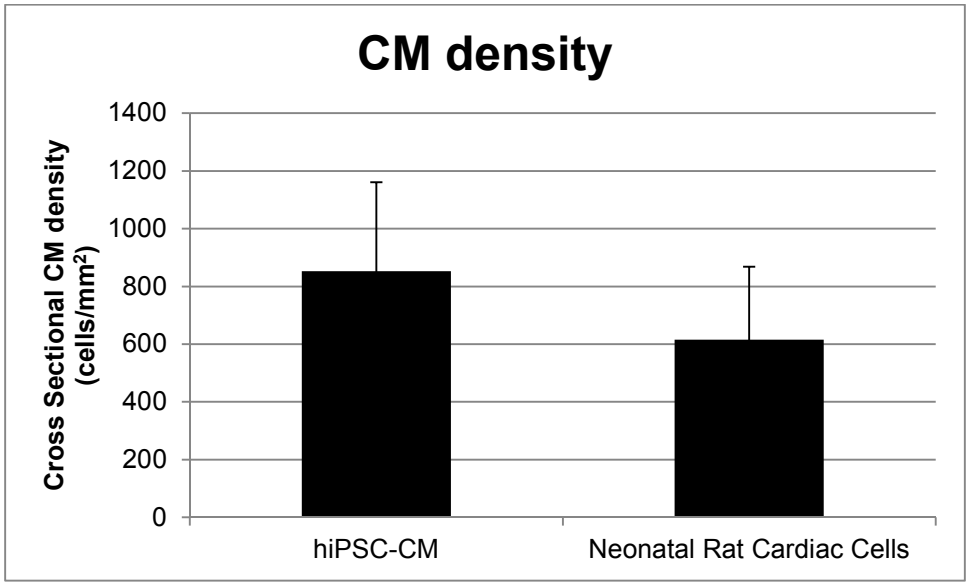

Figure 4.1: Cardiomyocyte (CM, cTnT+) cross-sectional density of patches created with hiPSC-CMs or neonatal rat cardiac cells. No significant difference in CM density was found

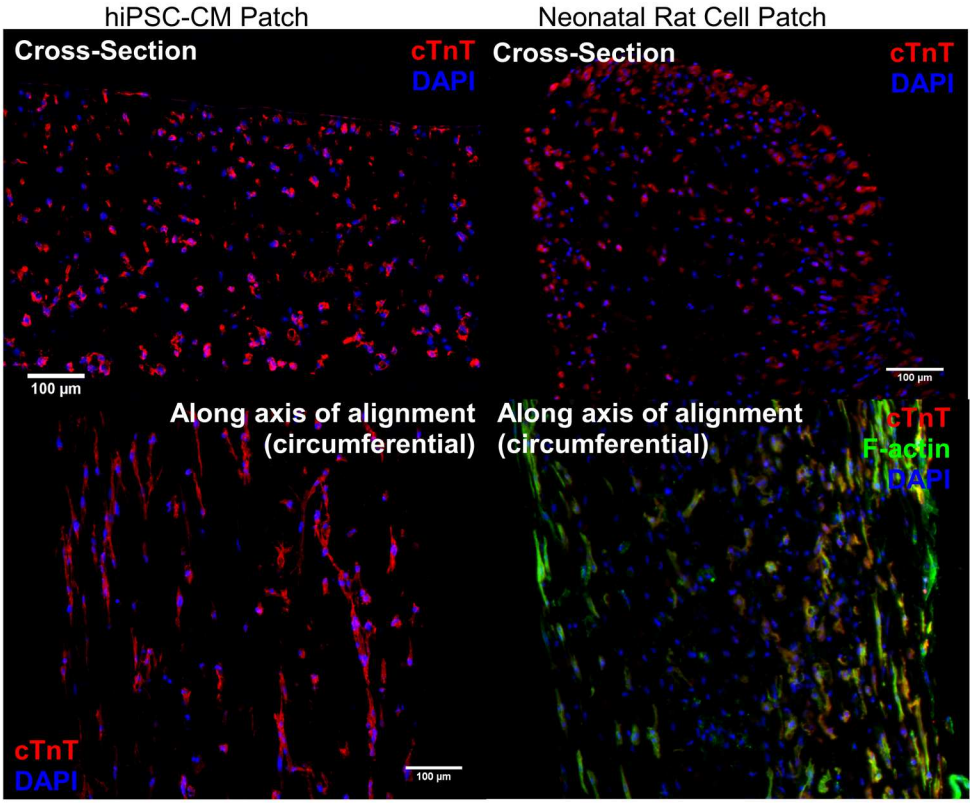

Figure 4.2: Histological comparison of ring patches constructed with hiPSC-CMs (left panels) and neonatal rat cardiac cells (right panels), showing circumferential alignment (bottom panels) of both cell types and uniform CM distribution of hiPSC-CMs in patch (top left).

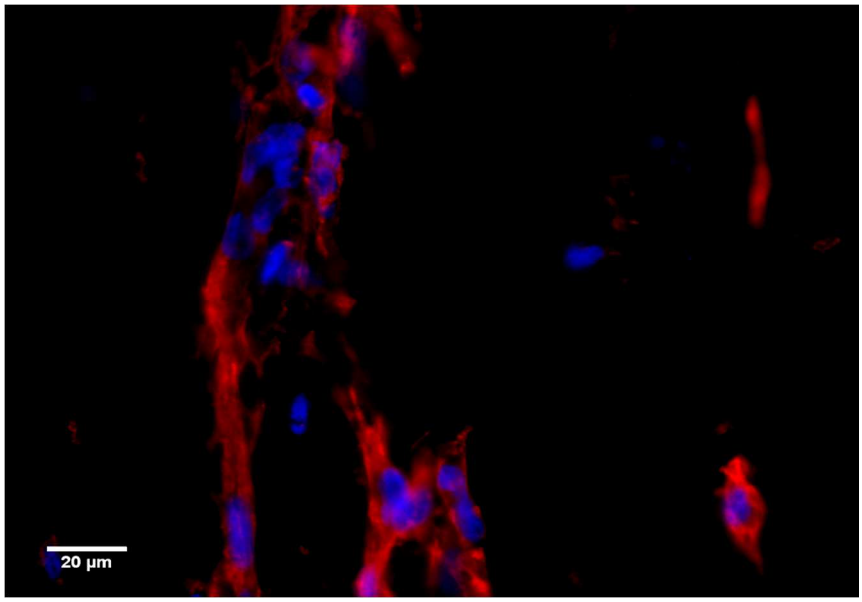

Figure 4.3: High Magnification View of elongated CMs in hiPSC-CM ring patch showing clustering of nuclei in CMs.

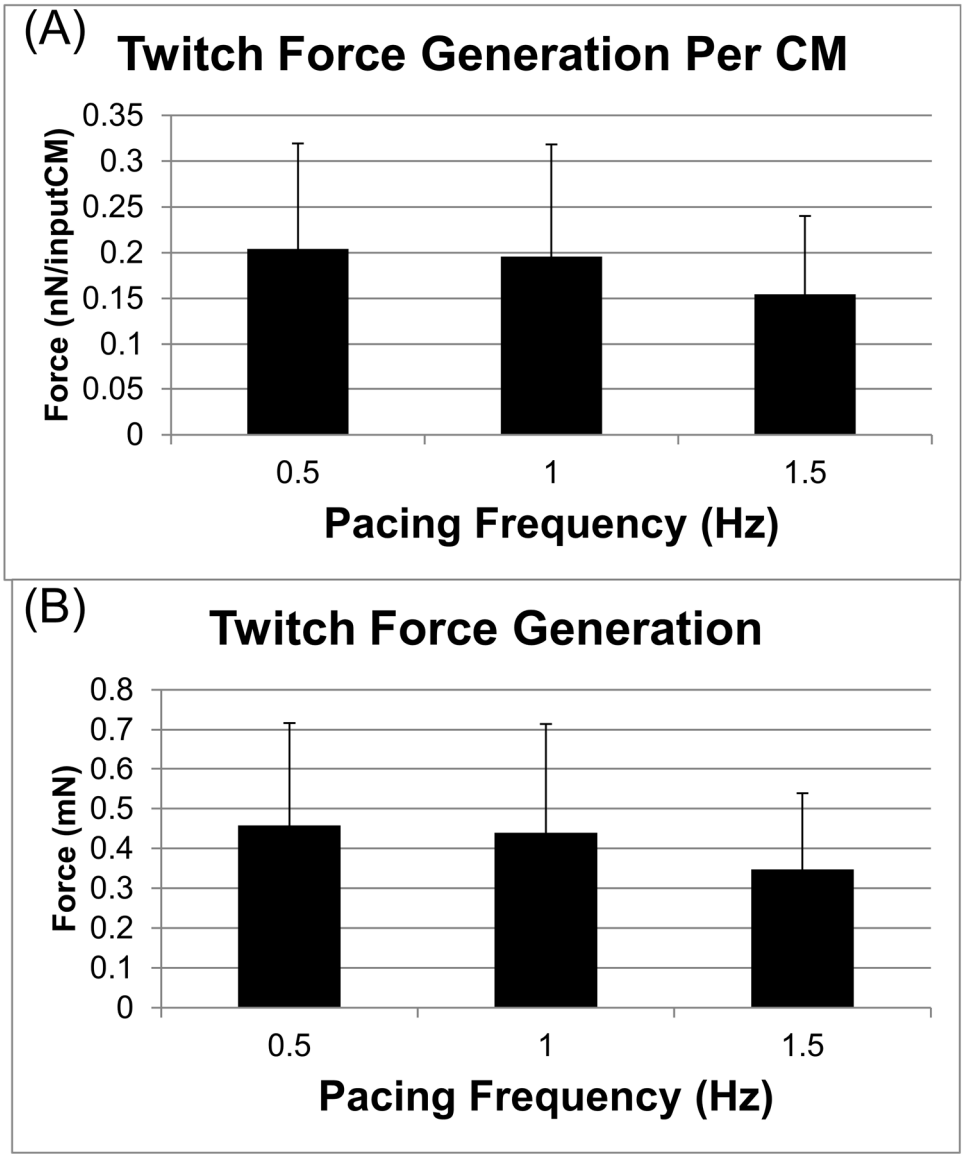

Figure 4.4 (continued on p 88)

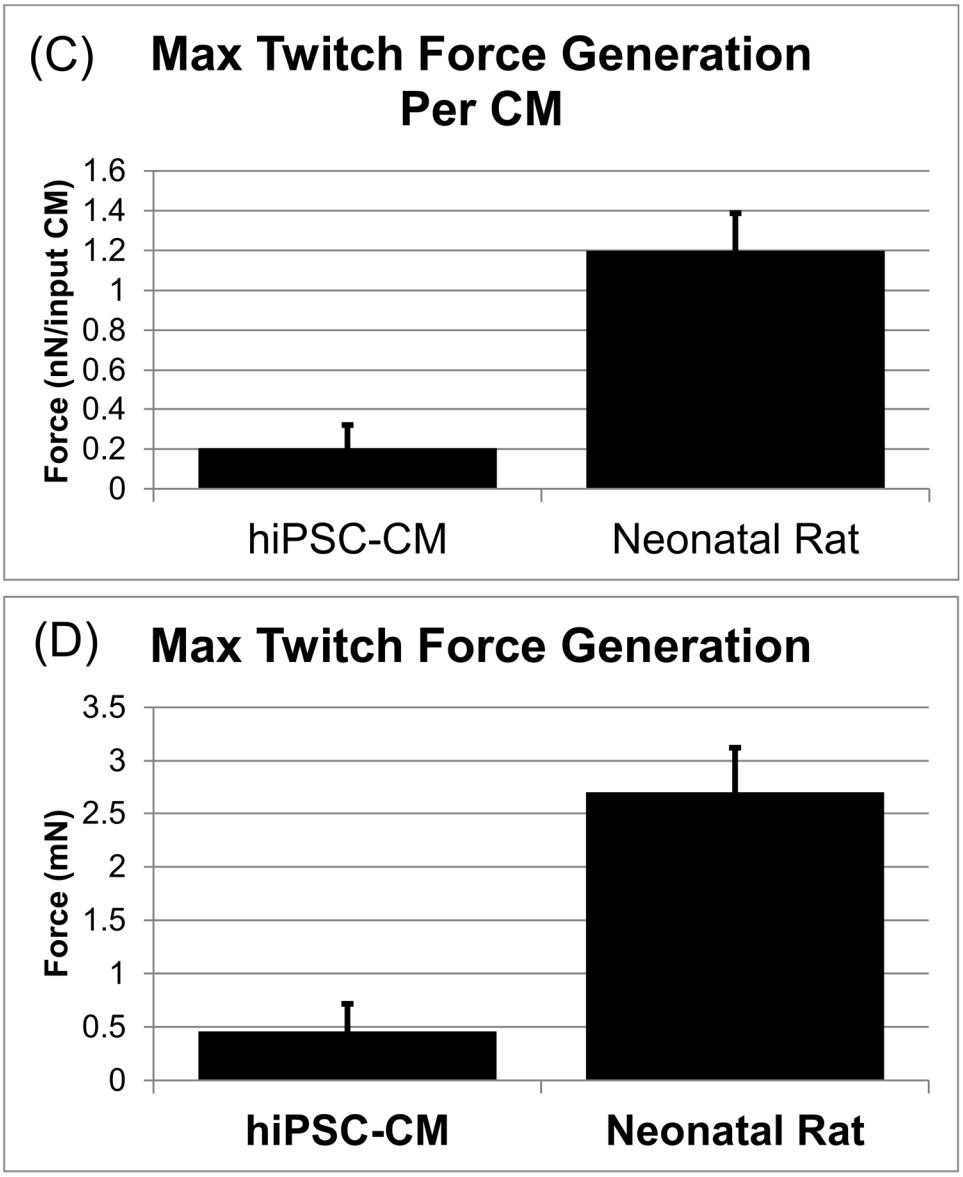

Figure 4.4: Contraction Force (Twitch Force) Generation of hiPSC-CM patches (A-B) and in comparison to similar patches constructed with neonatal rat cardiac cells (C-D).

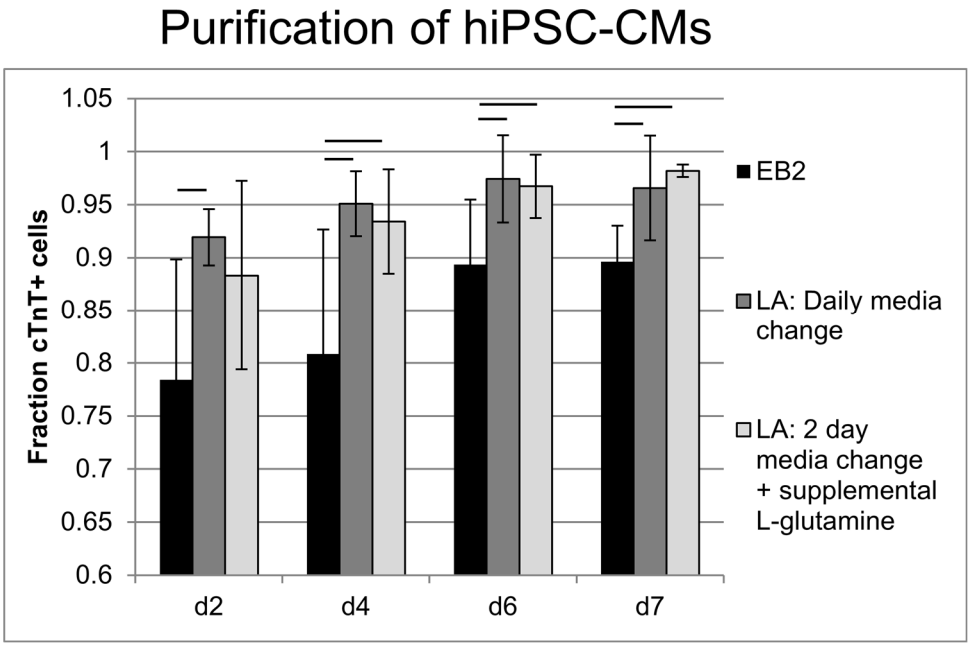

Figure 4.5: CM Purity (fraction cTnT+) after 2, 4, 6, or 7 days of exposure to Lactic acid (LA) media. Significance bars: $p < 0.05$.

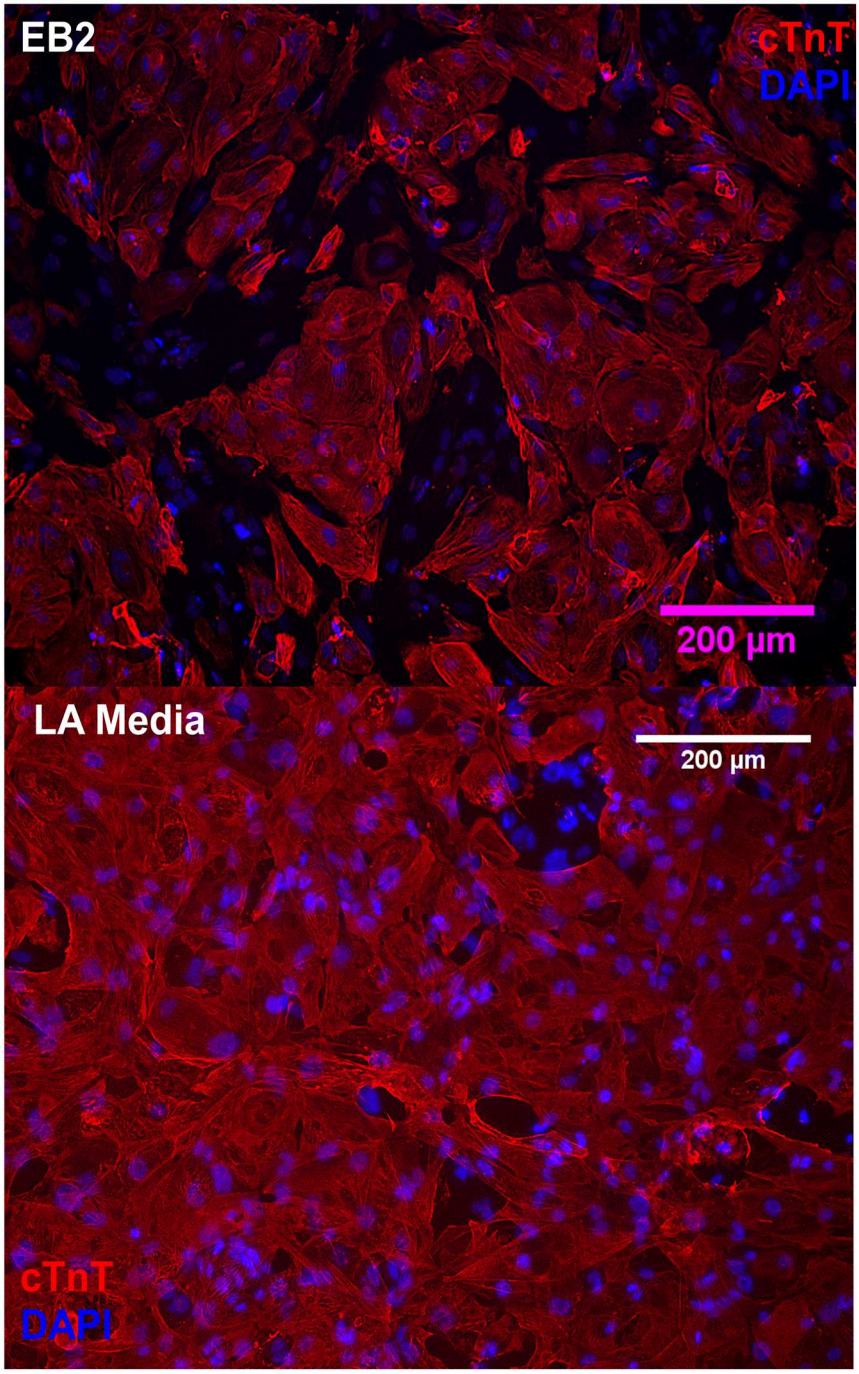

Figure 4.6: Histological Comparison of Unpurified (top, EB2) and Purified (Bottom, LA media) Cardiomyocytes.

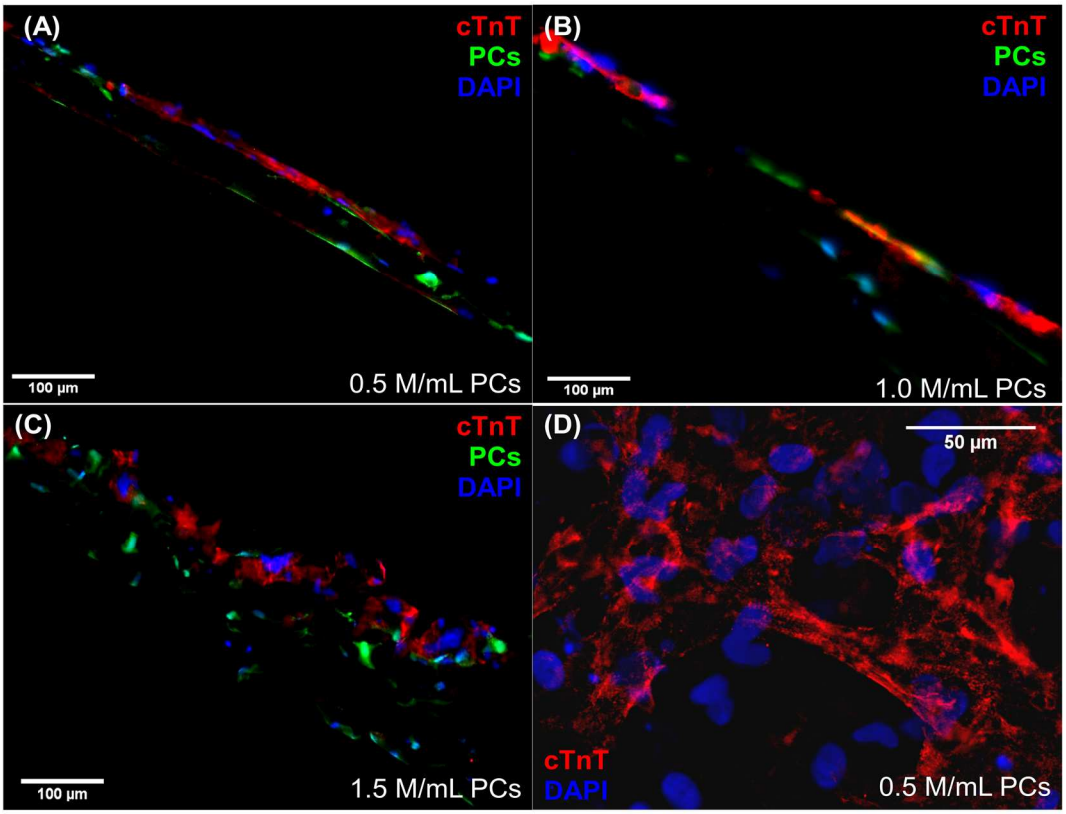

Figure 4.7: Cross-Sectional Views of 50 uL hemispheres constructed with purified hiPSC-CMs and varying numbers of PCs. (A-C). hiPSC-CMs in all conditions spread out along the top (media) surface of the hemispheres and displayed visible sarcomeric striations based on whole-mount staining of hemispheres

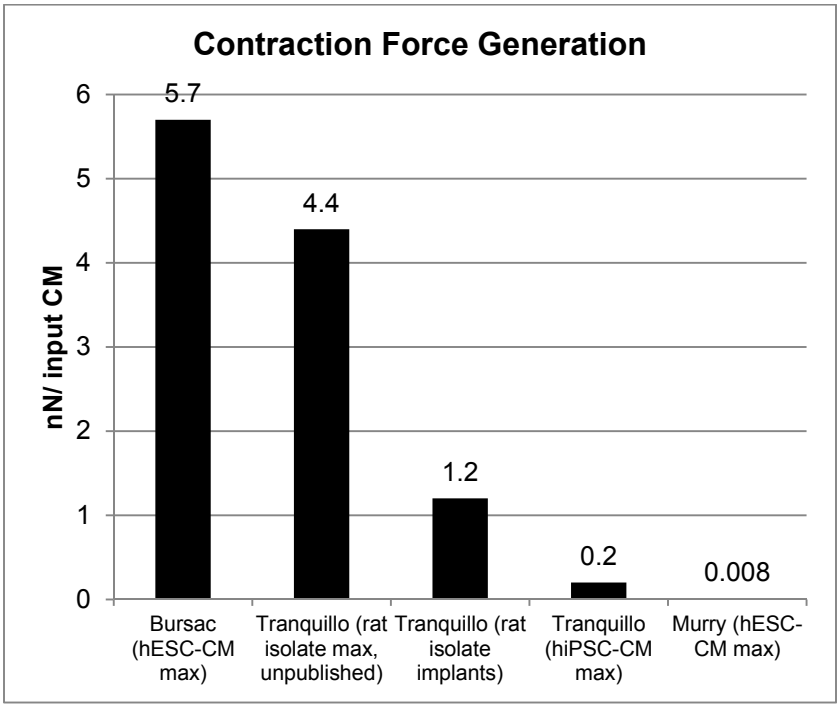

Figure 4.8: Contraction Force Generation of human pluripotent stem cell derived CM (hPSC-CMs) patches, state of the field. Bursac[25], Murry[10]

Chapter 5: Functional Effects of a Tissue-Engineered Cardiac Patch from Human Induced Pluripotent Stem Cell-Derived Cardiomyocytes in a Rat Infarct Model

5.1 Introduction

Human pluripotent stem cell derived CMs have been used for myocardial repair by direct myocardial injection, but engraftment rats are very low a few weeks after transplantation,[109, 110] which makes engineered tissues an attractive method to deliver CMs to the myocardium. There are only a few reports of an ECT prepared from hiPSC-CMs,entrapped in collagen-matrigel[10, 111] or fibrin-matrigel[112] scaffolds, and these were not implanted into infarcted myocardium. Thus, it is as yet unknown whether ECTs made from clinically-relevant hiPSC-CMs yield similar effects as ECTs made from hESC-CMs in an infarct model.

This study reports ECTs made from hiPSC-CMs entrapped in a fibrin gel and uses pericytes (PCs) as a non-CM cell population. PCs are vascular support cells that in the context of microvascular tissue engineering have been shown to regulate capillary stability and diameter.[48, 108, 113] PCs were chosen in this study to induce compaction of the fibrin gel, which is essential to concentrate and align CMs[37], and also to support the ingrowth of host microvessels into the ECT.[107] In addition, future strategies that include preformed microvessels in fibrin gel together with CMs may utilize a mixture of hiPSC-CMs, PCs, and endothelial

cells. This study demonstrates that PCs can be co-entrapped with hiPSC-CMs as a support cell type, eliminating the need for additional cell types in future studies.

Expanding upon a previous study in Chapter 3 reporting ECTs fabricated with neonatal rat cardiac cells, this study investigates the use of an aligned ECT, referred to as a patch, consisting of lactate-purified hiPSC-CMs and human PCs entrapped in a sacrificial fibrin gel to engraft into a nude rat acute infarct model and limit left-ventricular remodeling *in vivo*. Efficacy of the patch was assessed 4 weeks post-transplantation via echocardiography and histological characterization of scar size and patch engraftment, and compared to the effects of an engineered cardiac tissue created using only PCs.

5.2 Methods

5.2.1 Culture and purification of human iPSC-derived cardiomyocytes and human brain pericytes

Cells were purified, as detailed in Chapter 4, by using a media comprised of glucose-free DMEM supplemented with 4 mM lactic acid, NEAA, β-mercaptoethanol, penicillin/streptomycin, and 2 mM L-Glutamine (Sigma-Aldrich)[102] Cells were treated with lactate media for 4 days, changing lactate media twice, on days 4 and 6, before being returned to EB2 on day 8 for an additional 2 days prior to being harvested for construct preparation on day 10 of culture. The final cardiomyocyte purity was 94.2±2.9% cTnT+ cells.

5.2.2 Construction and Culture of Patches

Aligned patches containing both purified cardiomyocytes and pericytes (CM +PC) were constructed by mixing $2.2x10^6$ purified CMs and $3.4x10^5$ PCs with a fibrin-forming solution and injecting it into a 8mm-ID, 1.25 mL tubular mold as previously described[37] to create a final fibrin concentration of 3.3 mg/mL. The cell-containing, fibrin-forming solutions were incubated at 37°C for 15 min to allow formation of a fibrin gel. Gels were then removed from their casings and placed in EB20 culture medium supplemented with 2mg/mL aminocaproic acid (to limit fibrinolysis, Acros Organics) for the first 48 hours of culture, followed by culture in 2% serum medium for the remaining 12 days culture, 14 days total static culture.

Pericyte-only (PC) patches were constructed identical to CM + PC patches, containing $3.4x10^5$ PCs in a 1.25 mL, 3.3 mg/mL fibrin gel. hiPSC-CM only patches were not possible to construct because the cell induced fibrin gel compaction required to convert soft isotropic fibrin gel into a patch with functional CMs that can be sutured does not occur without the presence of non-CMs, as also reported by others. [11, 104]

5.2.3 Implantation of Patches into an Acute Nude Rat Infarct Model

Procedures used in this study were reviewed and approved by the Institutional Animal Care and Use Committee (IACUC) and Research Animal Resources (RAR) at the University of Minnesota.

Female Foxn1rnu nude rats (Harlan Sprague-Dawley) weighing 135-190 g were used in these studies. Rats were anesthetized using isoflurane, intubated, and received a left lateral thoracotamy to expose the heart. The pericardium was opened and MI was achieved by permanently ligating the left anterior descending (LAD) coronary artery with a 7-0 polypropylene suture. After a MI was established, a single patch was applied by removing one ring from its mandrel (Figure 5.1a) and cutting it into 3-8 mm long strips and suturing them parallel to each other over the epicardial surface of the left ventricle below the ligation suture, approximately parallel to the alignment of the surface myocardium (Figure 5.1b). After patch placement, the chest was closed and the animal was allowed to recover. Rats were administered 2.5 mg/kg ketoprofen and 15 mg/kg enrofloxacin (Baytril, Bayer) immediately post-operatively and daily for 3 and 5 days, respectively.

5.2.4 Cardiac Functional Analyis

Cardiac function was evaluated via echocardiograph assessments (Visual Sonics Vevo2100) of left ventricular ejection fraction and fractional shortening prior to ligation (baseline) and both 1 week and 4 weeks post-implantation. Hearts were harvested after 4 weeks *in vivo* for histological assessment.

5.2.5 Contraction Force Assessment of Patches

A subset of patches from the same batches were not implanted and instead subjected to twitch force assessment to evaluate their contractile force

generation. Twitch force measurements were recorded as previously described[5] on a custom-built testing system both spontaneously (when applicable) and in response to pacing. Briefly, CM-containing patches were placed in a media bath containing DMEM/F12 basal medium supplemented with 2mM $CaCl_2$, pre-tensioned between two posts, and subjected to field stimulation from two carbon electrodes. Data were recorded using LabVIEW and analyzed using a Matlab script.

5.2.6 Histology and Immunohistochemistry

Non-implanted patches and explanted hearts were fixed in 4% paraformaldehyde and frozen in embedding medium (Tissue-Tek OCT), and cryosectioned into 5 μm sections for immunohistochemistry and histological characterization. For immunofluorescence staining, sections were permeabilized with 0.01% Triton-X-100 (Sigma), blocked in 5% Normal Donkey Serum (Jackson Immunoresearch), incubated overnight at 4°C in primary antibody followed by a 60 minute incubation in secondary antibody at room temperature and a 10 minute incubation in Hoescht 3332 (LifeTech). Slides were mounted in fluorescent mounting medium (Dako) and imaged within 24 hours. Sections labeled for Isolectin B4 (IB4) were incubated for 10 minutes at room temperature. Information on immunofluorescence antibodies can be found in Appendix 4.

Infarct size was measured from Masson's Trichrome stained sections as the percentage of the surface area of the left ventricular anterior wall occupied by

scar. For each heart the infarct size was averaged from three areas of the heart: just below the ligation suture, mid-way between the ligation suture and the apex, and a section close to the apex. Left ventricular anterior wall thickness was measured across the infarcted region of the heart wall.

5.2.7 Protein Extraction and Western Blotting

Cells in each well of the 24-well plates used to compare unpurified and purified hiPSc-CMs were lysed at 4°C in a NP-40 lysis buffer consisting of 0.5% Nonidet P-40, 5% glycerol, 25 mM Tris (pH 7.4), 25 mM NaF, 225 mM NaCl, 0.025% sodium deoxycholate, 1 mM EDTA, 2 mM $NaVO_4$, and 1 mg/mL each of aprotinin, pepstatin, and leupeptin (Sigma-Aldrich). Total protein was assessed using a BCA protein assay (Pierce Biotechnology). 10 µg of protein from unpurified (n=4) and purified (n=5) hiPSC-CMs were loaded into the lanes of a 4-20% Mini-Protean TGX 10-well gel (BioRad) for protein separation and transfer. Western blot was conducted by assessing using primary antibodies for the α and β isoforms of myosin heavy chain and GAPDH (Santa Cruz Biotech), blocked in 5% blocking grade buffer (BioRad) with 0.1% Tween (Sigma-Aldrich), horseradish-peroxidase conjugated secondary antibodies (GE Healthcare Life Science) and chemiluminescence agent (Millipore). Expression intensity was analyzed using ImageJ software, and is outlined in Figure 5.11.

5.2.8 Statistical Analysis and Experimental Design

Three groups were investigated for this study: 1.) MI only (n=5): ligation only, no treatment; 2.) CM + PC patch (n=6): ligation + patch constructed with cardiomyocytes and pericytes; 3.) PC patch (n=4): ligation + patch constructed with PCs only.

Data are presented as means ± standard deviations. All results were analyzed using MiniTab statistical software. Student's t-tests and one-way analysis of variance (ANOVA) in conjunction with Tukey HSD post hoc testing was used to compare all groups. p-values <0.05 were considered significant.

5.3 Results

5.3.1 *In vitro* characterization of Patches

To establish that hiPSC-CMs can be co-entrapped with PCs to create an aligned, beating patch, patches were created and characterized *in vitro* prior to implantation. Both CM + PC and PC patches compacted into short tubes of comparable length from an initial length of 13 mm to less than 3 mm (Figure 5.1a). CM + PC patches had compacted down from an initial thickness of 2.83 mm to less than 0.5 mm (406±98.2 μm), and PC patches had a thickness of 403.8±87.6 μm, CMs (cTnT+ cells) made up 79.2±12.3% of the total cell number at implantation, with 8.8±6.3% of the cells being PCs (GFP+) and the remaining 12.0±6% of cells non-cardiomyocytes not purified from the CM cell culture, for a total cross-sectional cell density of 495±193.7 cells/mm^2 (Table 5.1, Figure 5.2a). The CM cross-sectional density was thus 405.7±63.1 CMs/mm^2. PC patches had

a final cell density of 63.3±9.9 cells/mm^2 compared to 40.4±43.9 cells/mm^2 for PCs in the CM + PC patches. Both CMs and PCs in both patches were well distributed across the patch thickness (Figure 5.2 a, d), elongated and aligned in the circumferential direction (Figure 5.2 b, c), and elongated CMs displayed organized sarcomeres (Figure 5.2c).

CM + PC patches generated measurable forces in response to multiple pacing frequencies (Figure 5.2 e, f). Average twitch force generation ranged from 0.35 to 0.46 mN (0.15-0.20 nN/input CM) over 0.5-1.5 Hz stimulation frequency. The maximum frequency in which a patch beat synchronously with pacing ranged between 1.5-2.0 Hz for each patch.

Cells within both CM + PC and PC patches had begun to deposit ECM throughout the scaffold during *in vitro* culture (Figure 5.3), despite the overall ECM remaining primarily fibrin at the time of implant (Figure 5.3 g, h). Collagen I (Figure 5.3 a, d) and basement membrane proteins Collagen IV and Laminin were present in both patches in the pericellular space and in the surrounding ECM (Figure 5.3 b, c, e, f). Cell-deposited fibronectin was not distinguishable histologically due to the presence of fibronectin from serum in the fibrin ECM (not shown). There was an increase in the amount of non-CM deposited Collagen IV in CM+ PC patches compared to PC only patches (Figure 5.3 i).

5.3.2 Functional Consequences of Patch Implantation

Echocardiography was conducted prior to infarction / patch implantation, and both 1 and 4 weeks post-operatively. 1 week post-op, all groups displayed a reduction in both left ventricular ejection fraction (LVEF) and fractional shortening (LVFS) relative to baseline (Figure 5.4a, Figure 5.5). However, animals that received CM + PC patches had higher LVEF and LVFS compared to both MI only controls and animals that received a PC patch (Figure 5.4 b, c). After 4 weeks post-op, LVEF and LVFS remained lower than baseline values, but the CM + PC patch group had higher LVFS than both MI only controls and PC patch animals, and higher LVEF than MI only controls. No improvements over MI only were seen with the administration of a PC patch at any time point. Additional ECHO data can be found in Table 5.2.

5.3.3 Left Ventricular Remodeling

Animals that received no patch (MI only) had infarct scars that covered 47.9±14.7% (range 30.7- 71.5%, median 45.4%) of the left ventricular free wall (Table 5.3, Figure 5.6). CM + PC patch animals had infarct sizes of 30.7±14.6% (range 15.9-50.0%, median 27.9%), smaller than MI only controls; PC patch animals had infarct sizes of 35.8±7.8% (range 27.3-46.1%, median 34.9%), not different than MI only or CM + PC patch animals. Wall thinning of the infarct area was seen in all groups compared to non-infarcted animals, with no reduction in wall thinning seen with the application of either CM +PC or PC patches. Patches

are not easily visualized in Figure 5.6. Additional measurements can be found in Table 5.4.

5.4.4 Patch Engraftment

After 4 weeks post-op, hearts that received CM + PC patches were observed to have a pale, thin tissue layer covering much of the left ventricular epicardial surface. This layer was found to be comprised of both scar tissue from the initial surgery and a thin, 81.3±33.5 μm layer of densely packed CMs located on the left ventricular epicardial surface (Figure 5.7a-c). The patch contained interspersed PCs (Figure 5.7b, e, f) and covered both infarcted and intact myocardium, separated from the host myocardium by a 103.3±33.1 μm non-myocyte interface zone (Figure 5.7a-d). Imaging of trichrome-stained sections revealed the extracellular matrix (ECM) of the engrafted patch to be primarily collagenous (Figure 5.7a). Elongation and circumferential alignment was observed in the majority of engrafted CMs (Figure 5.7c, e, f), but the cells were very small in size, indicating immaturity of the CMs. Gap junction protein connexin 43 was found between adjacent CMs within the engrafted patches (Figure 5.7e), which was only sparse after *in vitro* culture (Figure 5.8), although not concentrated at cell-cell junctions as observed in adult myocardium. These CMs were verified to be transplanted cells through Human Nuclear Antigen (HNA) staining 10.9±1.4% of imaged donor CMs stained positive for Ki67 (Figure 5.7d) at the 4 week time point, consistent with some level of CM proliferation over

4 weeks *in vivo*. Assuming no lateral contraction of the patches, after 4 weeks *in vivo* the number of cTnT+ nuclei in the engrafted patches increased 2-fold (102.9% increase). Little to no Ki67 positive cells were found in the patches at the end of *in vitro* culture (Figure 5.8).

Pericytes entrapped in PC patches did not survive 4 weeks *in vivo*, with few to none GFP+ and HNA+ cells being found within the host myocardium or along the epicardial surface of the heart. The ECM of patches was converted from being primarily fibrin at implant to collagenous after 4 weeks *in vivo*, similar to that of the infarct scar or adhesions from the chest wall, making it difficult to confidently identify the presence of a patch at this time point without the presence of HNA+ donor cells.

Two animals that received CM + PC patches died at the 1 week time point due to anesthesia. The patch on these animals was visible in trichrome, and contained somewhat sparsely distributed CMs and PCs with a few CMs Ki67+ (Figure 5.9). All other animals that survived the initial surgery lived to the 4 week time point.

CM + PC patches became vascularized via angiogenesis from the host based on isolectin B4 (IB4) staining, with small diameter vessels present in the patch 4 weeks post-op (Figure 5.10a). Active perfusion of the vessels was verified by the presence of red blood cells in H&E stained images of the

engrafted patches (Figure 5.10b). In the host myocardium, there were no differences in the density of IB4+ microvessels in infarcted myocardium among the groups after 4 weeks, but an increased density occurred in the area of myocardium bordering the infarct zone with the administration of a CM + PC patch (Figure 5.10c, d).

5.5 Discussion

This study demonstrated that the co-entrapment of hiPSC-CMs and human PCs in a fibrin gel results in a compacted, aligned, and beating cardiac patch (engineered cardiac tissue), and after 4 weeks *in vivo* the patch remained viable and resulted in a reduced infarct size (Table 1) and improved cardiac function compared to infarct-only controls (Figure 5). In contrast, a patch containing only PCs did not survive 4 weeks *in vivo* and resulted in no improvements in contractile function or reduction in infarct size. These results suggest that similar to our recent report of an ECT similarly made from a neonatal rat heart isolate and also implanted acutely,[37] the improvements seen with patch administration originate from cardiomyocytes. To our knowledge, this is the first demonstration of a cardiac patch utilizing hiPSC-CMs that not only remains viable, with CM proliferation, after 4 weeks *in vivo*, but also covers large portions of the left ventricular epicardial surface and contributes to the limitation of left ventricular remodeling post-infarction.

The creation of an ECT *in vitro* is a subject that has received increasing interest as a method to deliver cells to the injured myocardium, supplement the contractility of the left ventricular wall, and ultimately contribute to and facilitate cardiac regeneration. This study focused on limiting the loss of left ventricular contraction and infarct expansion by acute placement of the patch on the infarcted myocardium (rather than replacing infarct scar tissue with the patch in a second surgery), and to compare the use of hiPSC-CMs in a patch to a previous study utilizing neonatal rat cardiomyocytes and non-cardiomyocytes[37]. The same gel formulation was used in both studies, 1.25 mL of a 3.3 mg/mL fibrin gel in a tubular mold, and cultured for a total of 14 days. The concentration of cardiomyocytes was kept the same, with the neonatal rat study containing ~60% ($3x10^6$) of a heterogeneous population of non-cardiomyocytes, and the current study containing 15% ($3.4x10^5$) human PCs and 5% ($1.13x10^5$) non-cardiomyocytes that survived the purification process. However, the neonatal rat CM patches were stretch-conditioned prior to implantation, while these CM+PC patches were cultured statically for the entirety of culture. Early stage differentiated hiPSC-CMs have shown a relatively high proliferation ability compared to late stage mature hiPSC-CMs,[17] and we used the day 15-differentiated hiPSC-CMs in this study in an effort to maintain the hiPSC-CM proliferation after patch transplantation. Furthermore, immature CMs are more tolerant of perturbation and are more likely to survive transplantation than more mature CMs.[61] Both patches exhibited measurable twitch forces, although lower

for the hiPSC-CM patches (0.2 nN/input CM) compared to the neonatal rat cell patches (1.2 nN/input CM).[37]

In both the study utilizing neonatal rat CMs and the current study using hiPSC-CMs, a reduction in infarct size and improvements in cardiac function occurred with the implantation of a patch that contains both CMs and non-CMs while the implantation of patches containing non-CMs resulted in minimal (neonatal rat) or no (hiPSC-CM) improvement. However, near complete rescue of the myocardium resulted from the implantation of a neonatal rat cell patch[37], while moderate infarct sizes of 30.7±14.6% ($p<0.05$, Table 2) resulted from the implantation of a CM+PC patch in this study. These larger infarct sizes were associated with reduced improvements in cardiac function and thinning of the left ventricular wall, which were not observed with the application of the neonatal rat CM patch. Additionally, invasion of non-cardiomyocyte cells into the host was seen with the neonatal rat CM patch, but was not observed in this study. The reduced improvement found with the administration of a CM + PC patch compared to our previous neonatal rat patch may be due to several reasons. Different strains of rats were used (Fisher rats vs. athymic nude rats), a species mismatch of the transplanted cells (rat-rat vs human-rat), and a different initial maturation state of the transplanted cardiomyocytes (neonatal vs. embryonic/fetal). Additionally, there were fewer non-CM cells transplanted in the CM + PC patches in this study (0.45×10^6 cells vs 2.75×10^6 cells) and the

population of non-CM cells in the neonatal rat cell patches was a heterogeneous population consisting of cardiac fibroblasts as well as other non-characterized cells from the myocardial interstitium, including PCs. Pericytes are normally found in the myocardium as microvascular support cells, but the results from this study indicate that pericytes are likely not the migratory cell type seen in our neonatal rat patch study. Pericytes have been shown to minimally improve cardiac function and suppress fibrosis when transplanted into mouse myocardium[114], but these effects did not occur in this study, either due to the different source tissue, method of delivery or culture differences prior to implantation. Interestingly, while the PCs did not survive 4 weeks *in vivo* when transplanted as a PC only patch, they did survive when transplanted in the CM + PC patches, suggesting that not only are PCs required for the compaction and alignment of fibrin gels for patches containing CMs, but also that CMs are required for PC survival *in vivo*. In contrast, the hiPSC-CMs not only survived but appeared to proliferate based on co-localization of cTnT and Ki67 staining, which is a common marker for proliferation of stem cell-derived CMs[32, 115] but may also indicate multinucleation of CMs.[116, 117] It can be additionally noted that even though the non-cardiomoycytes that survived purification comprised only 5% of the total cell number at the time of ECT fabrication, they expanded over the 14 days of *in vitro* culture to comprise 12% of the final cell population at implant, higher numbers than PCs. These results indicate that future studies will have to further optimize the CM purification process and further characterize these non-

CM cell types to elucidate any potential contribution these cells contribute to myocardial protection post-infarction.

In both studies, the ECM of the patch was converted from fibrin to primarily collagen, and a collagenous interface zone developed, separating the host myocardium from the patch, suggesting the beneficial effects of the patches were not due to electrical integration of the CMs. The thin size of the engrafted patches in both studies makes any patch beating, if it occurred, an unlikely mechanism of functional improvement. In all, the mechanism by which the benefits afforded by CM + PC patch administration occurred are not clear, but the increase in microvessel density in the myocardium bordering the infarct could implicate paracrine mechanisms that stabilize the infarct scar and prevent further expansion. Although cell migration from the CM + PC patch into the host was not seen in this study, the increase in collagen IV deposition in vitro in the CM + PC patch compared to PC only patches following *in vitro* culture indicate altered behavior of pericytes in the presence of cardiomyocytes. Some of the ECM deposition could also be attributed to the entrapped non-CM cells remaining after the CM purification process.

There are no other reports thus far of ECTs made from hiPSC-CMs that have been implanted for comparison with this study. Improvement in cardiac function of nude rats was recently reported with the delayed administration of a scaffold-free cell sheet consisting of hiPSC-CMs co-cultured with endothelial and

vascular support cells,[104] but the cell sheets engrafted with limited success and did not substantially limit infarct expansion or left ventricular thinning[104]. In combination, this cell sheet and current study indicates a definite benefit from hiPSC-CMs administered to nude rat infarcts. However, optimization of this hiPSC-CM patch will be needed to achieve the near complete rescue of the myocardium we achieved with the neonatal rat patch.

This study provides preliminary data demonstrating not only the ability of an ECT containing hiPSC-CMs to remain viable after transplantation, but also with the potential for cell expansion. However, this study is limited by the acute infarct model used, limited sample size, and 4 week endpoint. For clinical applicability, an alternative, potentially autologous source of pericytes will need to be used, such as dermal pericytes,[118] and longer term studies in larger animals with delayed implantation will also be needed to assess the long term fate of the graft and any potential for teratoma formation of these hiPSC-CMs. Larger animal models will be additionally required to fully characterize the engraftment of immature, donor hiPSC-CMs with the adult, recipient myocardium, as rodent and human hearts have different intrinsic heart rates, which may hamper accurate assessment of electrophysiological integration

In conclusion, we created an aligned, force-generating engineered cardiac patch using hiPSC-CMs and PCs entrapped in a sacrificial fibrin gel and found that when transplanted onto acutely infarcted rat myocardium, the patch

remained viable and the CMs proliferated. This patch resulted in improved cardiac function and a reduced infarct size 4 weeks after transplantation, along with increased microvessel density in the host border zone myocardium, implicating potential paracrine-based, infarct-stabilizing mechanisms originating from the transplanted CMs.

5. 6 Acknowledgements

The authors thank Susan Saunders for technical assistance. This work was supported by NIH R01 HL108670 (to RTT) and HL95077 (to Zhang), and NIH U01 (TJK).

5.7 Figures and Tables

Table 5.1: Cell composition of patches pre-implantation

Patch	Cell Density (cells/mm^2)	%CM	%PC	Other Cell Types
CM + PC	495±193.7	79.2±12.3	8.8±6.3	12.0±6
PC	63.3±9.9	0	100	0

CM + PC: hiPSC-CM + pericyte patch, PC: Pericyte only patch. Data are mean ± standard deviation.

		CM + PC	PC	MI only
Baseline	Heart Rate (BPM)	383 ± 43.9	406±31.1	419±18.5
	Diameter;s (mm)	1.71±0.4 *, #	2.21±0.41 *, #	1.68±0.3 *, #
	Diameter;d (mm)	4.95±0.5 #	5.46±0.33 #	5.3±0.4 * #
	Volume;s (µL)	10.2±6.7	18.7±6.6	9.44±3.7
	Volume;d (µL)	118±28	147±20	137±21.5
	Stroke Volume (µL)	108±28.3 #	128±22.9	127±21.1 *, #
	Cardiac Output (mL/min)	42±14.2	52.6±12.5	53.7±10.5 #
	Ejection Fraction (%)	90.7±6.7	87.2±5.9	93.1±2.9
	Fractional Shortening (%)	65.1±9.7	59.6±8.8	68.4±5.0
1 week	Heart Rate (BPM)	388±58.2	362±47.6	397±27.4
	Diameter;s (mm)	2.97±0.4 #, +	4.08±0.8	4.16±0.6 #
	Diameter;d (mm)	5.54±0.6 #	5.91±1.0	5.77±0.4
	Volume;s (µL)	36.2±10.5	81±35.4	79.9±27.1
	Volume;d (µL)	154±38.5	182±66.2	167±23.2
	Stroke Volume (µL)	118±30.6	101±33.8	87.1±13.5
	Cardiac Output (mL/min)	46.7±16.3	35.6±11.1	34.7±6.7
	Ejection Fraction (%)	75.6±3.5	57.1±7.2	52.6±10.6
	Fractional Shortening (%)	46±4.0	31.6±4.6	28±7.0
4 week	Heart Rate (BPM)	394±14.6	362±70.3	375±35.4

Diameter;s (mm)	4.19±0.65 +	5.24±1.0	5.5±0.4
Diameter;d (mm)	6.58±0.33	7.06±1.0	6.91±0.3
Volume;s (μL)	83.8±32.4	142±63.2	152±25.3
Volume;d (μL)	227±24.3	269±83.6	252±27.6
Stroke Volume (μL)	143±23.6 +	127±31.4	100±13.6
Cardiac Output (mL/min)	56.7±10.8 +	44.7±10.5	37.3±6.1
Ejection Fraction (%)	63±10.2	48.9±11.3	40±5.4
Fractional Shortening (%)	36.1±7.5	26.3±7.7	20.6±3.2

Table 5.2: Additional ECHO data. All data are represented as mean ± standard deviation. *p,0.05 vs. 1 week # p<0.05 v.s 4 week +p<0.05 vs. MI only. BPM = beats per minute, s= systole, d= diastole. CM + PC = hiPSC-CM + Pericyte patch, PC = pericyte only patch, MI = infarction only, no treatment.

Table 5.3: Infarct Size and Left Ventricular Anterior Wall Thickness of 4-Week Implants.

Group	Infarct Size (%)	LV anterior wall thickness (mm)
MI only (n=5)	47.9±14.7	1.04±0.3
CM+PC patch (n=6)	30.7±14.6*	1.17±0.37
PC patch (n=4)	35.8±7.8	1.13±0.21
Non-Infarcted Heart (n=4)	-	2.47±0.21 * # $

All groups displayed a significant thinning of the LV anterior wall 4 weeks post-transplantation, but at the 4 week time point CM + PC patch recipient hearts had significantly smaller infarct sizes than MI only control animals. *$p<0.05$ vs. MI only, $^{\#}$ $p<0.05$ vs. CM + PC patch, $^{\$}$ $p<0.05$ vs. PC patch

Thickness (mm)	IVS	RV	LV RZ
CM+PC patch	2.42±0.33	1.26±0.27	2.79±0.23
PC patch	2.68±0.24	1.35±0.33	2.69±0.38
MI only	2.37±0.27	1.20±0.16	3.09±0.29

Table 5.4: Thickness Measurements of the Interventricular Septum (IVS), Right Ventricular Wall (RV), and the Non-Infarcted Remote Zone of the Left Ventricular Anterior Wall (LV RZ). Data are represented as mean± standard deviation. No significant differences were found between groups.

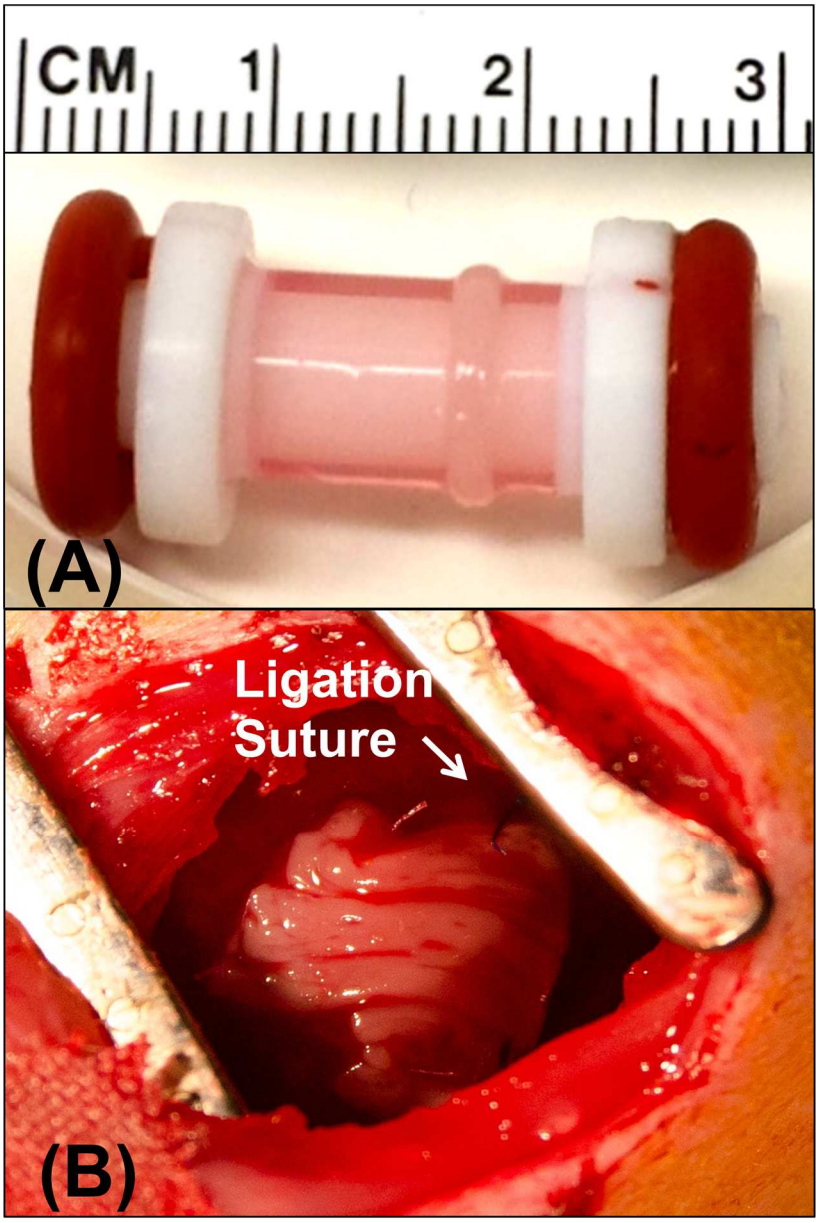

Figure 5.1: CM + PC patch at Implantation. (A) CM + PC patch in its mandrel prior to implantation. (B) Oblique view of the patch on heart after being cut into 3 strips and sutured onto the left ventricular epicardial surface. The ligation suture is marked by the white arrow.

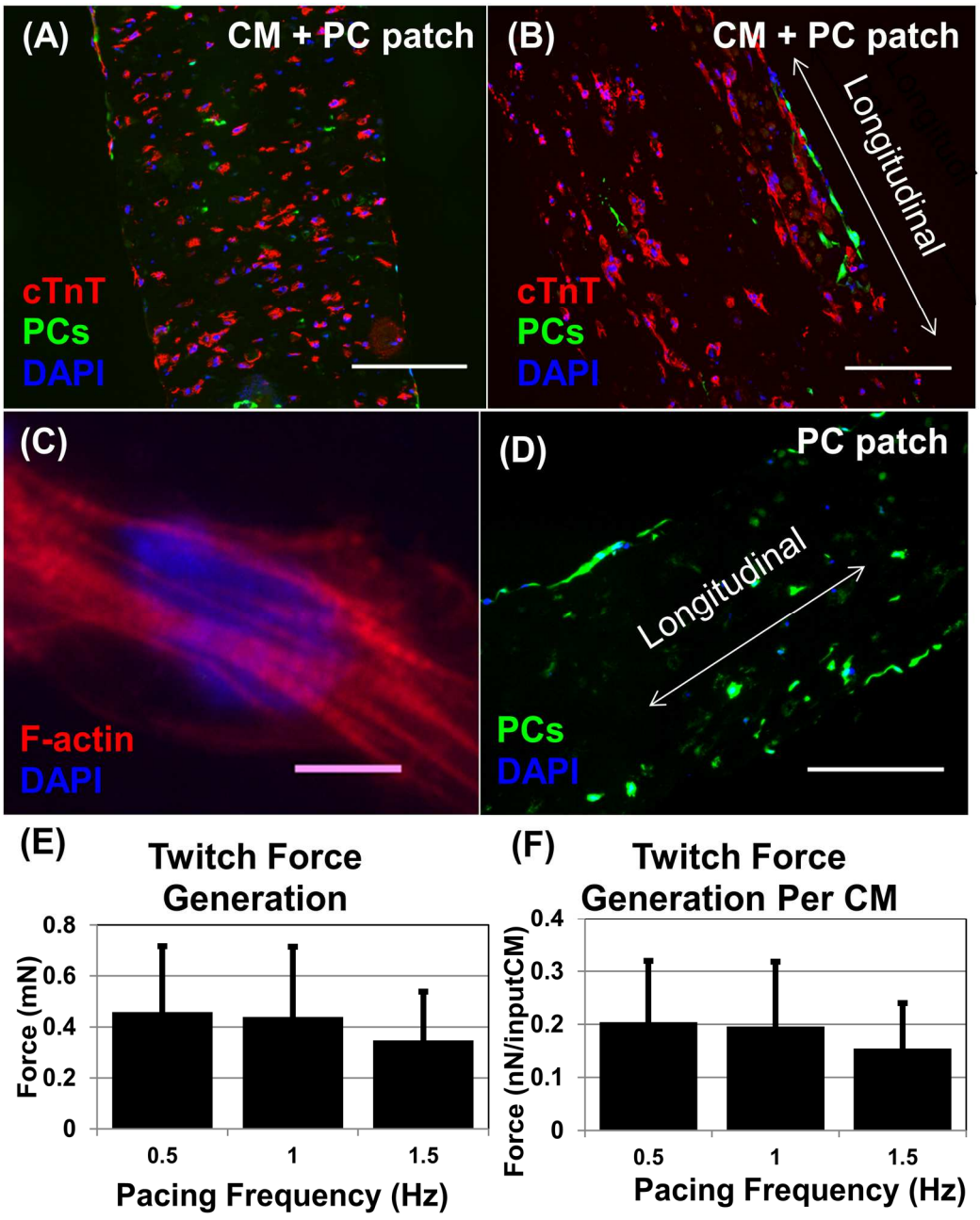

Figure 5.2: CM+ PC and PC patches prior to implantation: Cross-sectional (A) and longitudinal (B-D) sections of CM+ PC and PC patches showing uniform distribution (A), circumferential alignment (B), and striation (C) of entrapped

CMs. (D) Longitudinal section of PC patch showing uniform PC distribution and alignment. Scale = 200 μm (E-F) Twitch force generation of CM + PC patches prior to implantation. (E) Total force generation of patches, (F) Force generated normalized to number of cardiomyocytes seeded into gels at the beginning of culture.

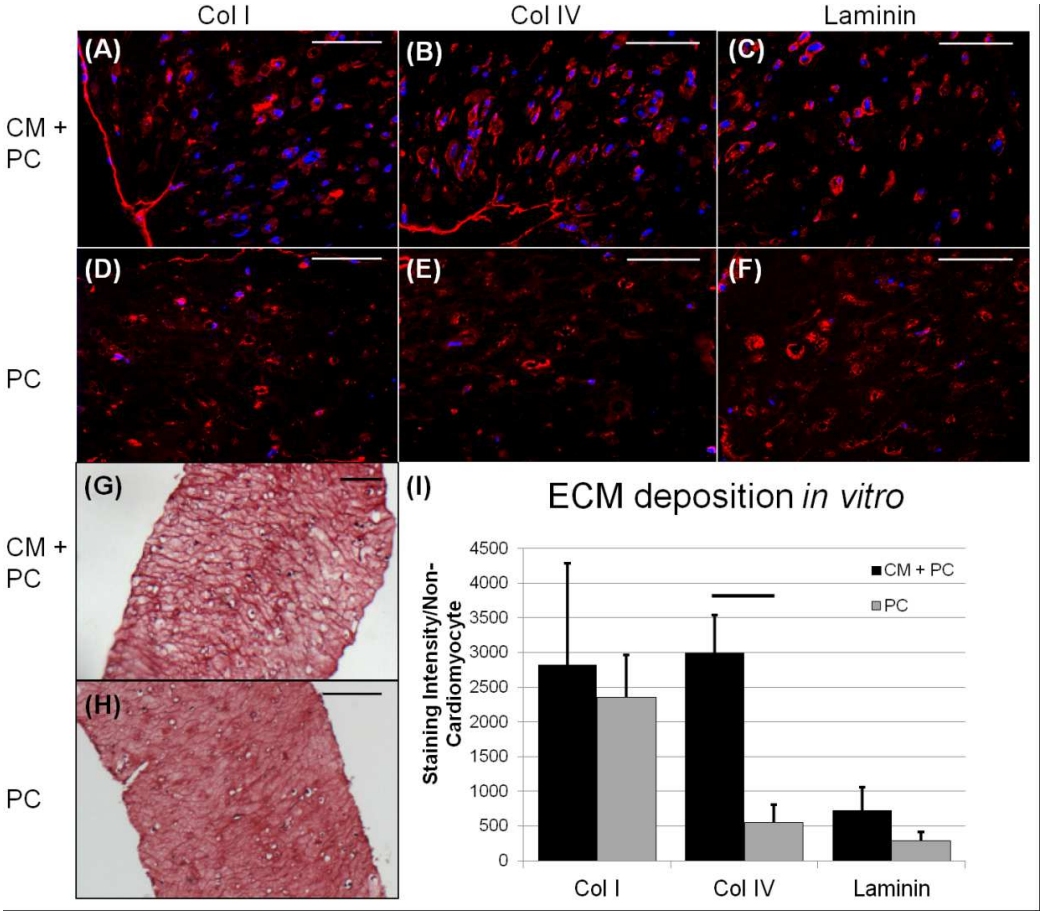

Figure 5.3: Cell-deposited ECM in CM + PC and PC patches. Collagen I deposition in CM + PC (A) and PC (D) patches in vitro. Basement membrane proteins Collagen IV (B, E) and Laminin (C, F) were also present in both CM +

PC and PC patches. Overall ECM of patches remained primarily fibrin at implant as seen in Masson's trichrome stained sections (G, H). More collagen IV was produced by non-cardiomyocytes in the CM + PC patch compared to the PC patch (I). Red: Matrix Protein; Blue: nuclei. Scale = 100 μm.

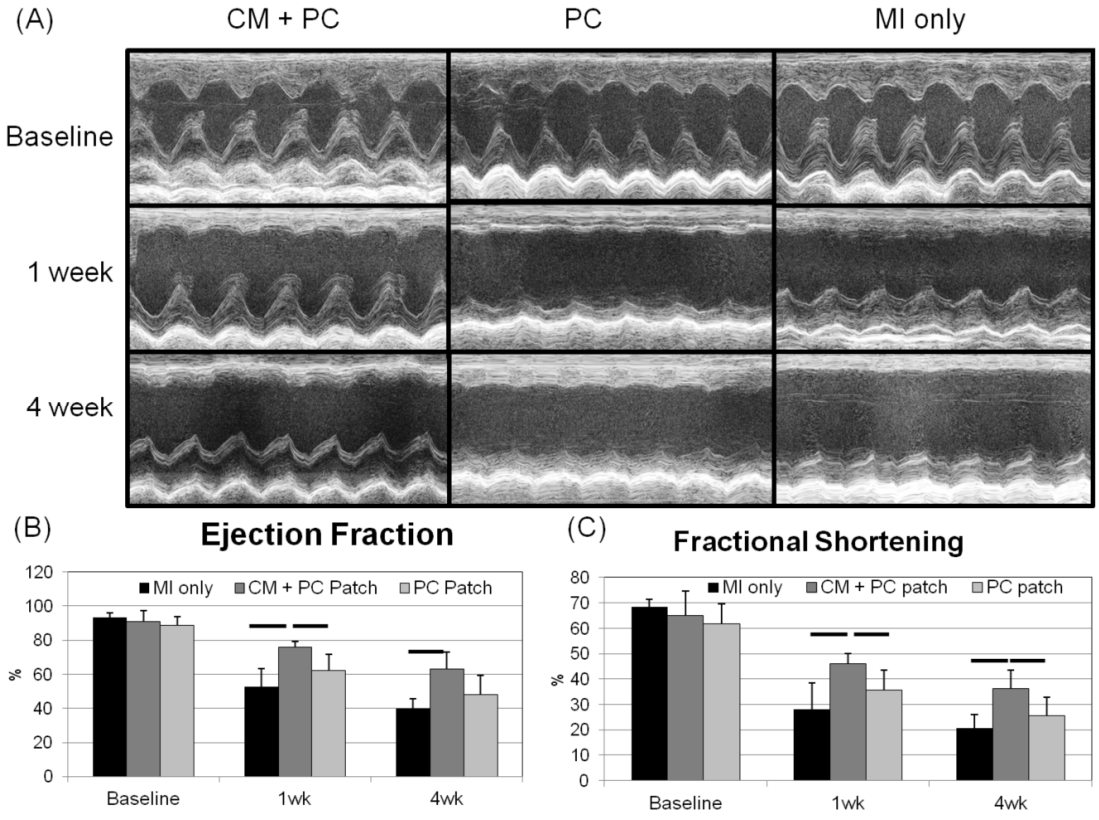

Figure 5.4: Echocardiography results 1 and 4 weeks post-infarction and transplantation. (A) Representative M-mode ECHO images of CM + PC patch recipient, PC patch recipient, and MI only hearts at each study time point. At the 1 week time point, animals receiving a CM + PC patch had improved LVEF and LVFS compared to both MI only controls and animals receiving PC patches (B, C). At 4 weeks post-infarction, animals receiving CM + PC patches had improved

LVFS over both groups and improved LVEF compared to infarct only controls (B, C). $p < 0.05$ is considered significant.

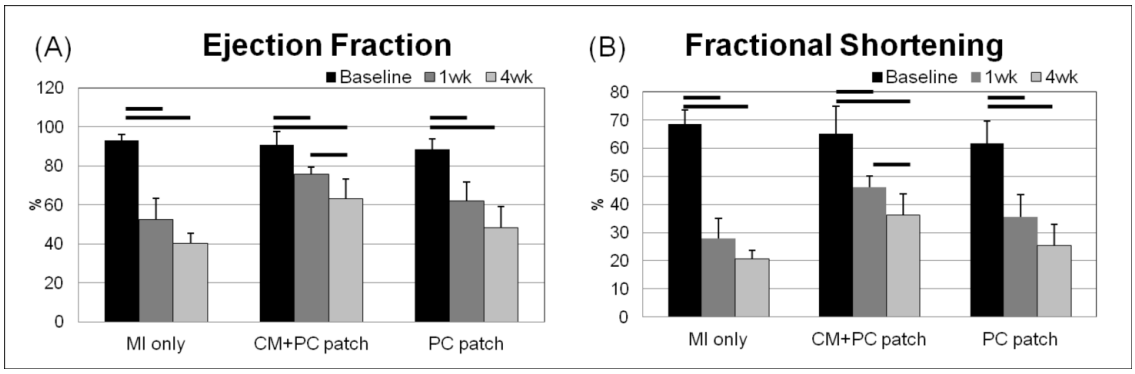

Figure 5.5: Additional echocardiography results both 1 week and 4 weeks post-transplantation. A significant reduction from baseline in both left ventricular ejection fraction (LVEF) and left ventricular fractional shortening (LVFS) was seen in all treatment groups both 1 week (A) and 4 weeks (B) post-infarction. A significant reduction in both LVEF and LVFS was also seen from week 1 to week 4 in the CM+PC patch group.

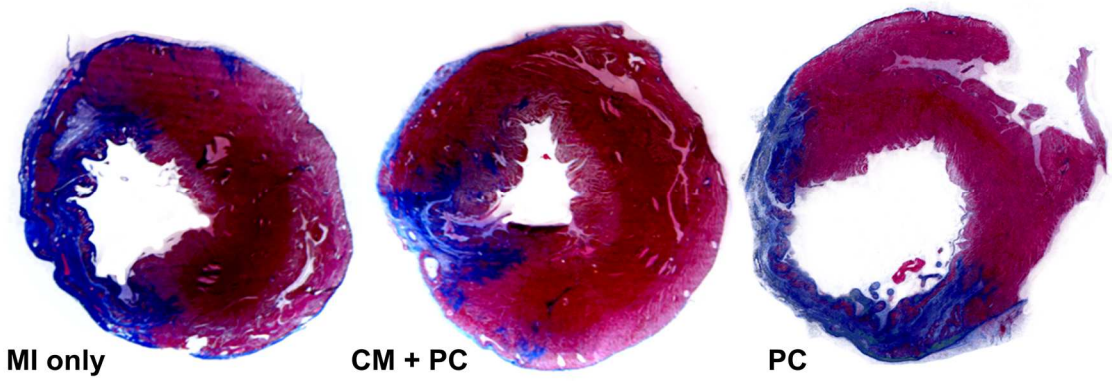

Figure 5.6: Masson's trichrome images of MI only, CM +PC, and PC patch hearts, showing representative infarct sizes (blue) and left ventricular anterior wall thicknesses. CM + PC patch recipient hearts had smaller infarct sizes than infarct only control animals, and no reduction in infarct size was seen in PC patch recipient hearts. Patch not easily visualized in sections.

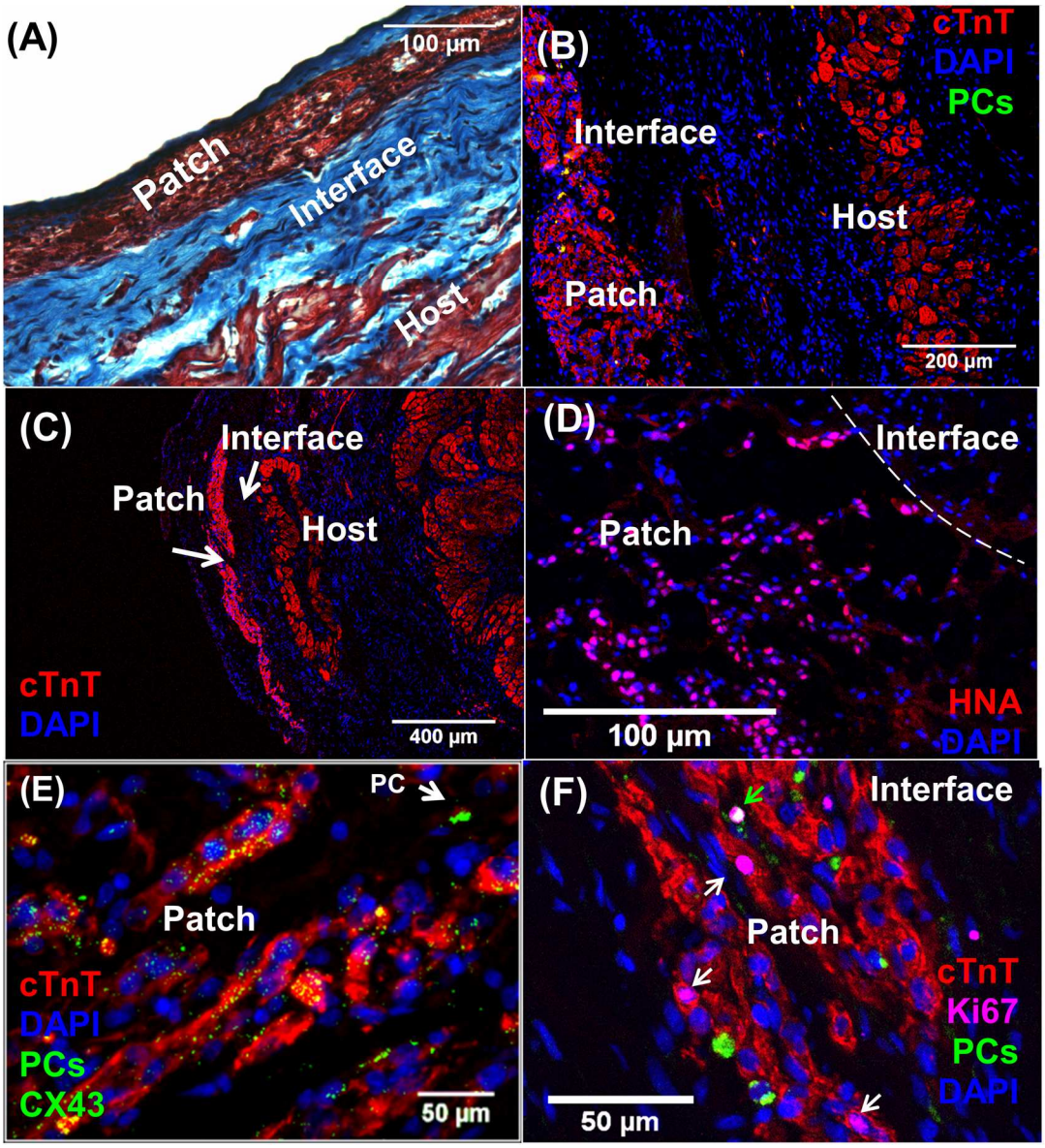

Figure 5.7: CM +PC patch engrafted onto heart 4 weeks post-transplantation. Top row: Masson's Trichrome image (A) showing engrafted patch on the epicardial surface of the heart surrounded by collagenous ECM, separated from the host myocardium by a collagenous non-cardiomyocyte interface zone. High (B) and low (C) magnification views of an engrafted patch on

top of infarcted myocardium. The patch was also present on top of intact myocardium far from the infarct zone. Bottom row: Inset of engrafted patch showing HNA+ cells within the patch (D), dispersal of pericytes (E, F) in the patch and CMs coupled via gap junctions (E). Some of the CMs (F, white arrows) in the patch were positive for Ki67 at the 4 week time point in vivo, indicating some level of CM proliferation in vivo. Green arrow = Ki67+ pericyte.

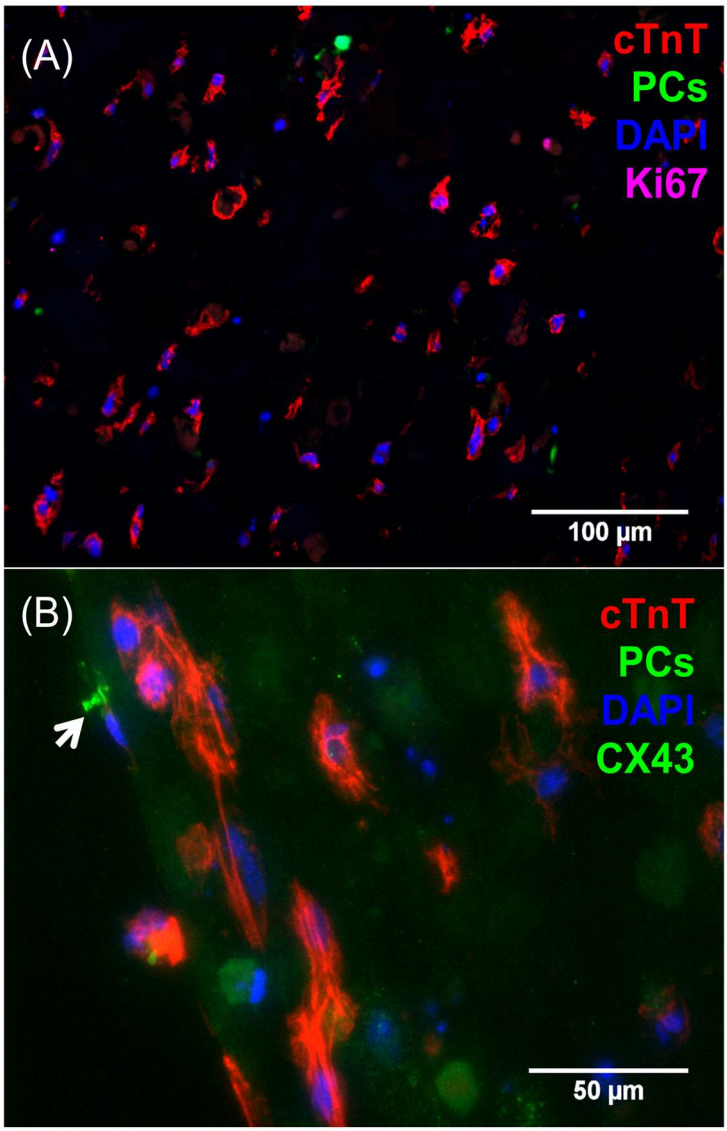

Figure 5.8: *In vitro* labeling of Ki67 and CX43. Cross-sectional (A) and longitudinal (B) images of *in vitro* CM + PC patches, indicating little to no presence of proliferating CMs (A) and gap junctions (B) in patches prior to transplantation.

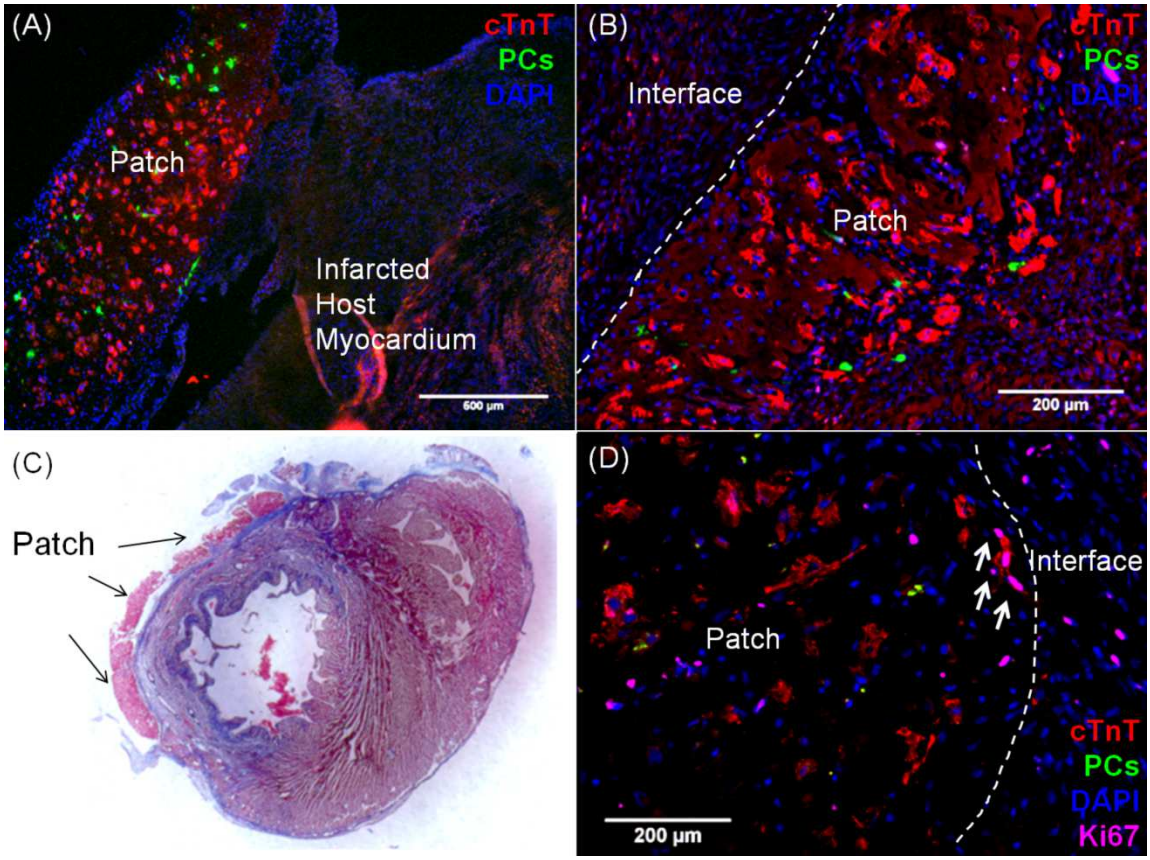

Figure 5.9: CM + PC patch engraftment 1 week post-op. Low magnification (A) and higher magnification (B) images of patches after 1 week in vivo. (C) Trichrome-stained section of a CM + PC patch recipient heart after 1 week in vivo, patch is indicated by black arrows. (D) Some transplanted CMs (white arrows were Ki67+ after 1 week in vivo. N= 2.

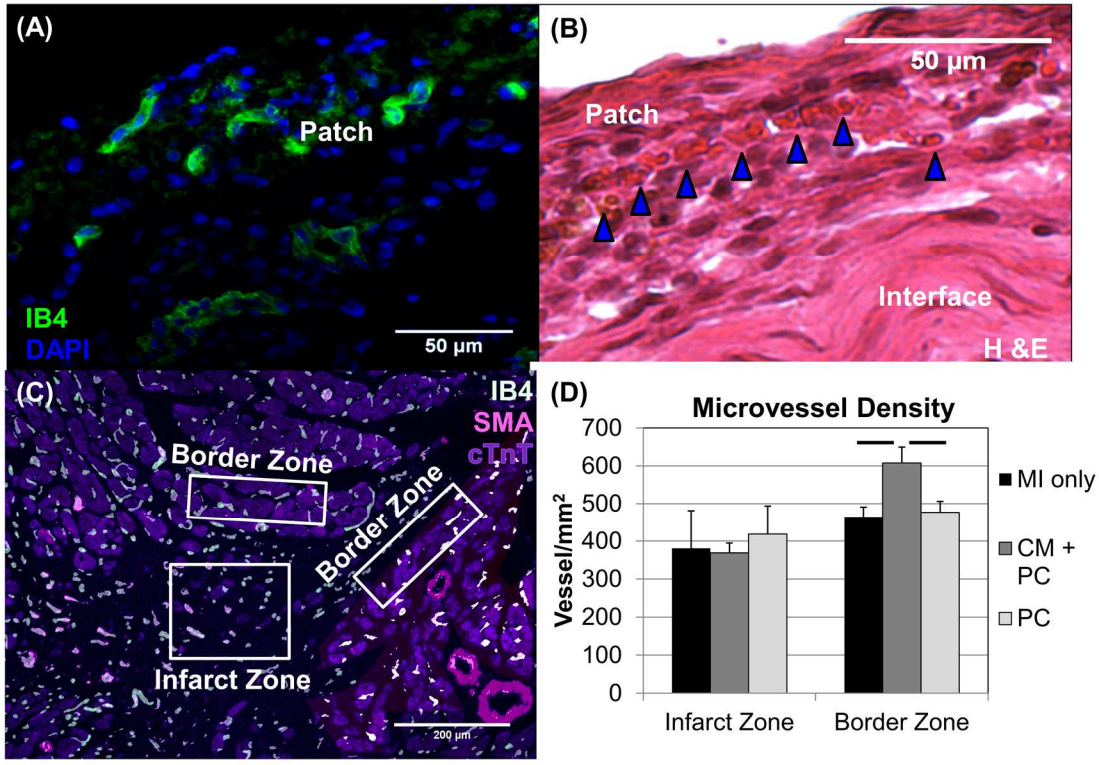

Figure 5.10: Host vascularization of CM + PC patch in vivo. (A) Isolectin B4 (IB4) + small diameter host vessels were found in the patch 4 weeks post-transplantation, and perfusion was indicated by the presence of red blood cells (blue arrows) in H&E stained slides (B). (C) Microvessel density in the host myocardium. An increase in microvessel density was seen in the areas of myocardium bordering the infarct zone with the administration of the CM + PC patch.

Chapter 6: The Effect of Cyclical Mechanical Stretch on the Maturation of Human Induced Pluripotent Stem Cell derived Cardiomyocytes

6.1 Introduction

Although it was shown in Chapters 4 and 5 that hiPSC-CMs are a promising cell source for cardiac repair post-infarction, concerns remain about the ability of these cells to successfully and safely engraft into the adult, human myocardium. A primary concerns stems from the relative maturation level of these cells. There is no definitive assessment of CM maturation, but human pluripotent stem cell –derived CMs (hPSC-CMs)are frequently described as resembling embryonic or fetal CMs, an immature phenotype. Yang, *et al*[105] reviewed the primary discrepancies between immature and mature CMs featured in Table 6.1. As evident from this work, immature CMs differ greatly from adult CMs in nearly all aspects, from cell morphology and intracellular organization to metabolism, force generation and electrophysiological properties. How these disparities affect cell engraftment, integration, and therapeutic efficacy of these cells in vivo has yet to be determined, largely due to the relative lack of success seen thus far in inducing maturation in pluripotent stem cell derived cardiomyocytes for comparative studies. Extended culture times and biochemical agents have been used to try and induce maturation in hPSC-CMs with limited success. Based on the results outline in chapter 2 showing that cyclic stretching increases the contractile force generation of neonatal rat CMs in a 3D

environment, in this study we seek to investigate whether or not stretch-conditioning can be used to induce maturation in hiPSC-CMs, and if so, to what degree in a smaller scale, 2D environment. Through protein analysis, we assess the relative quantities of α-sarcomeric actinin (αSA), and both the α and β isoforms of myosin heavy chan (α, β MHC) as a measure of the myofibril presence and assembly inside the cell, and also the ratio of the α to β isoforms of MHC, as the slow-twitch β isoform predominates as CMs progress towards the adult phenotype. In addition to these proteins, we assess the relative presence of Connexin 43 (CX43), a protein involved in cell-cell propagation of action potentials, and sarcoplasmic endoplasmic reticulum calcium (Ca^{2+}) ATPase (SERCA2A), a calcium reuptake pump located on the sarcomplasmic reticulum involved in CM relaxation post-stimulation. Extended relaxation time prevents re-initiation of contraction, leading to a reduction in the maximum stimulation frequency at which CMs can be paced.

6.2 Methods

6.2.1 Cyclic Mechanical Stretch Using the Flexcell System

Cells were exposed to cyclic mechanical stretch through the use of the Flexcell® Tension System. In this system, cells are cultured on distensible silicone membranes in a 6 well plate or 24 well plate format. Plates are placed over loading posts and vacuum is applied to the back side of the membrane, stretching it over the loading post (Figure 6.1). The pressure waveform the

membranes are exposed to is regulated on an external software system[119]. The 24 well plate system is capable of stretching cells at 1.2 – 8.0% biaxial strain, while the 6 well plate system can generate 0.8-21.8% uniaxial or biaxial strain (Flexcell, Int). Preliminary experiments in this study were conducted with a 5% amplitude square wave pulse at 1 Hz frequency with biaxial loading posts to compare the effects of using the 6 well or 24 well systems. Cells were exposed to cyclic stretch for 7 days prior to being harvested for protein and histological analysis.

6.2.2 Cell Culture

6.2.2.1 24-Well Plates

hiPSC-CMs were either seeded directly from thaw into Pronectin-conjugated 24 well Flexcell plates (Flexcell, Inc) (Figure 6.1a) at a seeding density of 100-120 $x10^5$ cells/cm^2, or thawed into T75 flasks coated with 2.5 μg/cm^2 fibronectin for 72 hours, per the standard culture protocol outlined in chapter 4, prior to harvesting and re-seeding into the Flexcell plate at a density of 100 $x10^5$ cells/cm^2. Once in the Flexcell plates, cells were cultured in EB20 for 48 hours post-seeding and EB2 for an additional 24 hours before initiation of stretch.

6.2.2.2 6-Well Plates

For use with a 6 well plate, hiPSC-CMs were seeded only into the center regions of the wells using a custom 17 mm diameter silicone seeding ring to conserve the number of cells required for experiments (Figure 6.2b). CMs were

seeded into plates directly from thaw, suspended in 800 µL of EB20 and placed into the center of the seeding ring. Cells were allowed to adhere for 24 hours inside the seeding ring before the ring was removed and the media replaced with 3 mL EB20/ well. The next day, media was changed to EB2 and cells were allowed to culture statically for an additional 24 hours prior to the initiation of stretch.

6.2.3 Protein Extraction and Western Blotting

To assess the protein changed in hiPSC-CMs after exposure to stretch, protein was extracted for Western Blot analysis. Cells were rinsed twice in cold PBS before being lysed at 4°C in a NP-40 lysis buffer consisting of 0.5% Nonidet P-40, 5% glycerol, 25 mM Tris (pH 7.4), 25 mM NaF, 225 mM NaCl, 0.025% sodium deoxycholate, 1 mM EDTA, 2 mM $NaVO_4$, and 1 mg/mL each of aprotinin, pepstatin, and leupeptin (Sigma-Aldrich). Cells were either lysed directly on the flexcell membranes in 100 µL lysis buffer for 5 minutes on ice before removing the lysate and placing it in a 1.6 mL eppendorf tube, or removed from the silicone membranes with a cell scraper and spun down in a 1.6mL eppendorf tube before adding 100 µL lysis buffer to the tube. Once in lysis buffer, all tubes were incubated for 15 minutes on an end-over-end rocker at 4°C. Lysate was then centrifuged for 15 minutes at 13-14 $x10^5$ RPM at 4°C. At the end of centrifugation, the supernatant was removed from the tubes and stored at -80°C until use for western blotting.

Total protein was assessed using a BCA protein assay (Pierce Biotechnology). 10 µg of protein was loaded into the lanes of a 4-20% Mini-Protean TGX 10-well gel (BioRad) for protein separation and transfer. Western blot was conducted by assessing using primary antibodies for the proteins connexin-43 (CX43), alpha sarcomeric actinin (αSA), α and β myosin heavy chain (MHC), sarcoplasmic reticulum Ca^{2+} ATPase (SERCA2A), and GAPDH. Blots were blocked in 5% blocking grade buffer (BioRad) with 0.1% Tween (Sigma-Aldrich), and horseradish-peroxidase conjugated secondary antibodies (GE Healthcare Life Science) and a chemiluminescence agent (Millipore). Expression intensity was analyzed using ImageJ software and normalized to expression of GAPDH.

6.2.4 Histology

For histological analysis, wells that were not harvested for protein analysis were rinsed twice with PBS and fixed in 4% paraformaldehyde (PFA) for 10 minutes at room temperature. Cell monolayers were permeabilized with 0.01% Triton-X-100 (Sigma), blocked in 5% Normal Donkey Serum (Jackson Immunoresearch), incubated for 60 minutes at room temperature in primary antibody followed by a 60 minute incubation in secondary antibody at room temperature and a 10 minute incubation in Hoescht 3332 (LifeTech). The silicone membranes were removed from the plates and inverted onto a glass slide with fluorescent mounting medium (Dako) for imaging on an inverted microscope.

6.2.4 Statistics

All data are presented as mean +/- standard deviation when sufficient sample sizes were available. Comparisons between statically cultured and stretches samples were conducted using Student's t-tests. P-values < 0.05 were considered significant.

6.3 Results

6.3.1 Adhesion of hiPSC-CMs to Pronectin-Conjugated Silicone membranes

6.3.1.1 24-well plates

When seeded directly from thaw into 24-well Flexcell plates, enough cells were available to fill all 24 wells of two plates. However, hiPSC-CMs did not adhere uniformly, with super-confluent cells clustered towards the center of the well and sparse to no cell adherence found toward the edges of the wells. Enough protein was harvested from each well to allow for western blot analysis.

To combat the issue of non-uniform seeding, cell-seeding inserts made by Flexcell were used to enhance cell seeding uniformity (Figure 6.2a). Cell-seeding inserts were placed in the base plate in place of loading posts and a small amount of vacuum (1% strain) was applied to hold the membranes taut during cell adhesion. Based on the results of the pre-plating experiments in Chapter 4, cells were allowed to adhere for 1 hour with the inserts before vacuum was

released and the plates cultured statically for 3 days, per standard protocol. This was not successful, and cells either did not adhere at all or adhered to the silicone with the same distribution as cells seeded without the seeding insert.

As an alternative method to seed cells into the plates at uniform distribution, cells were thawed into T75 flasks, per the standard thawing protocol outlined in chapter 4, and cultured for 3 days before being passaged and replated into the 24 well Flexcell plates at 100 x 10^5 cells/cm^2. There was a significant loss in cell number through this process, as ~20% of the CMs thawed into a flask can be recovered after 3 days in vitro, but CMs that did plate down did so in a relatively uniform manner. Thus, this approach was used for successive experiments with this setup.

6.3.1.2 6-well plates

Although the 24 well Flexcell plates allow for conservation of cells when running an experiment, a maximum of 8% stretch can be achieved with this system the only available loading posts are for biaxial stretch; there is no option for uniaxial stretch. Thus, 6 well plates were adapted to allow for the plating of cells in a confined region near the center of the well using silicone seeding rings as described in section 6.2.2.2. However, cell adhesion was very poor, with only 1 experiment of 4 having the hiPSC-CMs remain confluently adhered to the membranes for the duration of the study (Figure 6.3). Toxicity of the silicone seeding rings was ruled out, and after a thorough search of the literature and

available resources regarding Flexcell membrane coatings, it was found that in the deficiency was in the plate coatings themselves.

To accommodate for inconsistencies in the pronectin coatings, plates were re-coated with fibronectin prior to seeding cells onto the membranes. A number of conditions were attempted, and ultimately wells were coated overnight with EB20 media at 37ºC, followed by a rinse with PBS and then incubated again with 2.5 μg/cm^2 of fibronectin overnight on a shaker prior to seeding with cells. After the overnight coating, the fibronectin solution was removed and the wells were allowed to dry before placing the seeding rings in the wells and adding cells. The additional fibronectin coating interfered with the ability of the silicone seeding rings to form a tight seal with the underlying silicone membrane and nearly all wells had media leakage from the seeding rings in the first 24 hours of culture. However, this did not appear to affect the cell adhesion to the membranes, as all adherent cells were found within the bounds of the seeding rings, and cells adhered at confluence in these regions.

6.3.2 Changes in Protein Expression in Response to 7 days of 5% Biaxial Cyclic Stretching

6.3.2.1 24-Well Plates

When seeded directly from thaw into 24 well pronectin coated Flexcell plates (stretch initiated at day 3 of culture), an increase in the amount of αSA and near-significant increase in SERCA2A was found in samples that had been

exposed to 5% biaxial stretch. No difference was found in the presence of CX43, and insufficient sample size prevented any comparisons of MHCα, MHCβ, or the ratio of MHC α/β (Figure 6.4). Cells that were plated for 3 days prior to seeding into the flexcell plates (stretch initiated at day 6 of culture) did not generate enough replicates to draw conclusions, but data can be found in Figure 6.5.Cells that were cultured in flasks for 10 days prior to being replated into the Flexcell plates (stretch at day 13 post-thaw) resulted in decreases in the presence of αSA, MHCβ, SERCA2A, and an increase in the ratio of MHC α/β (Figure 6.6), contradicting both the results obtained when cells were plated directly from thaw and stretching was initiated at day 3 of culture, and any results that would be indicative of CM maturation.

6.3.2.1 6-Well Plates

Only one experiment was run with the 6-well plate setup, and this experiment was conducted without the additional fibronectin coating of the wells. These cells, plated from thaw into the flexcell plates (stretch initiation at day 3 post-thaw), showed an increase in the amount of αSA and SERCA2A in these cells, but a decrease in the amount of MHCβ (Figure 6.7).

6.4 Discussion and Future Work

No conclusions can be drawn from the data obtained to date investigating the use of stretch conditioning to induce maturation of hiPSC-CMs. Each experimental condition was run only once and thus it cannot be determined at

this time if the high degree of variability observed in these studies was an effect of the method of cell plating, time of stretch initiation, or inherent inter-experimental variability. It is evident from these preliminary trials that further optimization of cell seeding conditions, repeat experiments and higher sample numbers are required to elucidate the exact effect cyclic stretching has on hiPSC-CMs in a 2D environment.

Future work will utilize fibronectin-coated 6 well plates with cells thawed directly into the flexcell membranes. Not only will a comparison of statically cultured cells to those exposed to 5% biaxial stretch be investigated, but also the comparison of 5% and 10% biaxial stretch and 5% and 10% uniaxial stretch run side-by-side in the same experiment. Additional proteins will investigated, notably the isotype switch of cardiac troponin I (cTnI) from a slow skeletal isoform (ssTnI) to an adult phenotype (TnI), as it has recently been shown that this isotype switch can be used as a quantitative marker of cardiomyocyte maturation.[120] Relative presence of Kir2.1, an inward rectifier potassium channel, and Cav 1.2, one of the subunits of the L-type calcium channel, will also be assesses.

Through collaboration with the lab of Alena Talkachova (UMN Biomedical Engineering), optical mapping will be performed on these monolayers after the conclusions of the stretching regimen as a functional, electrophysiological measurement of cell maturation to complement the acquired protein data.

The only histological investigation conducted of thus far had been the assessment of the level of cell adherence. Future studies will label fixed cells for

αSA, CX43, and prelabeled with mitotracker to assess sarcomere size, CX43 organization, and the relative number of mitochondria in stretched and static cells. Sarcomere spacing should increase with cell maturation, CX43 expression should shift from being diffuse over the cell membrane to organized at cell-cell junctions, and the number of mitochondria should increase as CMs mature as a side effect of cellular hypertrophy and increased reliance on oxidative phosphorylation for energy production.

6.5 Figures

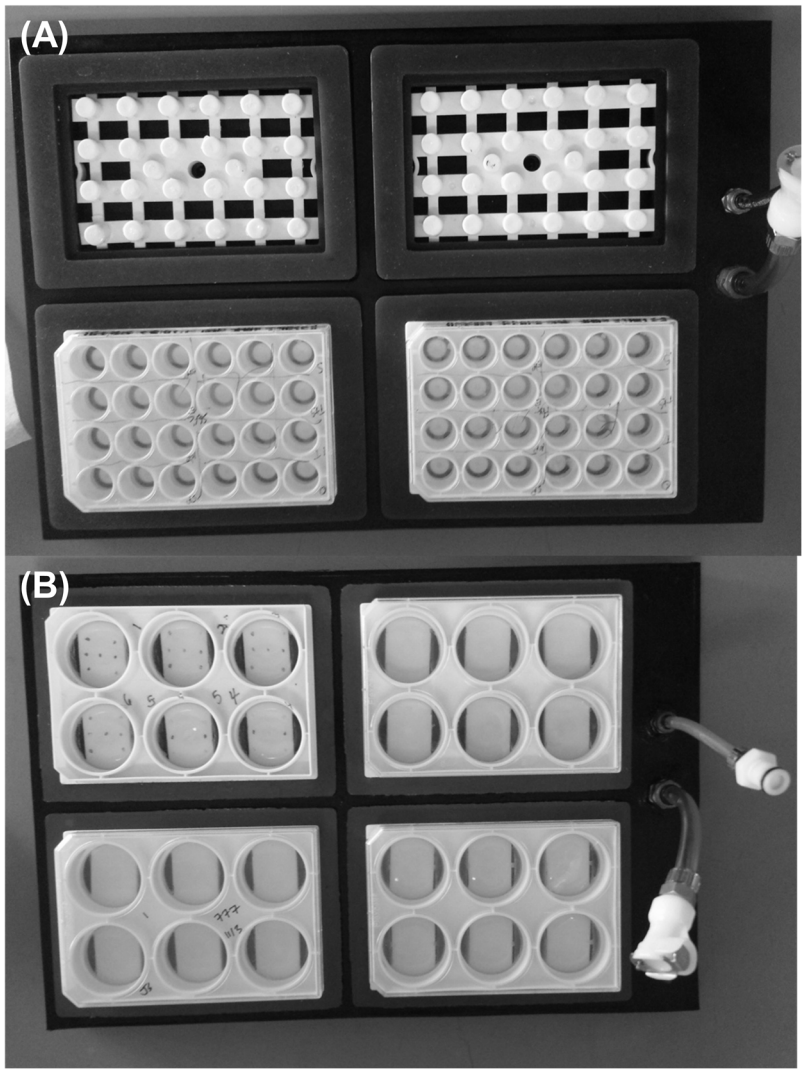

Figure 6.1: 24-well (A) and 6-well (B) Flexcell base plates with biaxial (A) and uniaxial (B) loading posts. Vacuum is applied through the inlet and outlet ports (A, B right side) to the back side of the silicone membranes, stretching them over the loading posts.

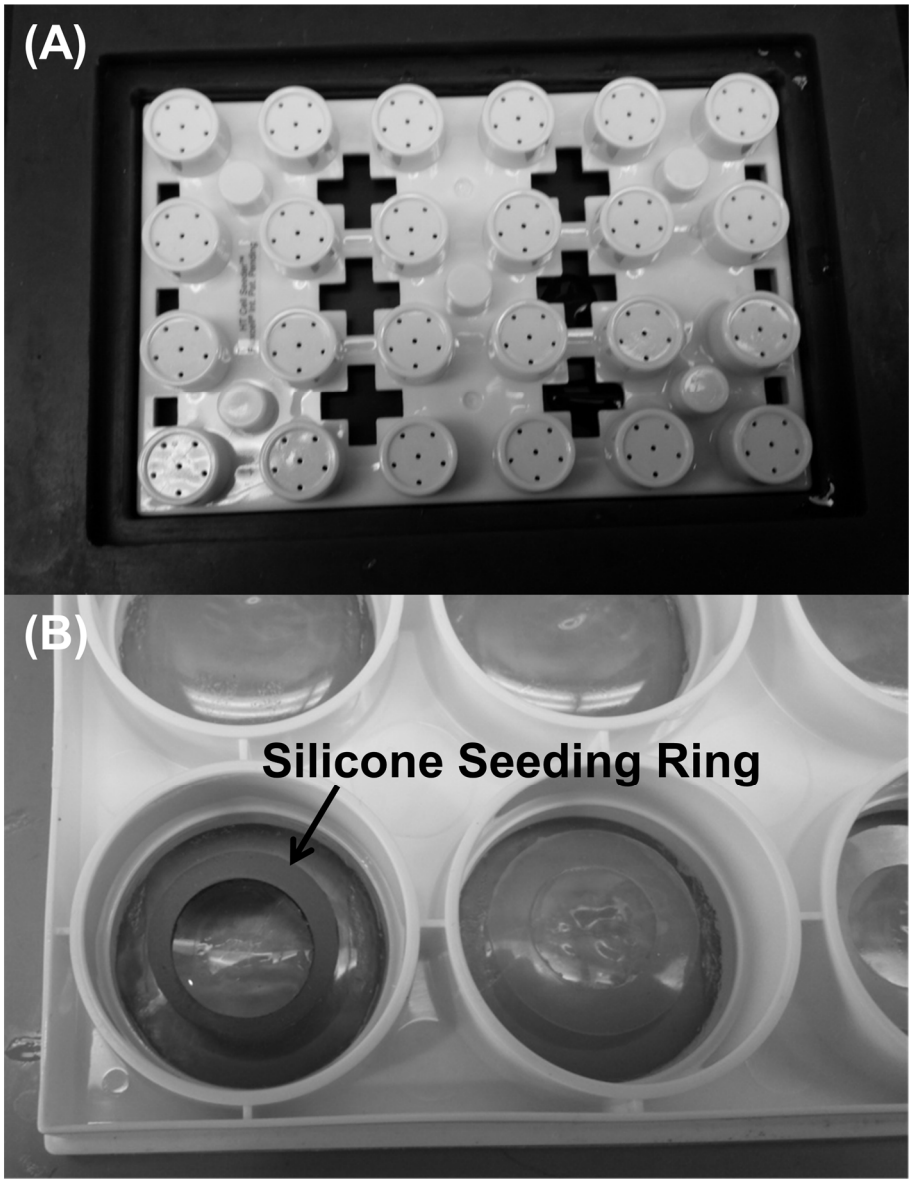

Figure 6.2: Cell Seeding Inserts for the 24-well system (A) and silicone seeding rings for the 6-well system (B). Cell suspension is placed inside the ring and incubated 24 hours before removing the ring and adding media to the entire well.

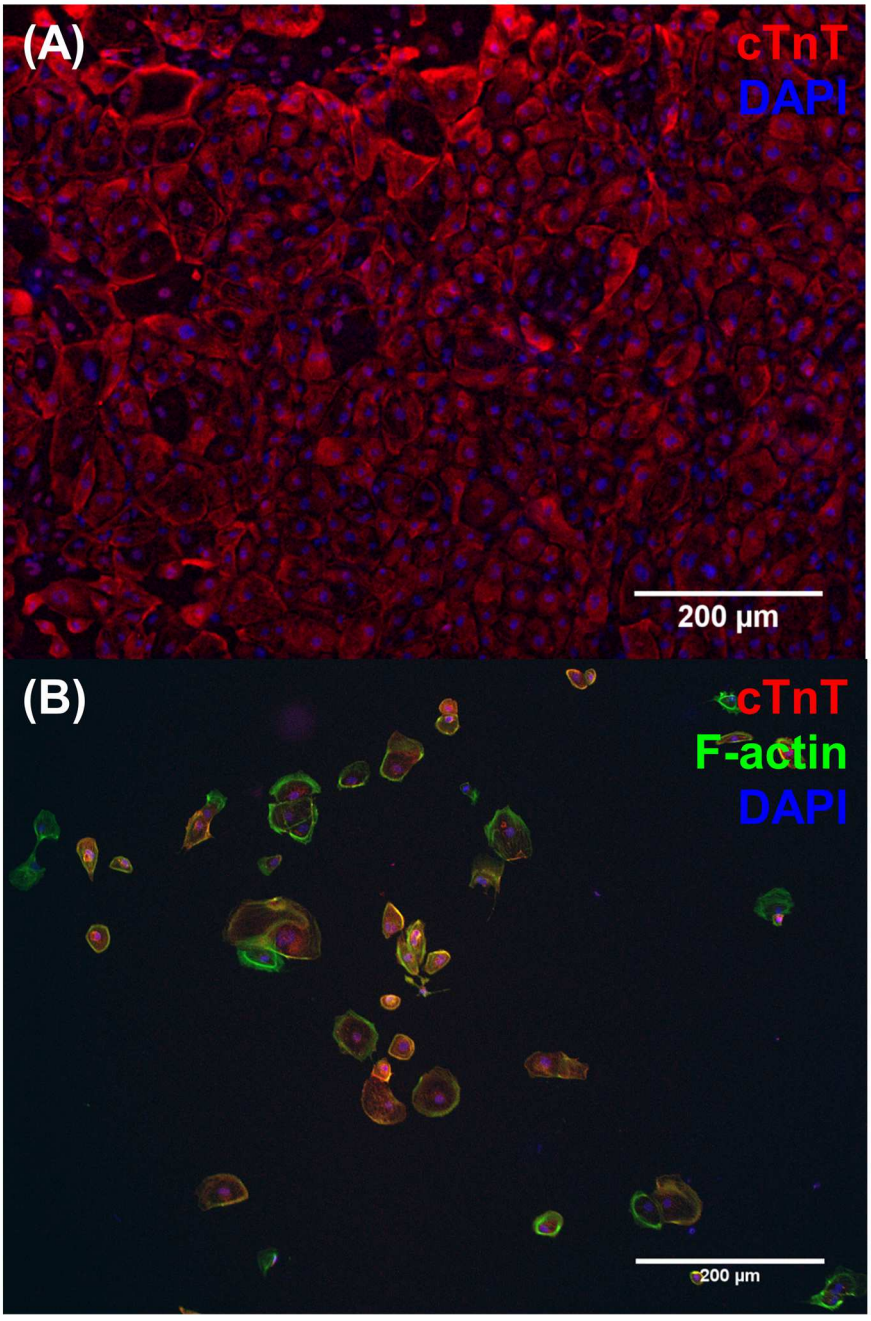

Figure 6.3: Representative images of successful (A) and unsuccessful (B) adhesion of hiPSC-CMs to the silicone membranes.

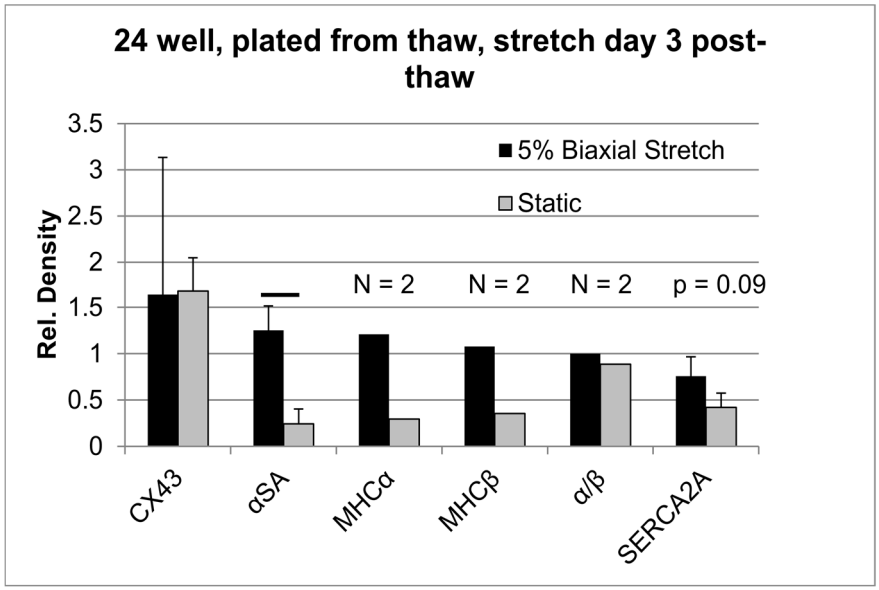

Figure 6. 4: Western blot protein analysis of hiPSC-CMs exposed to 5% biaxial stretch 3 days post-thaw and compared to statically cultured hiPSC-CMs. An increase in αSA was found in stretched samples compared to static. N=2-3.

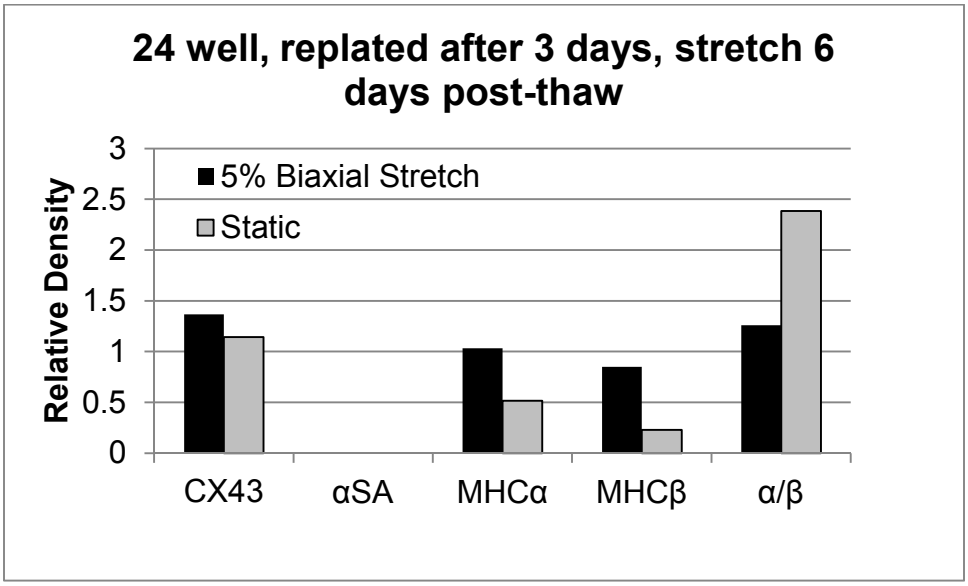

Figure 6. 5: Western blot protein analysis of hiPSC-CMs exposed to 5% biaxial stretch 6 days post-thaw and compared to statically cultured hiPSC-CMs. Insufficient sample sizes were available to make comparisons. N=2

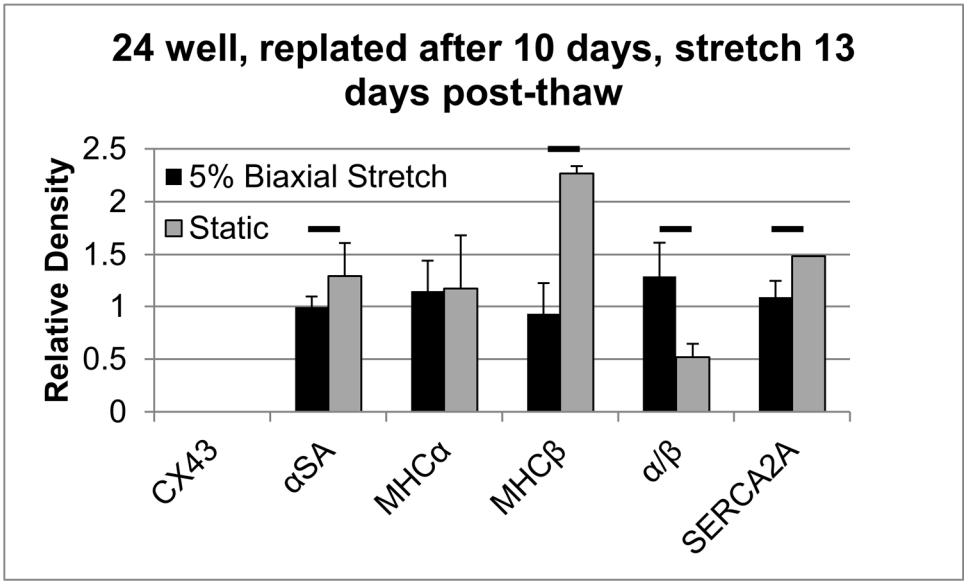

Figure 6.6: Western blot protein analysis of hiPSC-CMs exposed to 5% biaxial stretch 6 days post-thaw and compared to statically cultured hiPSC-CMs. A

decrease in the amount of αSA, MHCβ, SERCA2A, along with an increase in the ratio of MHC α/β was found in this study. N=3

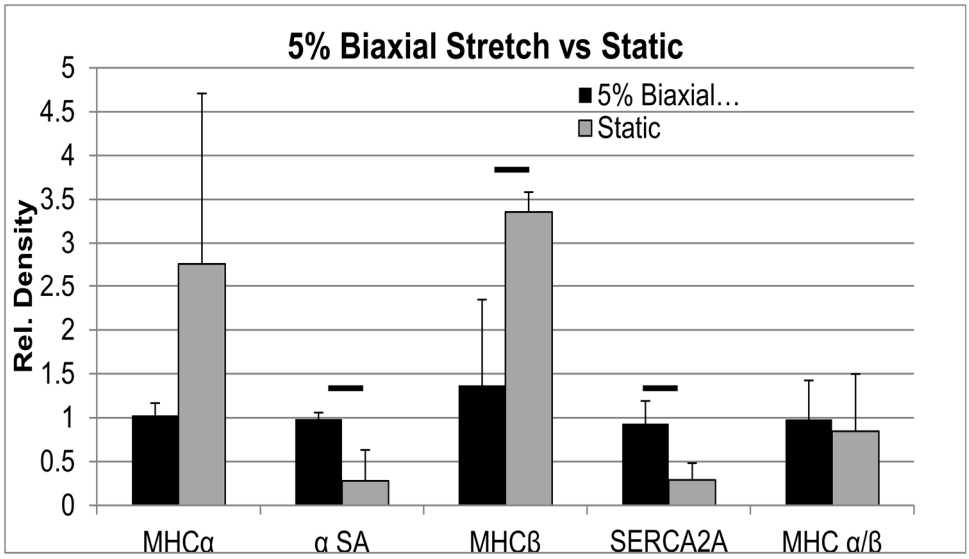

Figure 6.7: Western blot protein analysis of hiPSC-CMs exposed to 5% biaxial stretch 3 days post-thaw in 6-well plates and compared to statically cultured hiPSC-CMs. An increase in αSA and SERCA2A was observed in this study, along with a decrease in MHCβ. N=3-4

Chapter 7: Conclusions and Future Directions

7.1 Major Contributions

The work presented in this dissertation has had a sizeable contribution to the field of myocardial tissue engineering. Two manuscripts substantial manuscripts have been published, with one more in preparation, and this work has been presented at numerous oral and poster presentations at both internal and national conferences and meetings. The major conclusions from this work and its contribution to the literature are summarized here.

7.1.1 Contractile Force Generation of Neonatal Rat Cardiac Cell Patches Can be Increased Over 2-Fold through Cyclic Mechanical Stretch

This topic, included as supplemental material in a related publication[37] rather than a free-standing report, builds upon previous work establishing the ability to create aligned cardiac patches containing neonatal rat cardiac cells[5] and uses cyclic mechanical stimulation to increase the force generation of the cardiac patches (Chapter 2). Though similar techniques had been used elsewhere[44] and shown to induce some level of CM hypertrophy, this work verifies that cyclic stretching can be applied to fibrin-based engineered cardiac tissues and results in a increase in contractile force generation much larger than previous reports. This research also determined that the observed increase in force generation was sensitive to the amplitude of stretching and likely a stimulus

response rather than a sustained one, as the duration of stretching had no effect on the degree of force increase.

7.1.2 The Acute Implantation of a Cardiac Patch Containing Both Neonatal Rat Cardiomyocytes and Non-Cardiomyocytes Limits Left Ventricular Remodeling Post-Infarction

Following the work optimizing the neonatal rat cardiac cell patches detailed in chapter 2, this work assessed the capacity of a cardiac patch to not only survive in vivo after transplantation, but also to engraft and assist the injured myocardium post-infarction. It was found that not only do cells delivered to the myocardium via an engineered tissue engraft with high cell retention (36% survival at 4 weeks post-transplantation), but also have beneficial effects post-infarction, resulting in a limited infarct scar and preserved cardiac function with patch treatment.

The major finding and contribution of this work was that cardiomyocytes are required for the observed myocardial benefits, as a patch consisting of only non-cardiomyocytes resulted in reduced improvements. However, donor CMs were not coupled to the host myocardium, indicating a paracrine factor- mediated benefit of the patch originating from the co-culture of CMs and non-CMs.

7.1.3 A Fibrin-Based Cardiac Patch can be Constructed Using hiPSC-CMs

With the advent of iPSCs and the ability to differentiate them into beating cardiomyocytes, hiPSC-CMs became an attractive candidate for the creation of a

human cell-based cardiac patch. These cells had previously been entrapped in a collagen-matrigel scaffold with minimal elongation and contractile force generation. In the basic research covered in Chapter 4, we show that hiPSC-CMs can be entrapped in a fibrin gel without the support of additional growth factors, align, and generate forces higher than previously reported, albeit still substantially lower than the contractile forces generated by patches constructed with neonatal rat cardiomyocytes.

7.1.4 A Cardiac Patch Containing Both Purified hiPSC-CMs and PCs Engrafts Post-Transplantation with the Potential to Expand and Results in Improved Cardiac Function and Smaller Infarct Sizes

This work was the first publication in the literature that assessed the capacity of an engineered cardiac patch containing hiPSC-CMs to engraft and assist the injured myocardium post-infarction. As detailed in Chapter 5, we first demonstrated that hiPSC-CMs purified via lactate treatment can be co-entrapped with a defined non-CM cell population consisting of human PCs in a fibrin scaffold and over time can develop into a beating engineered tissue with static culture. When transplanted into a nude rat infarct model, patches containing both hiPSC-CMs and PCs resulted in improved cardiac function and smaller infarct sizes after 4 weeks in vivo compared to infarct-only controls. PC patches did not survive 4 weeks *in vivo* and provided no benefits to the host myocardium.

The major finding from this work was that transplanted hiPSC-CMs in CM+ PC patch recipient hearts successfully engrafted and 10.9% of imaged hiPSC-CMs were positive for Ki67, indicating some level of cell proliferation and/or cell maturation *in vivo*.

7.2 Future Directions

Although significant, much of the work detailed in this dissertation utilizing hiPSC-CMs remains preliminary and much work and further development is needed to bring hiPSC-CM based engineered tissues towards clinical trials and relevance.

7.2.1 Optimization of hiPSC-CM Patches

Although patches utilizing hiPSC-CMs were successfully created and transplanted in the work covered in this dissertation, the quality of these patches was far from optimal. Entrapped CMs remained small, with limited elongation and force generation. These insufficiencies may be due to a number of factors, including, but not limited to matrix properties, cell densities and culture conditions. The same basic gel formulation and CM seeding density as the neonatal rat cell patches was used in this work to enable side-by-side comparisons of the two cell types when entrapped in a fibrin scaffold. However, these conditions may not be optimal for hiPSC-CMs. Also, the culture media used in this work was the basic culture media used to culture cells when in 2D culture. No additional growth factors or media supplementation was used when

culturing these cells in a 3-dimensional environment, save the addition of ACA to limit fibronolysis. Additional media supplementation may be required to increase force generation For example, neonatal rat cardiac cell patches were supplemented with insulin and ascorbic acid to promote matrix deposition.

It can also be noted that the neonatal rat cardiac cell patches were stretch-conditioned prior to implantation while the hiPSC-CM patches were statically cultured. Future work will expand upon the preliminary 2D studies outlined in Chapter 6 to investigate the effect of cyclic stretching not only on hiPSC-CM maturation, but also on force generation when entrapped in a 3D matrix. Physiological hypertrophy is a component of CM maturation and leads to an increase in cell size and contractile force generation. Utilizing the methods available, hiPSC-CMs can be either pre-conditioned (stretch in 2D prior to entrapment in fibrin), exposed to stretch post-entrapment as in Chapter 2, or a combination of the two methods. Optimal stretching regimens will also need to be established to obtain the desired results.

7.2.2 Combination of a hiPSC-CM Patch with a Microvascular Patch to Enable the Creation of Large-Scale Engineered Cardiac Tissues

In order for the cardiac patches outlined in this dissertation to become clinically relevant, patches must be able to be created in larger sizes and thicknesses. Current patches rely on diffusion for oxygen and nutrient supply, limiting the thickness of the patch to > 1mm. In order to create larger scale

patches, a functional, perfusable microvasculature must be established within the patch to provide CMs throughout the thickness with oxygen and avoid a central necrotic region of the patch. Much work has already been completed in the creation of a microvessel network in fibrin gels[48], and the next steps will be to merge this patch with the patches created in this body of work. This will likely be no easy task, as both patches either have or will require significant optimization to obtain the optimal results from each individual cell type and finding optimal conditions to maintain both hiPSC-CMs and a microvessel network in vitro will be a significant undertaking.

7.2.3 Long Term and Large Animal Preclinical Models

The translational, animal studies covered in this dissertation are preliminary studies only and limited by the choice of animal model and the 4 week time scale. The rat model was chosen as a preliminary animal model due to its small size, limiting the number of cells required to complete these initial proof-of-concept studies. However, transplanting human cardiomyocytes into a rat model is not ideal, as human CMs, especially immature CMs, have lower native beating frequencies (<100 bpm) than rodent hearts (>400 bpm), potentially providing a basis for arrhythmic events and making it difficult to assess events originating from the patch. In order to fully assess patch engraftment, electrophysiological integration and long term effects of patch transplantation on donor myocardium.

References:

1. Caulfield JB, Leinbach R, Gold H. The relationship of myocardial infarct size and prognosis. *Circulation*. 1976;53:I141-144
2. Miniati DN, Robbins RC. Heart transplantation: A thirty-year perspective. *Annu. Rev. Med.* 2011;53:189-205
3. Reinecke H, Murry CE. Taking the death toll after cardiomyocyte grafting: A reminder of the importance of quantitative biology. *Journal of molecular and cellular cardiology*. 2002;34:251-253
4. Zimmermann WH, Melnychenko I, Wasmeier G, Didie M, Naito H, Nixdorff U, Hess A, Budinsky L, Brune K, Michaelis B, Dhein S, Schwoerer A, Ehmke H, Eschenhagen T. Engineered heart tissue grafts improve systolic and diastolic function in infarcted rat hearts. *Nature medicine*. 2006;12:452-458
5. Black LD, 3rd, Meyers JD, Weinbaum JS, Shvelidze YA, Tranquillo RT. Cell-induced alignment augments twitch force in fibrin gel-based engineered myocardium via gap junction modification. *Tissue engineering. Part A*. 2009;15:3099-3108
6. Brown MA, Iyer, Rohin K., Radisic, M. Pulsatile perfusion bioreactor for cardiac tissue engineering. *Biotechnology progress*. 2008;2008:907-920
7. Evans MJ, Kaufman MH. Establishment in culture of pluripotential cells from mouse embryos. *Nature*. 1981;292:154-156
8. Thomson JA, Itskovitz-Eldor J, Shapiro SS, Waknitz MA, Swiergiel JJ, Marshall VS, Jones JM. Embryonic stem cell lines derived from human blastocysts. *Science*. 1998;282:1145-1147
9. Kehat I, Kenyagin-Karsenti D, Snir M, Segev H, Amit M, Gepstein A, Livne E, Binah O, Itskovitz-Eldor J, Gepstein L. Human embryonic stem cells can differentiate into myocytes with structural and functional properties of cardiomyocytes. *The Journal of Clinical Investigation*. 2001;108:407-414
10. Tulloch NL, Muskheli V, Razumova MV, Korte FS, Regnier M, Hauch KD, Pabon L, Reinecke H, Murry CE. Growth of engineered human myocardium with mechanical loading and vascular coculture. *Circ Res*. 2011;109:47-59
11. Liau B, Christoforou N, Leong KW, Bursac N. Pluripotent stem cell-derived cardiac tissue patch with advanced structure and function. *Biomaterials*. 2011;32:9180-9187
12. Takahashi K, Yamanaka S. Induction of pluripotent stem cells from mouse embryonic and adult fibroblast cultures by defined factors. *Cell*. 2006;126:663-676
13. Yu J, Vodyanik MA, Smuga-Otto K, Antosiewicz-Bourget J, Frane JL, Tian S, Nie J, Jonsdottir GA, Ruotti V, Stewart R, Slukvin, II, Thomson JA. Induced pluripotent stem cell lines derived from human somatic cells. *Science*. 2007;318:1917-1920
14. Takahashi K, Tanabe K, Ohnuki M, Narita M, Ichisaka T, Tomoda K, Yamanaka S. Induction of pluripotent stem cells from adult human fibroblasts by defined factors. *Cell*. 2007;131:861-872
15. Zhang J, Wilson GF, Soerens AG, Koonce CH, Yu J, Palecek SP, Thomson JA, Kamp TJ. Functional cardiomyocytes derived from human induced pluripotent stem cells. *Circ Res*. 2009;104:e30-41

16. Zhang J, Klos M, Wilson GF, Herman AM, Lian X, Raval KK, Barron MR, Hou L, Soerens AG, Yu J, Palecek SP, Lyons GE, Thomson JA, Herron TJ, Jalife J, Kamp TJ. Extracellular matrix promotes highly efficient cardiac differentiation of human pluripotent stem cells: The matrix sandwich method. *Circ Res*. 2012;111:1125-1136
17. Lian X, Zhang J, Azarin SM, Zhu K, Hazeltine LB, Bao X, Hsiao C, Kamp TJ, Palecek SP. Directed cardiomyocyte differentiation from human pluripotent stem cells by modulating wnt/beta-catenin signaling under fully defined conditions. *Nature protocols*. 2013;8:162-175
18. Leri A, Kajstura J, Anversa P. Cardiac stem cells and mechanisms

of myocardial regeneration. *Physiol Rev*. 2005;85:1373-1416
19. Beltrami AP, Barlucchi L, Torella D, Baker M, Limana F, Chimenti S, Kasahara H, Rota M, Musso E, Urbanek K, Leri A, Kajstura J, Nadal-Ginard B, Anversa P. Adult cardiac stem cells are multipotent and support myocardial regeneration. *Cell*. 2003;114:763-776
20. Oh H, Bradfute SB, Gallardo TD, Nakamura T, Gaussin V, Mishina Y, Pocius J, Michael LH, Behringer RR, Garry DJ, Entman ML, Schneider MD. Cardiac progenitor cells from adult myocardium: Homing, differentiation, and fusion after infarction. *Proceedings of the National Academy of Sciences*. 2003;100:12313-12318
21. Laugwitz K-L, Moretti A, Lam J, Gruber P, Chen Y, Woodard S, Lin L-Z, Cai C-L, Lu MM, Reth M, Platoshyn O, Yuan JX-J, Evans S, Chien KR. Postnatal isl1+ cardioblasts enter fully differentiated cardiomyocyte. *Nature*. 2005;433:647-653
22. Messina E, De Angelis L, Frati G, Morrone S, Chimenti S, Fiordaliso F, Salio M, Battaglia M, Latronico MVG, Coletta M, Vivarelli E, Frati L, Cossu G, Giacomello A. Isolation and expansion of adult cardiac stem cells from human and murine heart. *Circulation Research*. 2004;95:911-921
23. Gaetani R, Doevendans PA, Metz CH, Alblas J, Messina E, Giacomello A, Sluijter JP. Cardiac tissue engineering using tissue printing technology and human cardiac progenitor cells. *Biomaterials*. 2012;33:1782-1790
24. Banerjee I, Fuseler JW, Price RL, Borg TK, Baudino TA. Determination of cell types and numbers during cardiac development in the neonatal and adult rat and mouse. *American journal of physiology. Heart and circulatory physiology*. 2007;293:H1883–H1891
25. Zhang D, Shadrin IY, Lam J, Xian HQ, Snodgrass HR, Bursac N. Tissue-engineered cardiac patch for advanced functional maturation of human esc-derived cardiomyocytes. *Biomaterials*. 2013;34:5813-5820
26. Morin KT, Tranquillo RT. Guided sprouting from endothelial spheroids in fibrin gels aligned by magnetic fields and cell-induced gel compaction. *Biomaterials*. 2011;32:6111-6118
27. Chouinard JA, Gagnon S, Couture MG, Levesque A, Vermette P. Design and validation of a pulsatile perfusion bioreactor for 3d high cell density cultures. *Biotechnology and bioengineering*. 2009;104:1215-1223
28. Stratman AN, Malotte KM, Mahan RD, Davis MJ, Davis GE. Pericyte recruitment during vasculogenic tube assembly stimulates endothelial basement membrane matrix formation. *Blood*. 2009;114:5091-5101

29. Kellar RS, Landeen LK, Shepherd BR, Naughton GK, Ratcliffe A, Williams SK. Scaffold-based three-dimensional human fibroblast culture provides a structural matrix that supports angiogenesis in infarcted heart tissue. *Circulation*. 2001;104:2063-2068
30. Yeong W, Sudarmadji N, Yu H, Chua C, Leong K, Venkatraman S, Boey Y, Tan L. Porous polycaprolactone scaffold for cardiac tissue engineering fabricated by selective laser sintering. *Acta Biomaterialia*. 2010;6:2028-2034
31. Engelmayr GC, Jr., Cheng M, Bettinger CJ, Borenstein JT, Langer R, Freed LE. Accordion-like honeycombs for tissue engineering of cardiac anisotropy. *Nature materials*. 2008;7:1003-1010
32. Caspi O, Lesman A, Basevitch Y, Gepstein A, Arbel G, Habib IH, Gepstein L, Levenberg S. Tissue engineering of vascularized cardiac muscle from human embryonic stem cells. *Circ Res*. 2007;100:263-272
33. Radisic M, Euloth M, Yang L, Langer R, Freed LE, Vunjak-Novakovic G. High-density seeding of myocyte cells for cardiac tissue engineering. *Biotechnology and bioengineering*. 2003;82:403-414
34. Dar A, Shachar M, Leor J, Cohen S. Optimization of cardiac cell seeding and distribution in 3d porous alginate scaffolds. *Biotechnology and bioengineering*. 2002;80:305-312
35. Li R-K, Jia Z-Q, Weisel RD, Mickle DAG, Choi A, Yau TM. Survival and function of bioengineered cardiac grafts. *Circulation*. 1999;100:II-63-Ii-69
36. Ifkovits JL, Devlin JJ, Eng G, Martens TP, Vunjak-Novakovic G, Burdick JA. Biodegradable fibrous scaffolds with tunable properties formed from photo-cross-linkable poly(glycerol sebacate). *ACS applied materials & interfaces*. 2009;1:1878-1886
37. Wendel JS, Ye L, Zhang P, Tranquillo RT, Zhang JJ. Functional consequences of a tissue-engineered myocardial patch for cardiac repair in a rat infarct model. *Tissue engineering. Part A*. 2014
38. Boudou T, Legant WR, Mu A, Borochin MA, Thavandiran N, Radisic M, Zandstra PW, Epstein JA, Margulies KB, Chen CS. A microfabricated platform to measure and manipulate the mechanics of engineered cardiac microtissues. *Tissue engineering. Part A*. 2012;18:910-919
39. Zimmermann WH. Tissue engineering of a differentiated cardiac muscle construct. *Circulation Research*. 2001;90:223-230
40. Ott HC, Matthiesen TS, Goh SK, Black LD, Kren SM, Netoff TI, Taylor DA. Perfusion-decellularized matrix: Using nature's platform to engineer a bioartificial heart. *Nature medicine*. 2008;14:213-221
41. Duan Y, Liu Z, O'Neill J, Wan LQ, Freytes DO, Vunjak-Novakovic G. Hybrid gel composed of native heart matrix and collagen induces cardiac differentiation of human embryonic stem cells without supplemental growth factors. *Journal of cardiovascular translational research*. 2011;4:605-615
42. Sekine H, Shimizu T, Hobo K, Sekiya S, Yang J, Yamato M, Kurosawa H, Kobayashi E, Okano T. Endothelial cell coculture within tissue-engineered cardiomyocyte sheets enhances neovascularization and improves cardiac function of ischemic hearts. *Circulation*. 2008;118:S145-152
43. Stevens KR, Kreutziger KL, Dupras SK, Korte FS, Regnier M, Muskheli V, Nourse MB, Bendixen K, Reinecke H, Murry CE. Physiological function and

transplantation of scaffold-free and vascularized human cardiac muscle tissue. *Proceedings of the National Academy of Sciences of the United States of America*. 2009;106:16568-16573
44. FINK C, ERGÜN S, KRALISCH D, REMMERS U, WEIL J, ESCHENHAGEN T. Chronic stretch of engineered heart tissue induces hypertrophy and functional improvement. *The FASEB Journal*. 2000;14:669 -679
45. Chiu LLY, Iyer RK, King J-P, Radisic M. Biphasic electrical field stimulation aids in tissue engineering of multicell-type cardiac organoids. *Tissue Engineering Part A*. 2011;17:1465-1477
46. Dvir T, Levy O, Shachar M, Granot Y, Cohen S. Activation of the erk1/2 cascade via pulsatile interstitial fluid flow promotes cardiac tissue assembly. *Tissue engineering*. 2007;13:2185-2193
47. Kolesky DB, Truby RL, Gladman AS, Busbee TA, Homan KA, Lewis JA. 3d bioprinting of vascularized, heterogeneous cell-laden tissue constructs. *Advanced Materials*. 2014:n/a-n/a
48. Morin KT, Dries-Devlin JL, Tranquillo RT. Engineered microvessels with strong alignment and high lumen density via cell-induced fibrin gel compaction and interstitial flow. *Tissue engineering. Part A*. 2014;20:553-565
49. Moya ML, Hsu YH, Lee AP, Hughes CC, George SC. In vitro perfused human capillary networks. *Tissue engineering. Part C, Methods*. 2013;19:730-737
50. Raghavan S, Nelson CM, Baranski JD, Lim E, Chen CS. Geometrically controlled endothelial tubulogenesis in micropatterned gels. *Tissue engineering. Part A*. 2010;16:2255-2263
51. Vantler M, Karikkineth BC, Naito H, Tiburcy M, Didie M, Nose M, Rosenkranz S, Zimmermann WH. Pdgf-bb protects cardiomyocytes from apoptosis and improves contractile function of engineered heart tissue. *Journal of molecular and cellular cardiology*. 2010;48:1316-1323
52. Morgan KY, Black LD. Mimicking isovolumic contraction with combined electromechanical stimulation improves the development of engineered cardiac constructs. *Tissue engineering. Part A*. 2014
53. Barash Y, Dvir T, Tandeitnik P, Ruvinov E, Guterman H, Cohen S. Electric field stimulation integrated into perfusion bioreactor for cardiac tissue engineering. *Tissue Engineering Part C: Methods*. 2011;16:1417-1426
54. Shapira-Schweitzer K, Habib M, Gepstein L, Seliktar D. A photopolymerizable hydrogel for 3-d culture of human embryonic stem cell-derived cardiomyocytes and rat neonatal cardiac cells. *Journal of molecular and cellular cardiology*. 2009;46:213-224
55. Milica Radisic PD, Vladimir G. Fast, Ph.D., Oleg F. Sharifov, Ph.D., Rohin K. Iyer, B.A.Sc., Hyoungshin Park, Ph.D., and Gordana Vunjak-Novakovic, Ph.D. Optical mapping of impulse propagation

in engineered cardiac tissue. *Tissue engineering. Part A*. 2009;15
56. Herron TJ, Lee P, Jalife J. Optical imaging of voltage and calcium in cardiac cells & tissues. *Circulation Research*. 2012;110:609-623
57. Sekine H, Shimizu T, Dobashi I, Matsuura K, Hagiwara N, Takahashi M, Kobayashi E, Yamato M, Okano T. Cardiac cell sheet transplantation improves

damaged heart function via superior cell survival in comparison with dissociated cell injection. *Tissue engineering. Part A*. 2011;17:2973-2980
58. Mihic A, Li J, Miyagi Y, Gagliardi M, Li SH, Zu J, Weisel RD, Keller G, Li RK. The effect of cyclic stretch on maturation and 3d tissue formation of human embryonic stem cell-derived cardiomyocytes. *Biomaterials*. 2014;35:2798-2808
59. Kawamura M, Miyagawa S, Miki K, Saito A, Fukushima S, Higuchi T, Kawamura T, Kuratani T, Daimon T, Shimizu T, Okano T, Sawa Y. Feasibility, safety, and therapeutic efficacy of human induced pluripotent stem cell-derived cardiomyocyte sheets in a porcine ischemic cardiomyopathy model. *Circulation*. 2012;126:S29-S37
60. Hasenfuss G, Mulieri LA, Blanchard EM, Holubarsch C, Leavitt BJ, Ittleman F, Alpert NR. Energetics of isometric force development in control and volume-overload human myocardium. Comparison with animal species. *Circulation Research*. 1991;68:836-846
61. Reinecke H, Zhang M, Bartosek T, Murry CE. Survival, integration, and differentiation of cardiomyocyte grafts: A study in normal and injured rat hearts. *Circulation*. 1999;100:193-202
62. Guo XM, Zhao YS, Chang HX, Wang CY, E LL, Zhang XA, Duan CM, Dong LZ, Jiang H, Li J, Song Y, Yang XJ. Creation of engineered cardiac tissue in vitro from mouse embryonic stem cells. *Circulation*. 2006;113:2229-2237
63. Isenberg BC, Tranquillo RT. Long-term cyclic distention enhances the mechanical properties of collagen-based media-equivalents. *Annals of biomedical engineering*. 2003;31:937-949
64. Naito H, Melnychenko I, Didie M, Schneiderbanger K, Schubert P, Rosenkranz S, Eschenhagen T, Zimmermann WH. Optimizing engineered heart tissue for therapeutic applications as surrogate heart muscle. *Circulation*. 2006;114:I72-78
65. Murry CE, Whitney ML, Laflamme MA, Reinecke H, Field LJ. Cellular therapies for myocardial infarct repair. *Cold Spring Harb Symp Quant Biol*. 2002;67:519-526
66. Tang XL, Rokosh G, Sanganalmath SK, Yuan F, Sato H, Mu J, Dai S, Li C, Chen N, Peng Y, Dawn B, Hunt G, Leri A, Kajstura J, Tiwari S, Shirk G, Anversa P, Bolli R. Intracoronary administration of cardiac progenitor cells alleviates left ventricular dysfunction in rats with a 30-day-old infarction. *Circulation*.121:293-305
67. Robey TE, Saiget MK, Reinecke H, Murry CE. Systems approaches to preventing transplanted cell death in cardiac repair. *Journal of molecular and cellular cardiology*. 2008;45:567-581
68. Simpson D, Liu H, Fan T-HM, Nerem R, Dudley SC. A tissue engineering approach to progenitor cell delivery results in significant cell engraftment and improved myocardial remodeling. *Stem Cells*. 2007;25:2350-2357 %U http://dx.doi.org/2310.1634/stemcells.2007-0132
69. Nakamura Y, Wang X, Xu C, Asakura A, Yoshiyama M, From AH, Zhang J. Xenotransplantation of long-term-cultured swine bone marrow-derived mesenchymal stem cells. *Stem Cells*. 2007;25:612-620
70. Phillips CA, Petrofsky JS. Myocardial material mechanics: Characteristic variation of the circumferential and longitudinal systolic moduli in left ventricular dysfunction. *Journal of Biomechanics*. 1984;17:561-568

71. Jalil JE, Doering CW, Janicki JS, Pick R, Shroff SG, Weber KT. Fibrillar collagen and myocardial stiffness in the intact hypertrophied rat left ventricle. *Circulation Research*. 1989;64:1041-1050
72. Muller-Ehmsen J, Whittaker P, Kloner RA, Dow JS, Sakoda T, Long TI, Laird PW, Kedes L. Survival and development of neonatal rat cardiomyocytes transplanted into adult myocardium. *Journal of molecular and cellular cardiology*. 2002;34:107-116
73. Toma C, Pittenger MF, Cahill KS, Byrne BJ, Kessler PD. Human mesenchymal stem cells differentiate to a cardiomyocyte phenotype in the adult murine heart. *Circulation*. 2002;105:93-98
74. Zeng L, Hu Q, Wang X, Mansoor A, Lee J, Feygin J, Zhang G, Suntharalingam P, Boozer S, Mhashilkar A, Panetta CJ, Swingen C, Deans R, From AH, Bache RJ, Verfaillie CM, Zhang J. Bioenergetic and functional consequences of bone marrow-derived multipotent progenitor cell transplantation in hearts with postinfarction left ventricular remodeling. *Circulation*. 2007;115:1866-1875
75. Hatzistergos KE, Quevedo H, Oskouei BN, Hu Q, Feigenbaum GS, Margitich IS, Mazhari R, Boyle AJ, Zambrano JP, Rodriguez JE, Dulce R, Pattany PM, Valdes D, Revilla C, Heldman AW, McNiece I, Hare JM. Bone marrow mesenchymal stem cells stimulate cardiac stem cell proliferation and differentiation. *Circ Res*. 2010;107:913-922
76. Mouquet F, Pfister O, Jain M, Oikonomopoulos A, Ngoy S, Summer R, Fine A, Liao R. Restoration of cardiac progenitor cells after myocardial infarction by self-proliferation and selective homing of bone marrow-derived stem cells. *Circ Res*. 2005;97:1090-1092
77. Pfister O, Mouquet F, Jain M, Summer R, Helmes M, Fine A, Colucci WS, Liao R. Cd31- but not cd31+ cardiac side population cells exhibit functional cardiomyogenic differentiation. *Circ Res*. 2005;97:52-61
78. Wang X, Hu Q, Nakamura Y, Lee J, Zhang G, From AH, Zhang J. The role of the sca-1+/cd31- cardiac progenitor cell population in postinfarction left ventricular remodeling. *Stem Cells*. 2006;24:1779-1788
79. Neidert MR, Lee ES, Oegema TR, Tranquillo RT. Enhanced fibrin remodeling in vitro with tgf-β1, insulin and plasmin for improved tissue-equivalents. *Biomaterials*. 2002;23:3717-3731
80. Grassl ED, Oegema TR, Tranquillo RT. Fibrin as an alternative biopolymer to type-i collagen for the fabrication of a media equivalent. *Journal of biomedical materials research*. 2002;60:607-612
81. WIMAN B, COLLEN D. Molecular mechanism of physiological fibrinolysis. *Nature*. 1978;272:549-550
82. Ye Q, Zünd G, Benedikt P, Jockenhoevel S, Hoerstrup SP, Sakyama S, Hubbell JA, Turina M. Fibrin gel as a three dimensional matrix in cardiovascular tissue engineering. *European Journal of Cardio-Thoracic Surgery*. 2000;17:587-591
83. Grassl ED, Oegema TR, Tranquillo RT. A fibrin-based arterial media equivalent. *Journal of Biomedical Materials Research Part A*. 2003;66A:550-561
84. Zhang D, Shadrin IY, Lam J, Xian H-Q, Snodgrass HR, Bursac N. Tissue-engineered cardiac patch for advanced functional maturation of human esc-derived cardiomyocytes. *Biomaterials*. 2013;34:5813-5820

85. Cheng W, Li B, Kajstura J, Li P, Wolin MS, Sonnenblick EH, Hintze TH, Olivetti G, Anversa P. Stretch-induced programmed myocyte cell death. *The Journal of Clinical Investigation*. 1995;96:2247-2259
86. Feygin J, Mansoor A, Eckman P, Swingen C, Zhang J. Functional and bioenergetic modulations in the infarct border zone following autologous mesenchymal stem cell transplantation. *American Journal of Physiology - Heart and Circulatory Physiology*. 2007;293:H1772-H1780
87. Feygin J, Hu Q, Swingen C, Zhang J. Relationships between regional myocardial wall stress and bioenergetics in hearts with left ventricular hypertrophy. *American Journal of Physiology - Heart and Circulatory Physiology*. 2008;294:H2313-H2321
88. Kakkar R, Lee RT. Intramyocardial fibroblast myocyte communication. *Circ Res*. 2010;106:47-57
89. Mirotsou M, Jayawardena TM, Schmeckpeper J, Gnecchi M, Dzau VJ. Paracrine mechanisms of stem cell reparative and regenerative actions in the heart. *Special Issue: Cardiovascular Stem Cells Revisited*. 2011;50:280-289
90. Nichol JW, Engelmayr GC, Jr., Cheng M, Freed LE. Co-culture induces alignment in engineered cardiac constructs via mmp-2 expression. *Biochemical and biophysical research communications*. 2008;373:360-365
91. Plotnikov EY, Khryapenkova TG, Vasileva AK, Marey MV, Galkina SI, Isaev NK, Sheval EV, Polyakov VY, Sukhikh GT, Zorov DB. Cell-to-cell cross-talk between mesenchymal stem cells and cardiomyocytes in co-culture. *Journal of cellular and molecular medicine*. 2008;12:1622-1631
92. Ruwhof C, van Wamel AET, Egas JM, van der Laarse A. Cyclic stretch induces the release of growth promoting factors from cultured neonatal cardiomyocytes and cardiac fibroblasts. *Molecular and cellular biochemistry*. 2000;208:89-98
93. van Wamel AET, Ruwhof C, van der Valk-Kokshoorn LM, Schrier P, van der Laarse A. Stretch-induced paracrine hypertrophic stimuli increase tgf-β1 expression in cardiomyocytes. *Molecular and Cellular Biochemistry*. 2002;236:147-153
94. Roger VL, Go AS, Lloyd-Jones DM, Benjamin EJ, Berry JD, Borden WB, Bravata DM, Dai S, Ford ES, Fox CS, Fullerton HJ, Gillespie C, Hailpern SM, Heit JA, Howard VJ, Kissela BM, Kittner SJ, Lackland DT, Lichtman JH, Lisabeth LD, Makuc DM, Marcus GM, Marelli A, Matchar DB, Moy CS, Mozaffarian D, Mussolino ME, Nichol G, Paynter NP, Soliman EZ, Sorlie PD, Sotoodehnia N, Turan TN, Virani SS, Wong ND, Woo D, Turner MB. Heart disease and stroke statistics--2012 update: A report from the american heart association. *Circulation*. 2012;125:e2-e220
95. Zhang L, Guo J, Zhang P, Xiong Q, Wu SC, Xia L, Roy SS, Tolar J, O'Connell TD, Kyba M, Liao K, Zhang J. Derivation and high engraftment of patient-specific cardiomyocyte sheet using induced pluripotent stem cells generated from adult cardiac fibroblast. *Circulation: Heart Failure*. 2015;8:156-166
96. Anderson D, Self T, Mellor IR, Goh G, Hill SJ, Denning C. Transgenic enrichment of cardiomyocytes from human embryonic stem cells. *Mol Ther*. 2007;15:2027-2036
97. Huber I, Itzhaki I, Caspi O, Arbel G, Tzukerman M, Gepstein A, Habib M, Yankelson L, Kehat I, Gepstein L. Identification and selection of cardiomyocytes

during human embryonic stem cell differentiation. *The FASEB Journal*. 2007;21:2551-2563
98. Elliott DA, Braam SR, Koutsis K, Ng ES, Jenny R, Lagerqvist EL, Biben C, Hatzistavrou T, Hirst CE, Yu QC, Skelton RJP, Ward-van Oostwaard D, Lim SM, Khammy O, Li X, Hawes SM, Davis RP, Goulburn AL, Passier R, Prall OWJ, Haynes JM, Pouton CW, Kaye DM, Mummery CL, Elefanty AG, Stanley EG. Nkx2-5egfp/w hescs for isolation of human cardiac progenitors and cardiomyocytes. *Nat Meth*. 2011;8:1037-1040
99. Dubois NC, Craft AM, Sharma P, Elliott DA, Stanley EG, Elefanty AG, Gramolini A, Keller G. Sirpa is a specific cell-surface marker for isolating cardiomyocytes derived from human pluripotent stem cells. *Nat Biotech*. 2011;29:1011-1018
100. Fong C, Peh GL, Gauthaman K, Bongso A. Separation of ssea-4 and tra-1–60 labelled undifferentiated human embryonic stem cells from a heterogeneous cell population using magnetic-activated cell sorting (macs) and fluorescence-activated cell sorting (facs). *Stem Cell Rev and Rep*. 2009;5:72-80
101. Ye L, Zhang S, Greder L, Dutton J, Keirstead SA, Lepley M, Zhang L, Kaufman D, Zhang J. Effective cardiac myocyte differentiation of human induced pluripotent stem cells requires vegf. *PloS one*. 2013;8:e53764
102. Tohyama S, Hattori F, Sano M, Hishiki T, Nagahata Y, Matsuura T, Hashimoto H, Suzuki T, Yamashita H, Satoh Y, Egashira T, Seki T, Muraoka N, Yamakawa H, Ohgino Y, Tanaka T, Yoichi M, Yuasa S, Murata M, Suematsu M, Fukuda K. Distinct metabolic flow enables large-scale purification of mouse and human pluripotent stem cell-derived cardiomyocytes. *Cell stem cell*. 2013;12:127-137
103. Yu J, Hu K, Smuga-Otto K, Tian S, Stewart R, Slukvin II, Thomson JA. Human induced pluripotent stem cells free of vector and transgene sequences. *Science*. 2009;324:797-801
104. Masumoto H, Ikuno T, Takeda M, Fukushima H, Marui A, Katayama S, Shimizu T, Ikeda T, Okano T, Sakata R, Yamashita JK. Human ips cell-engineered cardiac tissue sheets with cardiomyocytes and vascular cells for cardiac regeneration. *Scientific reports*. 2014;4:6716
105. Yang X, Pabon L, Murry CE. Engineering adolescence: Maturation of human pluripotent stem cell-derived cardiomyocytes. *Circ Res*. 2014;114:511-523
106. Twardowski RL, Black LD, 3rd. Cardiac fibroblasts support endothelial cell proliferation and sprout formation but not the development of multicellular sprouts in a fibrin gel co-culture model. *Annals of biomedical engineering*. 2014;42:1074-1084
107. Chang WG, Andrejecsk JW, Kluger MS, Saltzman WM, Pober JS. Pericytes modulate endothelial sprouting. *Cardiovascular research*. 2013;100:492-500
108. Armulik A, Genove G, Betsholtz C. Pericytes: Developmental, physiological, and pathological perspectives, problems, and promises. *Developmental cell*. 2011;21:193-215
109. Ye L, Chang Y-H, Xiong Q, Zhang P, Zhang L, Somasundaram P, Lepley M, Swingen C, Su L, Wendel Jacqueline S, Guo J, Jang A, Rosenbush D, Greder L, Dutton James R, Zhang J, Kamp Timothy J, Kaufman Dan S, Ge Y, Zhang J. Cardiac repair in a porcine model of acute myocardial infarction with human induced pluripotent stem cell-derived cardiovascular cells. *Cell stem cell*. 2014;15:750-761

110. Chong JJ, Yang X, Don CW, Minami E, Liu YW, Weyers JJ, Mahoney WM, Van Biber B, Cook SM, Palpant NJ, Gantz JA, Fugate JA, Muskheli V, Gough GM, Vogel KW, Astley CA, Hotchkiss CE, Baldessari A, Pabon L, Reinecke H, Gill EA, Nelson V, Kiem HP, Laflamme MA, Murry CE. Human embryonic-stem-cell-derived cardiomyocytes regenerate non-human primate hearts. *Nature*. 2014;510:273-277
111. Nunes SS, Miklas JW, Liu J, Aschar-Sobbi R, Xiao Y, Zhang B, Jiang J, Masse S, Gagliardi M, Hsieh A, Thavandiran N, Laflamme MA, Nanthakumar K, Gross GJ, Backx PH, Keller G, Radisic M. Biowire: A platform for maturation of human pluripotent stem cell-derived cardiomyocytes. *Nat Meth*. 2013;10:781-787
112. Hirt MN, Boeddinghaus J, Mitchell A, Schaaf S, Börnchen C, Müller C, Schulz H, Hubner N, Stenzig J, Stoehr A, Neuber C, Eder A, Luther PK, Hansen A, Eschenhagen T. Functional improvement and maturation of rat and human engineered heart tissue by chronic electrical stimulation. *Journal of molecular and cellular cardiology*. 2014;74:151-161
113. Smith AO, Bowers SLK, Stratman AN, Davis GE. Hematopoietic stem cell cytokines and fibroblast growth factor-2 stimulate human endothelial cell-pericyte tube co-assembly in 3d fibrin matrices under serum-free defined conditions. *PloS one*. 2013;8:e85147
114. Chen CW, Okada M, Proto JD, Gao X, Sekiya N, Beckman SA, Corselli M, Crisan M, Saparov A, Tobita K, Peault B, Huard J. Human pericytes for ischemic heart repair. *Stem Cells*. 2013;31:305-316
115. Xu C. Characterization and enrichment of cardiomyocytes derived from human embryonic stem cells. *Circulation Research*. 2002;91:501-508
116. Nadal-Ginard B. Myocyte death, growth, and regeneration in cardiac hypertrophy and failure. *Circulation Research*. 2003;92:139-150
117. Hein S. Progression from compensated hypertrophy to failure in the pressure-overloaded human heart: Structural deterioration and compensatory mechanisms. *Circulation*. 2003;107:984-991
118. Helmbold P, Nayak RC, Marsch WC, Herman IM. Isolation and in vitro characterization of human dermal microvascular pericytes. *Microvascular Research*. 2001;61:160-165
119. Weinbaum J, Schmidt J, Tranquillo R. Combating adaptation to cyclic stretching by prolonging activation of extracellular signal-regulated kinase. *Cel. Mol. Bioeng.* 2013;6:279-286
120. Bedada FB, Chan SS, Metzger SK, Zhang L, Zhang J, Garry DJ, Kamp TJ, Kyba M, Metzger JM. Acquisition of a quantitative, stoichiometrically conserved ratiometric marker of maturation status in stem cell-derived cardiac myocytes. *Stem cell reports*. 2014;3:594-605
121. Syedain ZH, Meier LA, Reimer JM, Tranquillo RT. Tubular heart valves from decellularized engineered tissue. *Annals of biomedical engineering*. 2013;41:2645-2654

Appendix 1: Supplemental Studies

A1.1 Grooved Molds for the Creation of Aligned Patches With Uniform CM Distribution

A1.1.1 Motivation

As seen in Chapters 2 and 3, although cells from neonatal rat cardiac isolates were seeded homogenously within the fibrin biomaterial scaffold at casting, after 2 weeks in vitro culture, CMs were not uniformly distributed throughout the gel. CMs were sparsely distributed throughout most of the patch and concentrated at very high densities in small regions located close to the ends of the ring near the ablumenal surface of the ring (Figure 3.2). This 'edge effect' occurs for yet unknown reasons, but may be partially due to a number of factors, among them minute changes in regional patch mechanics or microstructure at some stage of gel compaction. As the gel compaction process in the presence of multiple cell types is very complex and difficult to assess on the scales mentioned, an alternate solution was proposed. Rather than attempt to elucidate and subsequently control the dynamic mechanical and microstructural environments of the compacting gels, a new mold design sought to capitalize on this 'edge effect' and create a patch that consisted of entirely 'edges.'

A1.1.2 Mold Design

The new molds were designed in the style of rectangular slab gels with a series of parallel grooves. The design of the molds was intended to match size

as close as possible to the 1.25 mL, 13 mm wide, 2.83 mm thick cylindrical gels created with ring patches. As a result, the inner chamber was 38 mm long with the center 24 mm containing the grooves and 7 mm on each end being open, without grooves to allow for the placement of foam or glass rods for patch anchorage. The groove features do not extend the full thickness of the mold, with the top 2 mm remaining open, to enable the gel forms and compacts as a single piece of tissue rather than individual strips. Grooved molds were constructed as an assembly of 45 pieces consisting of end pieces, grooves, and spacers, all either custom machined or laser cut out of thin materials. Glass rods and silicone o-rings were used to thread the pieces together and hold them taut. End pieces were machined out of Ultem, spacers were laser cut out of 0.8 mm thick Teflon and the grooves were laser cut out of 250 μm thick poly ether ether ketone (PEEK) or 127 μm thick polycarbonate to create 800 μm wide grooves separated by 127 μm. Pieces were cleaned and sterilized unassembled and then assembled by stacking pieces together on glass rods and held in place by silicone o-rings (Figure A1.1). Schematics of individual pieces can be found in (Figure A1.2). Due to the millimeter-scale height of some of the features, it was not feasible to create a grooved mold using microfabrication, and 3D printing was not available during the design process. Additionally, the modular design enables patches of different volume to be created by simply altering the number of grooves, creating either a narrower or wider slab. Additionally, for optimization purposes the laser-cut slats and spacers can be rapidly and relatively

inexpensively redesigned and constructed to allow for changes in the overall design.

A1.1.3 Preliminary Results with Neonatal Rat Cardiac Cells and hiPSC-CMs

Once assembled, gels were cast with the same gel formulation and cell composition as the ring-mold patches. Gels were cast by placing the assembled mold upside down on a slab of silicone rubber and pipetting the cell-containing, gel-forming solution into the underside (now upward facing) of the mold, filling it to the tops of the grooves. Gels were allowed to polymerize for 6 minutes at room temperature before being moved to a 37ºC incubator for the remaining 10 minutes of polymerization. After polymerization, the molds were picked up using sterile tweezers and placed upright into a dish containing the appropriate culture media for the cell type (See chapter 2, chapter 4). Gels were cultured statically for 14 days prior to being harvested for histological analysis.

The resultant, compacted patch was approximately 1.5 cm in length after being removed from the mold, retained its ridge-like features (Figure A1.3), and beat both spontaneously and in response to pacing. However, optimization of the casting and culture process for these grooved molds was conducted concurrently with preliminary studies creating ring-shaped patches with unpurified hiPSC-CMs. As found in Chapter 4 (Chapter 4.3, Figure 4.2), hiPSC-CMs are substantially uniformly distributed after 14 days static culture, making the use of a grooved mold to enhance CM distribution in patches unnecessary.

A1.2 Implantation of Decellularized Neonatal Rat Cardiac Cell Patches

The material discussed in the following appendix was adapted from the following: Wendel et al, *Functional Consequences of a Tissue-Engineered Myocardial Patch for Cardiac Repair in a Rat Infarct Model*. Poster Presented at: AHA 2013. American Heart Association Scientific Sessions. Dallas, TX. November 2013.

A1.2.1 Motivation

In chapter 3, it was found that animals that received a CM+ patch had improved cardiac function and smaller infarct sizes than animals that received no treatment or a CM- patch. Additionally, animals that received CM- patches also resulted in some benefits, although to a lesser extent than CM+ recipient patches. One aspect of the patches that was not investigated in Chapter 3 as a potential source of the benefits seen was that of the transplanted matrix itself. Here we decellularized a subset of CM+ patches created for implantation in Chapter 3 and transplanted them onto the LV epicardial surface of Fisher rats acutely post-infarction

A1.2.2 Methods

Stretch-conditioned CM+ patches were created in Chapter 2. CM+ patches were chosen to be decellularized, as it was shown in Figure 3.3 that CM+ patches contain more cell-deposited matrix than CM- patches and thus any effects of cell-deposited matrix will be more prevalent with decellularized CM+ patches. Following a pre-established protocol[121], patches were kept on their latex

mandrels, rinsed in PBS, and exposed to a solution of 1% Sodium Dodecyl Sulfate (SDS) for 2 hours on a shaker. Patches were then removed from their mandrels and exposed to SDS for an additional 2 hours floating freely in solution. Patches were then rinsed in deionized H_2O (DIH2O) and the SDS was removed by exposing the patch to a solution of 1% Triton-X-100 in DIH2O for 30 minutes. Patches were then moved back onto their latex mandrels and rinsed in PBS containing 1% Penicillin/Streptomycin for 36 hours, with 6 changes of PBS over the time frame. Patches were then incubated in culture medium containing DNAse at a dilution of 1:1000 for 4 hours at 37ºC, followed by a 24 incubation in culture medium at 37ºC. Lastly, decellularized patches were rinsed in PBS and stored at 4ºC until needed for transplantation.

Decell patches were sutured into the LV epicardium of n = 5 Fisher rats as three 8 mm strips identical to patches implanted in Chapter 3. ECHO was conducted 1 week and 4 weeks post-op, and hearts were explanted at 4 weeks for histological analysis.

A1.2.3 Results

CM+ patches were successfully decellularized with no evidence of cells present in the patches observed through H&E or DAPI staining. There was a qualitative increase of matrix porosity and decrease in the presence of deposited matrix proteins (Figure A1.4, A1.5). If validated these results would potentially be indicative of protein degradation and loss through the decellularization process

and would lead to a subsequent decrease in mechanical properties, though this was not investigated in this study and no conclusions can be made.

No improvements in infarct size and cardiac function were seen with the administration of the decell patch, as shown in Figures A1.6-A1.7 and Table A1.1. Due to the absence of cells and that the ECM of the patches is remodeled to a collagenous ECM over 4 weeks in vivo, it was difficult to differentiate any potential residual patch from scar tissue or adhesions from the chest wall. As a result, the fate of these patches in vivo is unknown. The combination of this inability to characterize the patch in vivo, the lack of improvement seen with the administration of a decell patch, and the potential loss of protein through decellularization, this treatment was neither further characterized nor pursued further.

A1.3 Figures and Tables

Table A1.1: Infarct Size and LV Thickness Measurements, Adapted From Table 3.2

Group	Infarct Size	LV free wall thickness
Sham (no ligation)	**-**	**2563.9± 306μm * # $**
MI only	**68.8 ±9.7 %**	**637.2 ± 28.9μm**
MI + DC patch	**53.5 ±5.2%**	**680.5±88.2μm**
MI + CM- patch	**34.0 ±5.6% ***	**932.7±345.6μm ***
MI + CM+ patch	**16.32±13.5%*#**	**1905.0±514.5μm * # $**

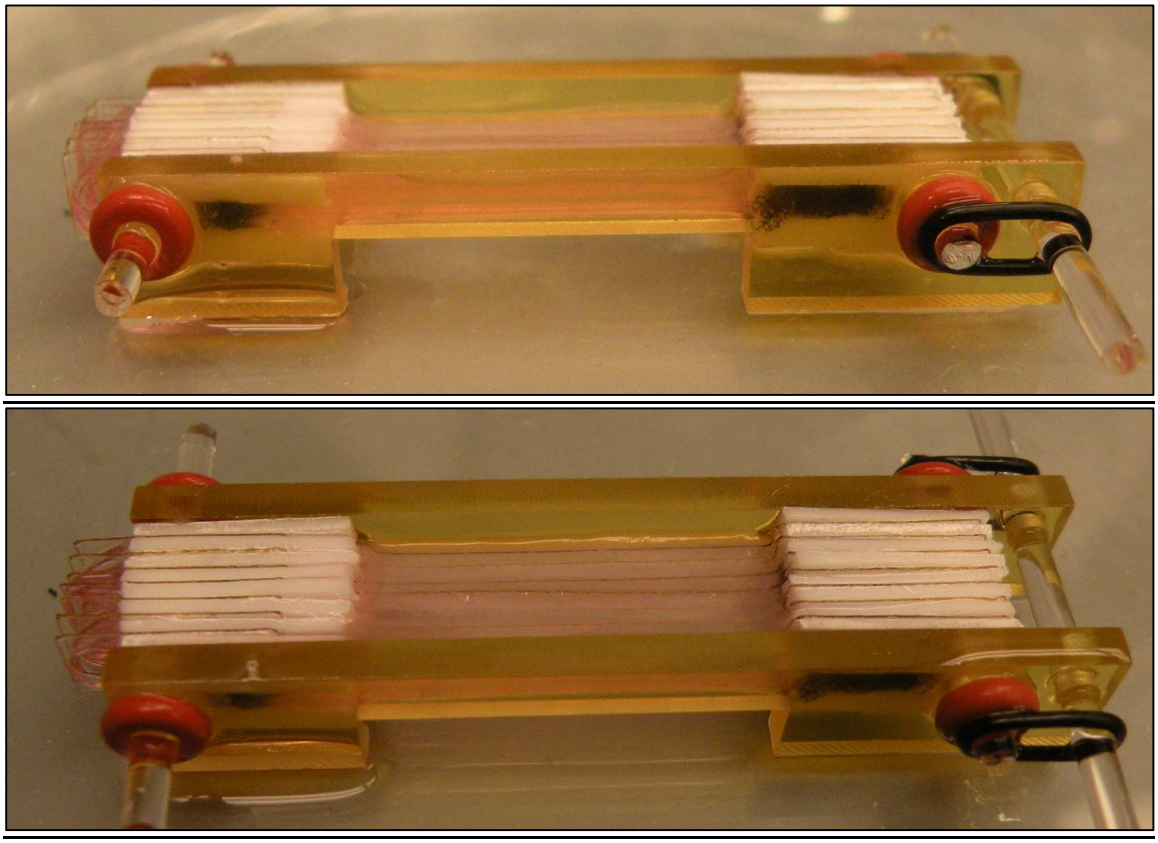

Figure A1.1: Assembled Grooved Mold With Patch After 2 Weeks Static Culture. This is an image of an early phase design. Later versions featured spacers and grooves open on the top side rather than closed as pictured. Foam was used to anchor the tissues at the edges of the slabs.

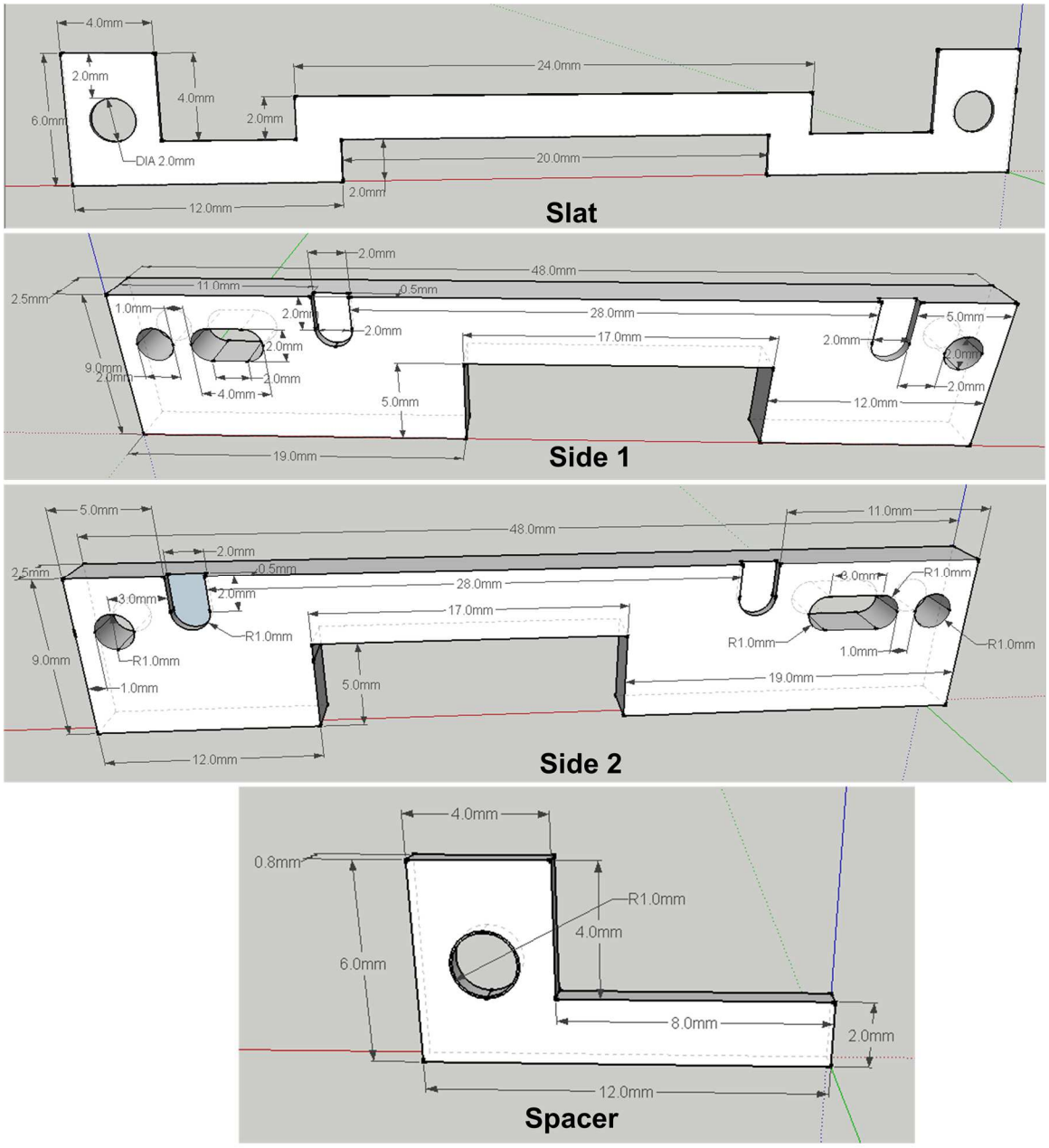

Figure A1.2: Schematics of Grooved Mold Pieces

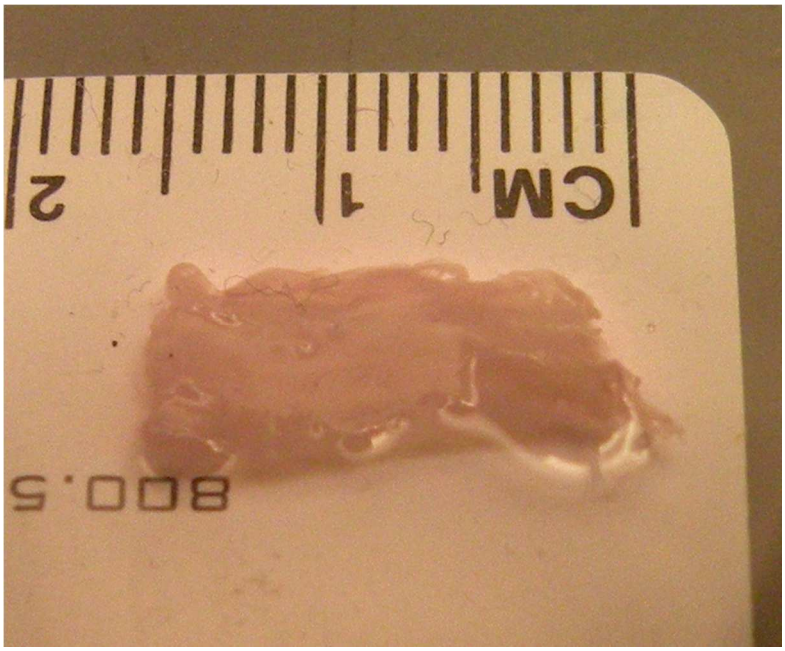

Figure A1.3: Grooved Patch After Removal From the Mold

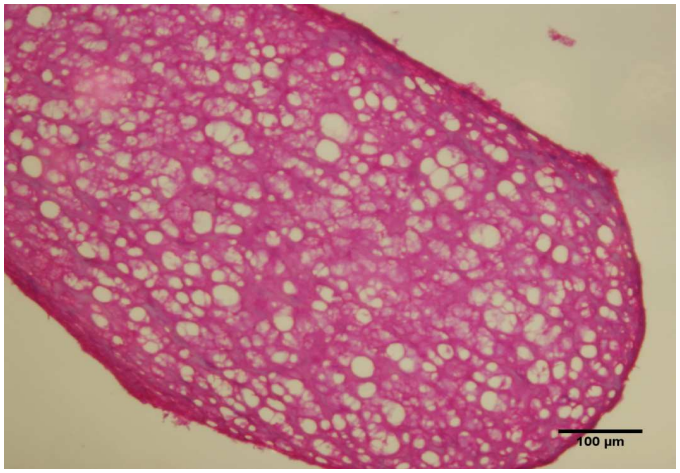

Figure A1.4: H&E –stained section of a decellularized CM+ patch. No observable nuclei were found in the patch, but a qualitative increase in porosity of the patch was observed.

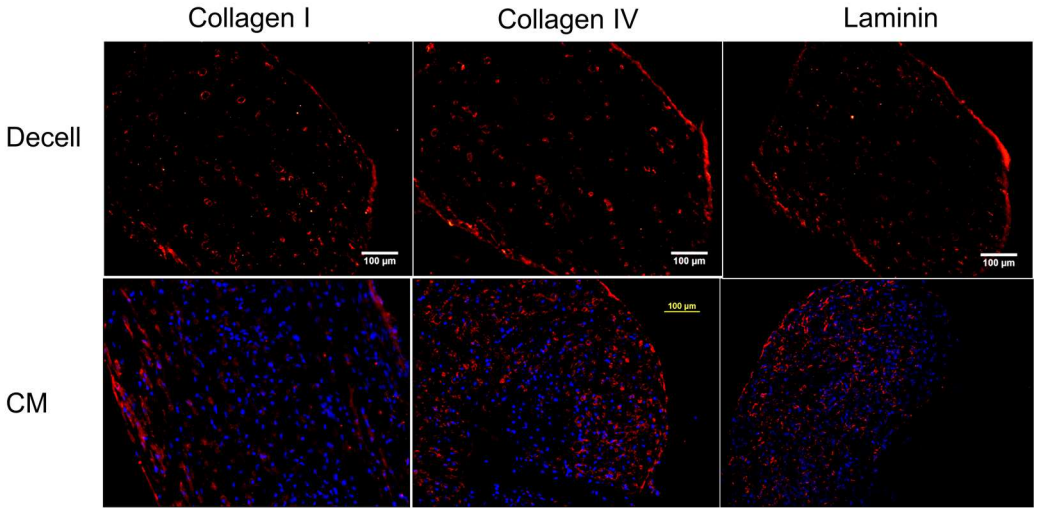

Figure A1.5: Adapted From Figure 3.3. ECM labeling of decellularized CM+ patch and a CM+ patch.

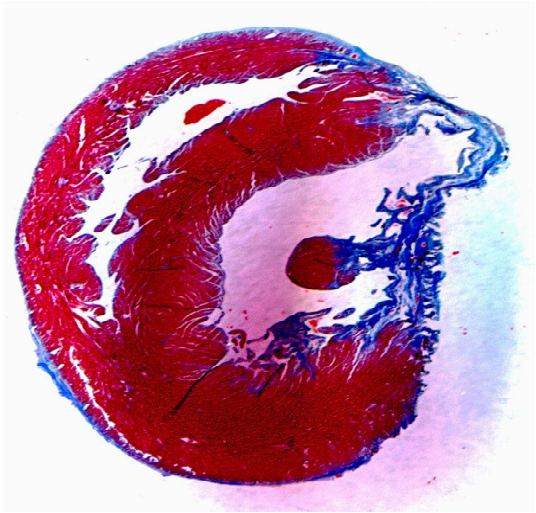

Figure A1. 6: Masson's Trichrome- Stained section of a DC patch recipient heart 4 weeks- post infarction and transplantation

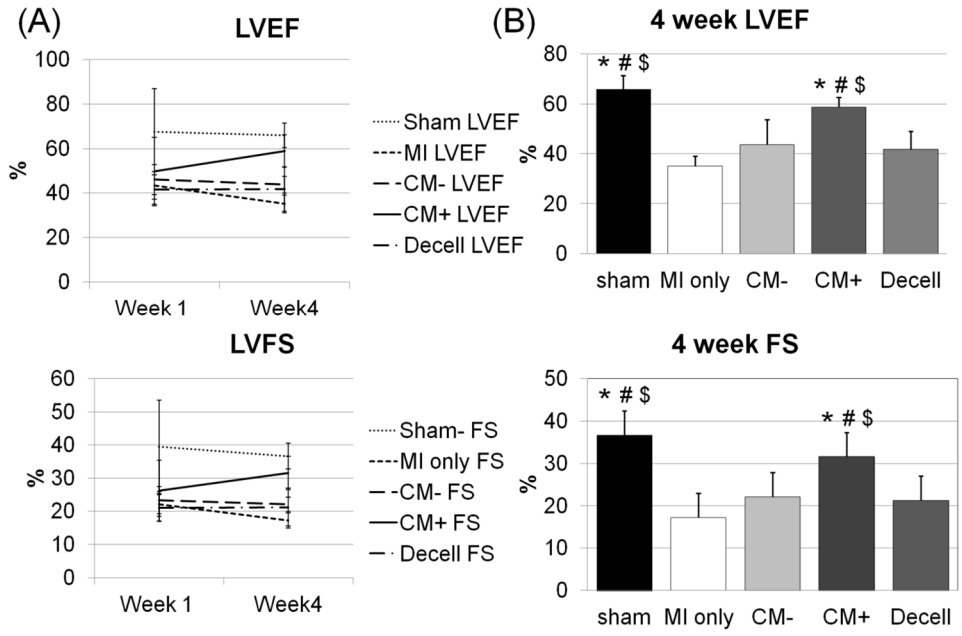

Figure A1.8: Echocardiography results 1 week and 4 weeks post-implantation. Adapted from Figure 3.4.

Appendix 2: Cell Count Matlab Code

Contained in this appendix is the User's Manual written to run the cell count matlab script. The code itself can be obtained from the lab server.

Matlab Cell Count Code: User's Manual

(I) Running the Code:

a. Hit Run on the .m file window

b. Select the directory to the folder containing the files to import

c. Sequentially select the grayscale image files corresponding to Blue, Red, Green and Far Red channels to import. The directory window title will show which file to import at a given time (i.e. File Selector: Green = pick the image corresponding to the Green/FITC/GFP channel)

d. Scale and Objective

   i. User Prompt: Have the scale and objective changed?

   ii. If the scale and objective are the same as the defaults, select 'no'

   iii. If they are different, select 'yes' and enter the scale (1 pixel = X um) in the command window and hit enter. Then enter the objective (5, 10, 20 or 40) and hit enter.

   iv. If you selected 'yes,' the command prompt will reappear. Select 'no' the second time.

e. Thresholding Images: Composite and Component image examples are shown in Figures A2.1 and A2.2

i. An intensity histogram will appear for the ‘Blue’ channel. Select the level to threshold the DAPI image (Figure A2.3a).

ii. A second image will then appear with the original grayscale image on the left and the thresholded (binary) image on the right (Figure A2.3b).

iii. A prompt will appear asking ‘Try another initial guess?’ If the binary image is an adequate representation of the image, select ‘no’. If it does not, select ‘yes’ and pick a new threshold on the histogram.

iv. Repeat this process until a representative binary image is obtained

f. Repeat this process for the ‘Red’, ‘Green’, and ‘Far Red’ images. (Figure X.4)

g. A figure will appear with the title ‘area’ (Figure A2.5) The white region represents the calculated area of the tissue section in the image.

i. Select an Area: User Prompt: ‘Select a Region?’ If you wish to calculate the cell distribution in both the total tissue section and a sub-region, select ‘yes’ (select ‘no’ if you do not).

ii. A binary image of the DAPI channel will appear. Select points to outline a sub-region of the tissue section (Figure A2.6)

iii. A second user prompt will appear, select ‘no’. At this time the program is not set up to record multiple sub-regions.

h. Done! Some representative intersection images will appear (Figure A2.7-A2.9), along with a data table with cell numbers, densities and

percentages (Figure A2.10). Copy and paste this into an excel sheet because that's what you ran this whole code to get.

(II) Optimization

a. Scale and Objective: Obviously, you have to know the pixel/um conversions for every objective for whatever microscope the slides were imaged on. The conversions provided in the command window are for the Tranquillo lab microscope

b. Thresholding: Thresholding parameters must be optimized for the proteins you are staining for.

    i. Change the ordering, number of uses and parameter size of the bwmorph operations.

c. Size of the Structuring Elements (Lines 124, 128, 132, 136). Changing this size will affect the time it takes to run the code but also effect the accuracy of background removal

(III) Limitations

a. This code fails at higher magnifications of tissue sections and most magnifications of plated cell monolayers due to the minimal overlap of cytosolic proteins with nuclei.

b. This code was developed to detect cytosolic proteins for cell counting. The use of cell-membrane proteins has not been investigates and is not recommended for use with this code.

(IV) Figures:

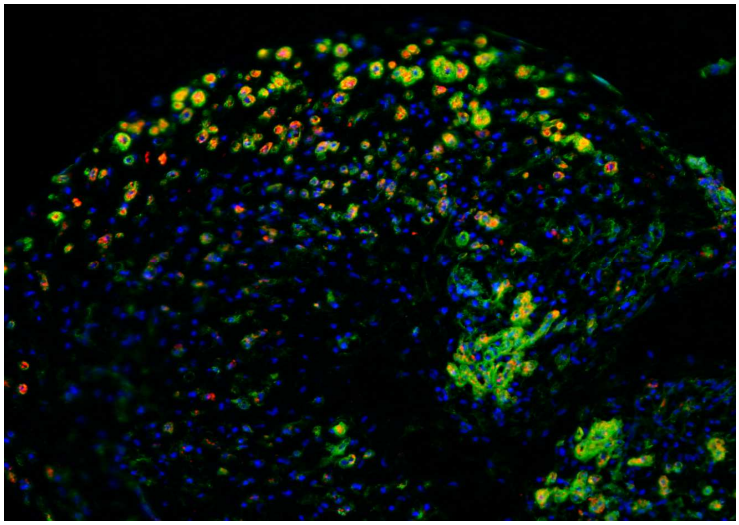

Figure A2.1: Color Composite Image of Sample Image run in this code

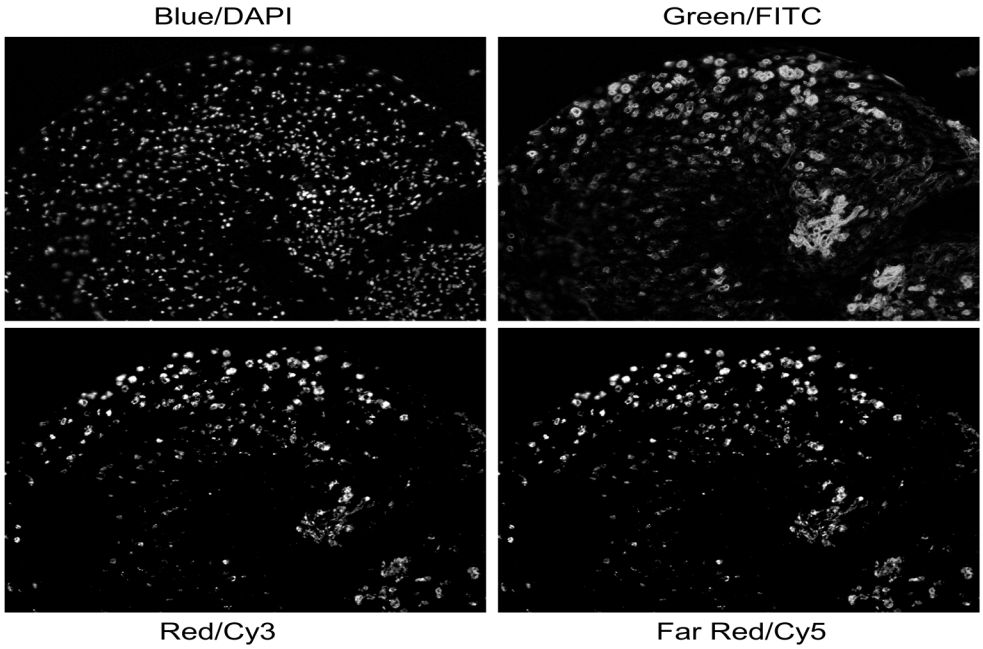

Figure A2.2: Grayscale component images of the four channels analyzed in this code. Note: The composite image in Figure X.1 only features labels in the Cy3, GFP/FITC, and DAPI channels. For example purposes, Far red/Cy5 is a duplicate of the Cy3 channel.

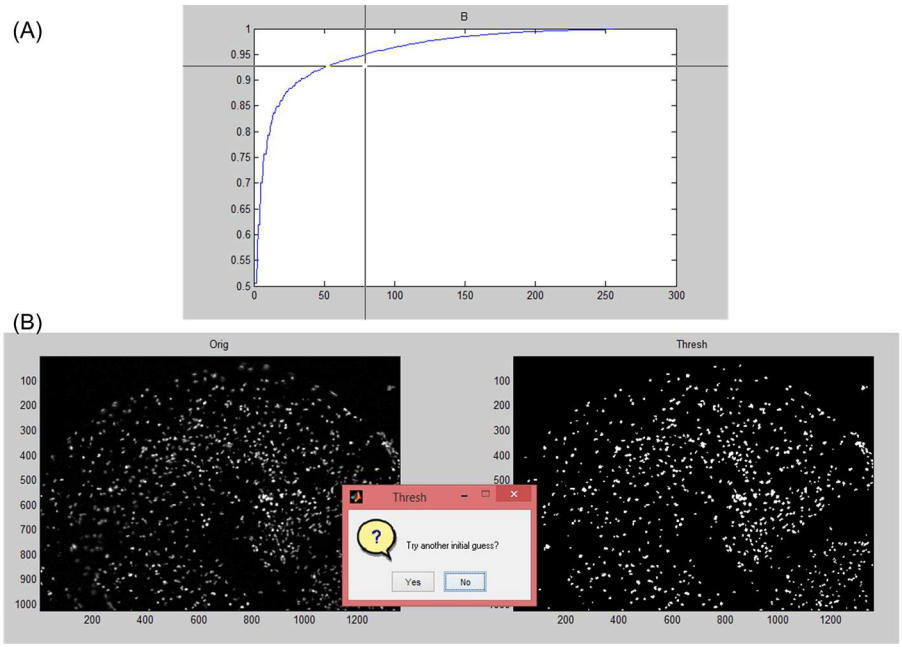

Figure A2.3: Thresholding of the Blue/DAPI channel. (A) shows the intensity histogram where a threshold is selected and (B) shows the resultant original and thresholded binary images.

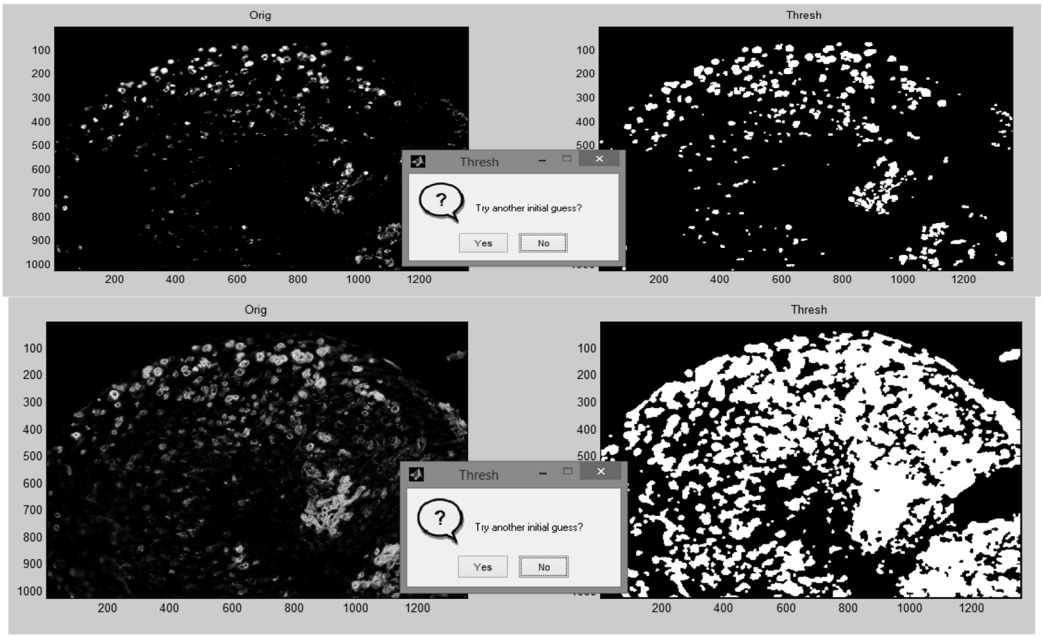

Figure A2.4: Thresholding for the Cy3 (top) and GFP/FITC channel images.

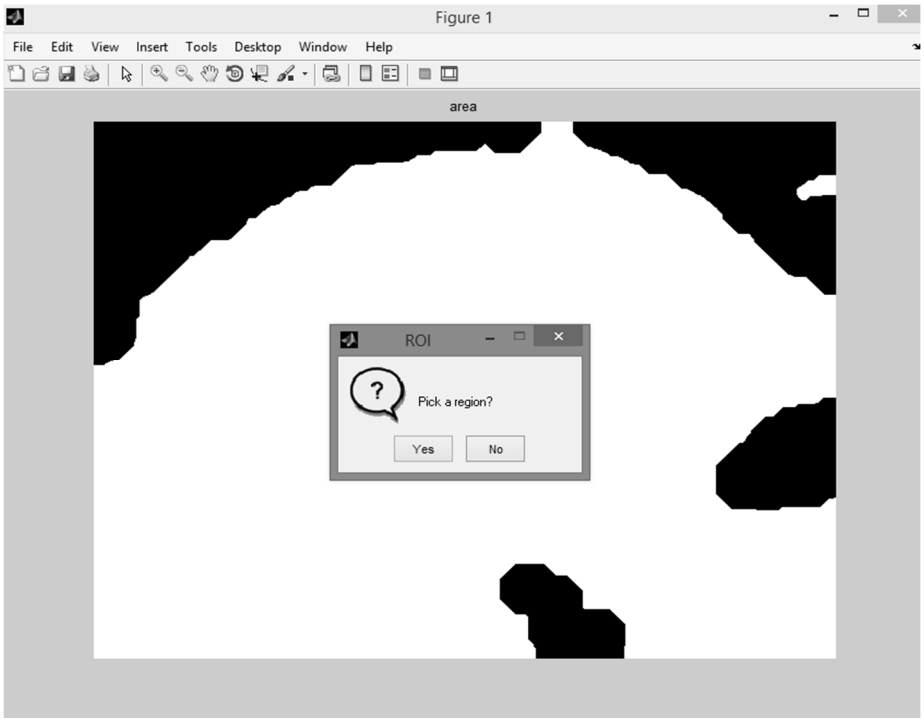

Figure A2.5: Section area (white) and region of interest selector

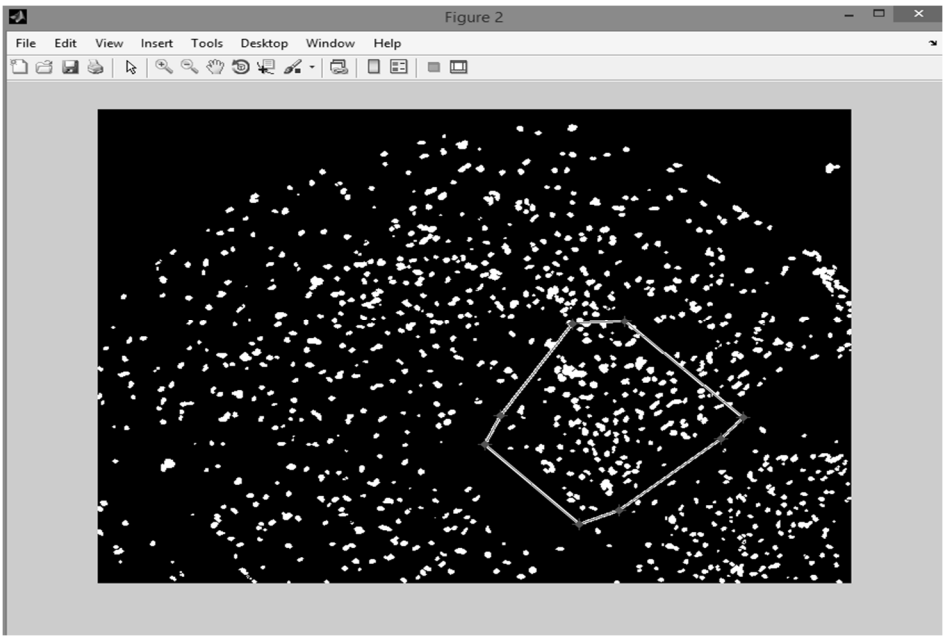

Figure A2.6: Selecting a Region of Interest

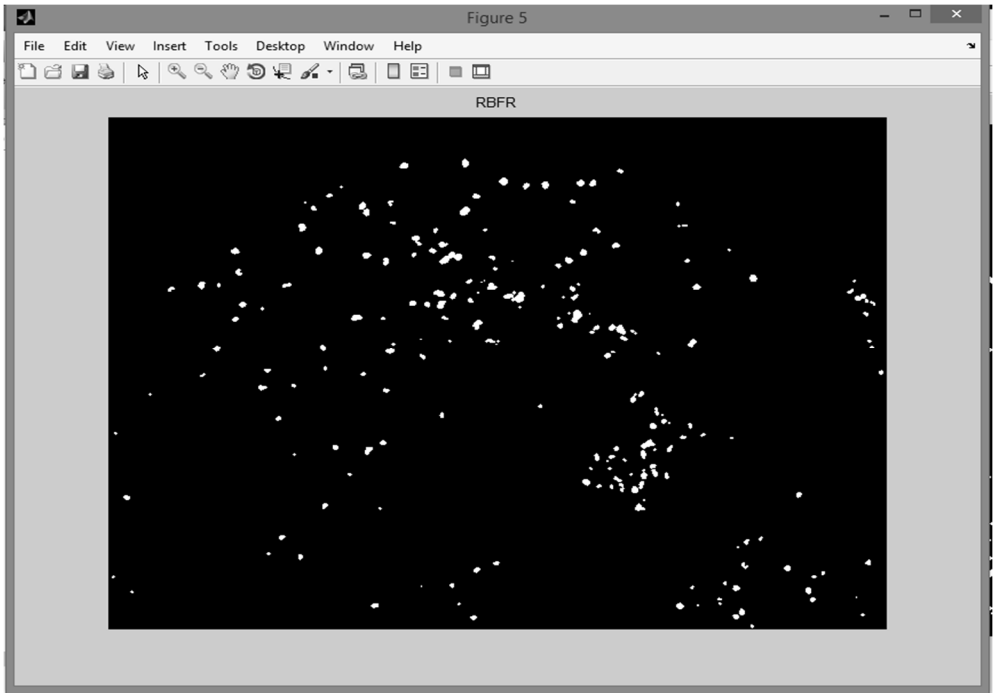

Figure A2.7: Sample output: overlay of DAPI+ nuclei with Cy3 and Cy5. Note the imperfect separation of nuclei, and the presence of particles smaller than nuclei, indicating some processing optimization is needed for the component image processing and thresholding.

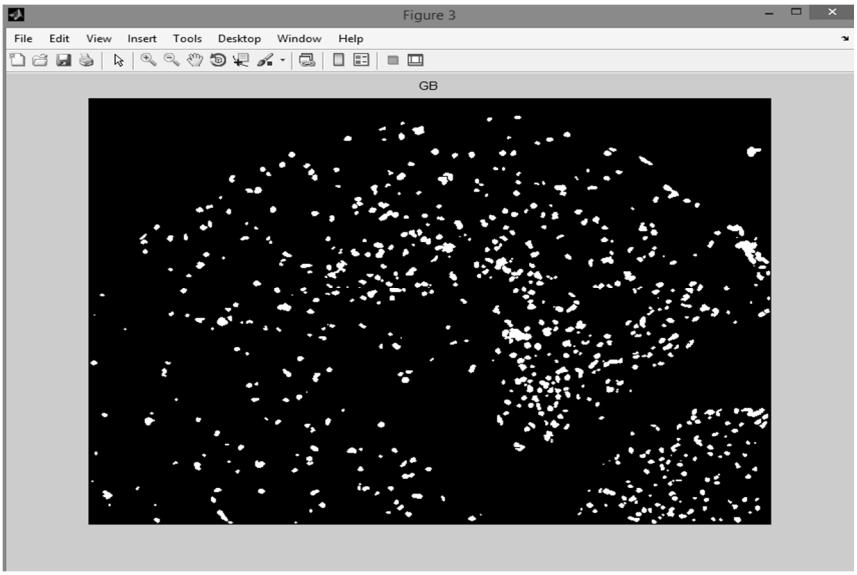

Figure A2.8: Sample output: Overlay of DAPI+ nuclei with FITC/GPF + structures

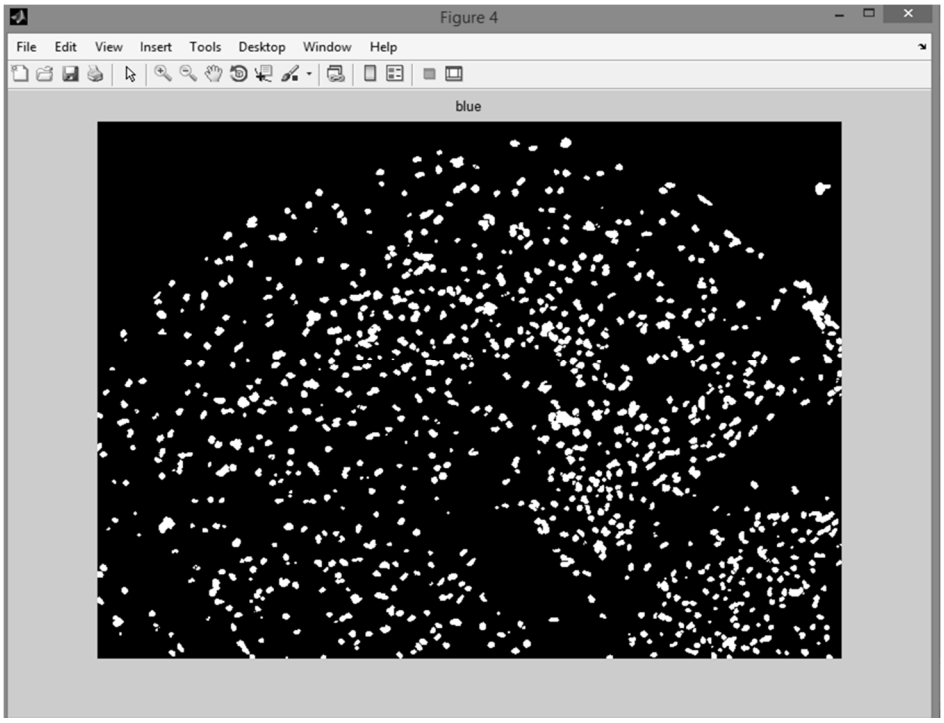

Figure A2.9: Sample Output: DAPI+ nuclei. Note the incomplete singling out of individual nuclei, indicating optimization is needed in the processing and thresholding of the DAPI image.

0	#	density (cells/mm^2)	% of cells in section	% of total cells
Blue	1081	4.0656e+03	0	0
Green	409	1.5382e+03	0	0
Red	259	974.0852	0	0
Far Red	334	1.2562e+03	0	0
B/G	206	774.7551	0.1906	0
B/R	265	996.6509	0.2451	0
B/FR	100	376.0947	0.0925	0
B/G/R	163	613.0343	0.1508	0
B/G/FR	81	304.6367	0.0749	0
B/R/FR	100	376.0947	0.0925	0
B/G/R/FR	81	304.6367	0.0749	0
Select Area Blue	105	1.5846e+04	0	0.0971
Select Area Green	27	4.0748e+03	0	0.0660
Select Area Red	14	2.1128e+03	0	0.0541
Select Area Far Red	41	6.1876e+03	0	0.1228
Select Area B/G	88	1.3281e+04	0.8381	0.4272
Select Area B/R	61	9.2060e+03	0.5810	0.2302
Select Area B/FR	61	9.2060e+03	0.5810	0.6100
Select Area B/G/R	59	84.8012	0.5619	0.3620
Select Area B/G/FR	54	77.6147	0.5143	0.6667
Select Area B/R/FR	54	77.6147	0.5143	0.5400
Select Area B/G/R/FR	54	77.6147	0.5143	0.6667

Table A2.1: Data Table Output from code

Appendix 3: Protocols

MOLD CLEANING AND PREPARATION PROTOCOL

1.) Disassemble Molds
2.) Put mold parts into a beaker with ~10% (enough to make the solution look pink-ish) Formulated Cleaning Concentrate in DIH20.
3.) Sonicate for 1h
4.) Rinse beaker and mold parts well with tap H20
5.) Return mold parts to beaker and fill with DIH20
6.) Sonicate for 1h
7.) Drain and dry mold parts on the benchtop on a clean blue chuck.
8.) Autoclave: 10-20min exposure, 10min exhaust. Don't let the mold parts sit in the autoclave after the cycle is complete. The extra heat exposure will cause the casings to break during assembly.
9.) Coat in 5% pluronic (sterile) for 1-3h in a sterile beaker in the hood.
10.) Remove pluronic and refilter. It can be used 3x. Let the mold parts dry on a sterile drape in the hood
11.) Once dry, assemble the molds on the drape using sterile gloves to maintain sterility. When done, place assembled molds into a cleaned and autoclaved jar.

Molds can be cleaned and assembled ahead of time and stored at RT

Product Info:

Detergent: Branson GP Formulated Cleaning Concentrate

NEONATAL RAT CARDIAC CELL ISOLATION

Checklist

4 litters Sprague-Dawley rats, supposedly 48 hrs old: order by 4pm Friday for Wednesday delivery (Thursday isolation) or by 4pm Wednesday for Monday delivery (Tuesday isolation)

Solutions:

MyoMedia: 5 mL FBS- frozen in aliquots in our freezer

5 mL Pen/Strep - frozen in aliquots in west side freezer

50 mL Horse Serum – frozen in 45 and 5 mL aliquots in our freezer

5 mL 100x ACA – in our fridge

435 mL DMEM- in our fridge and/or cold room

-combine and sterile filter

PBS Glucose: 1.98g D-glucose

500mL sterile PBS

5 mL P/S

-Combine, dissolve and sterile filter

Stop Solution: 25mL FBS

5mL P/S

470mL DMEM

-combine and sterile filter

Insulin: In aliquots in Main fridge if not in our fridge, 2mg/mL (1000x)

AA: In 0.5 and 1 mL aliquots in west side fridge (1000x)

If not already made for the day, 50 mg/mL in DD H20 and filter sterilized. AA is kept by the scale. Filter sterilizers are in the cabinet with the bottles.

5% Pluronic Solution: 50g Pluronic +800mL water

- Stir until dissolved, then bring up to 1L and sterile filter

Equipment Needed:

Sterile Tool Packet containing**:** Hemostat

Fine tweezers

Large scissors

Microscissors

Scalpel handle (#4)

Mold casings (syringe parts): autoclaved and coated in 5% Pluronic for 1.5h+. Make sure you have ejectors (smaller syringe parts) too.

Mold Parts: cleaned and autoclaved, enough for 15/litter to be on the safe side

Plastic jars for culturing finished constructs: cleaned and autoclaved, have 6 small and 6 large on hand minimum

4-across 50mL conical tube rack

12mL and 6mL syringes

18 and 30 GA needled: at least 10 of each on hand

Sterile Drapes: At least 6 on hand

Sterile gloves: at least 6 on hand

3 ice buckets: 1 large, 2 small

Carcass bucket: with small black trash bag in it

2 x100mm Petri dishes/litter

Scalpel Blades, #20: 1/litter on hand

Sterile gauze: 2 sheets

50mL conical

Sterile dropper pipet

Shaker in incubator

Collagenase, type 2

Notes:

Day before: - Assemble mold parts, make stop solution and PBS glucose if needed

Day of: -thaw serums and make media as late as possible. Thaw FBS aliquot in cold water. Make AA before starting if not already made.

- Place shaker in incubator

Neonatal Rat Cardiac Cell Isolation (for 4 litters of rats, scale down for fewer litters)

Start warming 1 bottle PBS glucose. The other stays cold.

Weigh out collagenase: want 200mL of 300U/mL. current lot is 200U/mg. Dump into 250mL bottle

Fill and label 8 petri dishes (2/litter) with cold PBS. Place 4 open on ice, reserve other 4 (all in hood)

Label 4 50mL conicals and place in hood

Place two petri dishes (or small beakers) in hood and fill with 20-40mL betadine each

Place mold casings in pluronics (in hood) if not already coated

Lay down sterile drape on each side and dump tool packets onto them. Don't touch without sterile gloves on. Also open and dump scalpel blades onto drape

Weigh pups, then put on ice and into the hood.

Glove up (sterile), assemble scalpel + blade and hemostat + gauze (gauze not completely sterile- don't touch!) and place in betadine dish

Swap pup torsos with betadine, euthanize and remove hearts. Place hearts in PBS glucose dishes on ice.

Once finished with rats, trim upper 1/3 off of each heart with micro scissors. Place remaining 2/3 (supposedly the ventricles only) in the other PBS glucose dish.

Mince heart pieces with micro scissors into as small of chunks as you can get (without taking too much time) and when done remove heart pieces and PBS glucose and place in 50mL conical. Rinse the dish a few times with the excess PBS glucose. Place tubes on ice.

Make up collagenase solution: 200mL warm PBS glucose into bottle with collagenase. Filter sterilize into another bottle.

Start warming up stop solution

Draw off most of the PBS glucose from the tubes and add 7mL collagenase solution apiece. Incubate 7 min on shaker in bottom incubator.

Place 8 50mL conicals in the hood.

After the first collagenase digestion, titrate gently on slow 4 times and aspirate off liquid (mostly crap and dead cells). Replace collagenase solution and incubate 7 min.

Titrate 5 times on slow. Remove supernatant and place in 50mL conical. Add 7mL collagenase to tubes with chunks and 10 mL stop solution to tubes with cells.

For remaining titrations (7 total) titrate 10 times on fast.

Filter cells through 70um cell sieves into new tubes, fill with warm DMEM and spin down for 5 min at 1.6

Resuspend cells in 50mL DMEM each and spin again, then resuspend into 20mL total and count.

Resuspend cells to 23.5mil cells/mL and put on ice

During the digestions and while the cells are spinning, dry off mold casings, thaw serums to make fresh media and start assembling mold parts and make fibrinogen and thrombin solutions:

Aligned molds: Fill with agarose first then place in fridge until cold

Fibrinogen aliquots are in freezer with horse serum, make sure the right lot #,

Thrombin aliquots are in the -80. 20 mM HEPES in saline is in the west fridge door. CaCl is in one of the fridges.

1.25 mL/ME total solution. 4:1:1 Fibrinogen: cells: thrombin. Add fibrinogen and cells first, then add thrombin and inject. Draw up into syringe with larger gauge needle (green) then switch to pink for injecting into molds. Keep needle upright as much as possible and watch out for bubbles.

Place molds in small jar and incubate upright for (15-20: 20 for 2mg/mL) min. Then eject into DMEM and place in labeled jars with fresh, supplemented media.

*pre-aliquot the media (enough for 1-2 jars apiece) and heat only until warm before adding MEs

(Optional) Fix extra cells for FACS analysis in 4% PFA for 15 min. then spin, resuspend, spin, resuspend and place in fridge

Replace media ~12h later (next morning) and gently nudge constructs with Pasteur pipette to make sure they are not sticking to the endcaps.

Change media and pick constructs every MWF. Harvest at d14.

<u>Percoll:</u>

If making constructs enriched for myocytes, extra step after spinning cells down and counting.

Percoll gradients: 9mL percoll stock solution in HBSS (in our fridge) + 11mL HBSS (usually by microscope)

10mL each into two 15mL tubes. Gently place cells for separation on top of gradients then spin at 2200rpm for 20 min.

Reserve top layer, aspirate off middle, and collect bottom cells.

Spin down cells in DMEM and count.

Preplating: (A more reliable method to enrich for CMs)

45min in PP media (15%FBS, 1%P/S in DMEM).

Non-myocytes adhere to the TCP in this time, CMs remain in suspension.

1 step = ~60-70% CMs, 2 steps~90-95% CMS.

PATCH CONSTRUCTION PROTOCOL: GENERIC

Checklist

Solutions:

Culture Media for final product

Basal media

Trypsin, FBS, whatever is needed to harvest cells

20mM HEPES buffer in saline:
10mL HEPES
490 mL saline
-combine and sterile filter

Fibrinogen Solution (for 1 mL total solution):

Final fibrinogen conc. ->	2 mg/mL	3.3 mg/mL	4 mg/mL
Fibrinogen stock (36mg/mL)	0.037mL	0.0614mL	0.0744 mL
20mM HEPES in saline	0..633mL	0.6053 mL	0.592 mL

Thrombin Solution:

Final fibrinogen conc. ->	2 mg/mL	3.3 mg/mL	4 mg/mL
Thrombin stock (80U/mL)	4.2 uL	5.2 uL	9.3 uL
2M CaCl	1.9uL	1.9uL	1.9uL
Basal Media	0.161 mL	0.161 mL	0.156 mL

(the ratio of fibrinogen/thrombin remains the same for all concentrations in this formulation)

5% Pluronic Solution: 50g Pluronic +800mL water

- Stir until dissolved, then bring up to 1L and sterile filter

Equipment Needed:

Mold casings (syringe parts or tubing): autoclaved and coated in 5% Pluronic for 1.h+. Make sure you have ejectors (smaller syringe parts) too.

Mold Parts: cleaned and autoclaved, coated in 5% Pluronic if using small molds

Plastic jars for culturing finished constructs: cleaned and autoclaved, have 6 small and 6 large on hand minimum

12mL and 6mL syringes

18 and 20 GA needled: at least 10 of each on hand

Sterile Drapes: At least 6 on hand

Sterile gloves: at least 6 on hand

50mL conicals

Ice Bucket with Ice in it

Prep (day of, but prior to casting)

-assemble molds

Large molds: - Pluronic coat mold casings for 1.0h+ and let dry on a sterile drape in hood. Pour pluronic back into bottle. It can be used 3x.
- agarose-fill mandrels
- assemble molds (sterilely)

Small molds: - Pluronic coat everything for 1h+ and let dry on a sterile drape in hood
- assemble molds

- make sure enough media is made

Harvest Cells

Per optimized protocol for each cell type, harvest CMs last since they are the most sensitive cell type

Casting:

Large Molds: 1.25 mL/gel total solution.

4:1:1 Fibrinogen: cells: thrombin.

Important: Keep all cells, fibrinogen, and thrombin solutions on ice until mixing. Warm cells will die quicker and the fibrin polymerization is accelerated at higher temperatures. Keeping it cold gives you more working time.

Also, If there are particles in the fibrinogen solution, that's not good. It means the fibrinogen has started to fall out of solution. Warm it up to 37C until the solution is clear again and then put it back on ice to chill.

- Add fibrinogen and cells first to a 50mL conical, then add thrombin and mix. Quickly (it's already started polymerizing) draw up into syringe with larger gauge needle (18GA/green) then switch to pink/20GA and inject the solution into molds. Keep needle upright as much as possible and watch out for bubbles.

- Place molds in small jar and incubate upright for (15-20: 20 for 2mg/mL) min. Then eject into a 100mm petri dish with warm basal media in it. Pick mold up by the endcaps with a pair of sterile tweezers and place in labeled jars with fresh, warm media.

    *pre-aliquot the media (enough for 1-2 jars apiece) and heat only until warm before adding the gels

- Replace media ~12h later (next morning) and gently pick constructs

    - To pick gels: use a sterile Pasteur pipet and gently nudge edge of gel along mandrel to ensure it is not adherent to the Teflon.
    - Culture and exchange media every other day (or MWF) until harvest.

Analysis:

Uniaxial tensile testing

Alignment mapping

Contraction force testing

Histology

PATCH CONSTRUCTION PROTOCOL: HEMISPHERES

Supplies Needed

- Tissue Punch of desired size
- Well plate of appropriate size (large enough to fit the tissue punch), sterile
- Heating source, either a bunson burner or a tissue culture hood sterilizer
- Tissue Culture Hood
- Cells and Reagents to cast fibrin gels (see fibrin casting protocol)
- Dental pick

Procedure:

Stamping of Tissue Culture Plate

1.) Bring sterile well plate, tissue punch, and heating source into the tissue culture hood
2.) Heat the tissue punch for 10-30s until hot
3.) Use the heater tissue punch to create a stamp in a single well of the well plate, evenly applying pressure to create a circular region of melted plastic, rotating as needed.
    *This may take some practice, too little pressure or too cool of a tissue punch may result in an incomplete ring while too much pressure could cause the plate to crack or create a hole in the well.
4.) Correct defects in the ring, if they appear, with a heated dental pick
5.) Repeat steps 2-4 for each well you wish to place a hemisphere into.
    *This process can be done ahead of time, as long as the plate is stored such that it remains sterile.

Casting of Hemispheres

1.) Prepare fibrinogen and thrombin solutions and cells as per standard protocol
2.) To cast a hemisphere, mix the component solutions in a batch of appropriate volume (per standard casting protocol) and then gently add the desired volume of cell-laden gel forming solution into the center of one of the stamped rings. The gel solution should be bounded by the melted plastic and look like a rounded droplet on the plastic (i.e. hemisphere)
3.) Continue this process for the remaining hemispheres. Be careful not to bump the plate or they will spill.
4.) Let hemispheres sit in the tissue culture hood for 6 minutes before carefully transferring them to a 37C incubator for 15 additional minutes.
5.) At the end of polymerization, remove well plate form the incubator and return to the tissue culture hood. Add an appropriate amount of media for the number and

type of cells entrapped, with a minimum enough to cover the hemisphere entirely.

6.) Change media 24h (the next day) after casting to remove any excess thrombin and dead cells. After that, media can be changed 3x weekly, or whatever is deemed optimal for the entrapped cell types. Supplement media with ACA to reduce fibrinolysis.

Sample of Stamp Diameters and the Hemisphere Sizes That Can Be Made With Them:

Diameter of Stamp (mm)	Volume of Hemisphere (uL)
4.5	25
6	50
7.25	75
10	150
11	225
13.25	400
17	750
20	1000
22	1200
23	1400

Use this information as a starting point to calculate the volumes for different diameter stamps

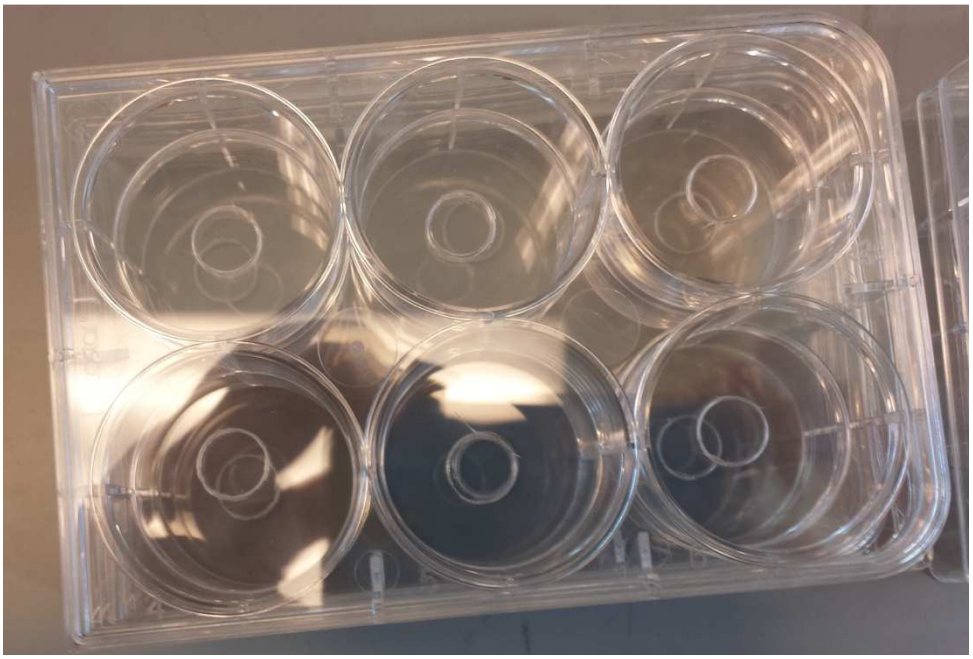

Example of stamped rings in a tissue culture well plate

CONTRACTION FORCE (AKA TWITCH FORCE) TESTING

Equipment:

The Biggies:
Contraction Force Tester (*force transducer + movable media bath on optical board)*: Located on shelf next to incubators #8 and 9
Stimulator *(S88X GRASS, Astromed, Inc):* also on shelf next to the incubators.
Filter *(900 Tunable Active Filter, Freq Devices Inc):* also on shelf next to incubators
Laptop *(crappy little Acer):* usually found on the shelf next to the incubators, on my bench or put away in the bottom drawer next to Krissy's desk.
Small 37C Incubator: the one on Pat's bench. It will not fit onto one of the shelves where the rest of the equipment is, put it on a cart and roll it up next to the shelves.
DAQ card: good luck finding it. Most frequent locations: on the same shelves as the above equipment, on the cart with the pressure transducer (which also moves around a lot).

Other Miscellaneous things you will need:
Foam: the black blocks of it located either on the shelves or on top of the fridge in Tranquillo East
Contraction Force Media: 2uM CaCl + 1000x AA in DMEM, warm. 10mL for each sample you plan on **testing**
Tweezers
Pipet-aid
Waste Container for used contraction force media
24well plate to store tested samples

Setting up the System:

1. Place the Contraction force tester into the small incubator. Put foam underneath it to limit noise in your data. Let warm up for ~5min before doing anything.
2. There is a cable coming from the filter that ends in 2 wires. Red goes into A/1 + and Black to A/1 – on the DAQ card. There should also be a black ground wire connected to the A/1 – wire. That goes into the ground slot. Screw all wires into their ports tightly.
3. Plug the USB port of the DAQ card into the laptop
4. Plug in the force transducer output display box. Make sure it is set to 5g rather than 0.5g.
5. Plug in and start up the computer. This may take a while.
6. Turn on the filter. The switch is on the backside. Don't mess with the settings, they are fine as is.

7. Turn on the stimulator. The switch is on the front panel (pictured). It will start up and ask you to change settings or hit enter. Hit enter.
8. Connect the alligator clips from S1 output on the stimulator (they should be the ones without covers) to the electrode wires on the contraction force tester.
9. Once the computer is setup, go into the contraction force testing folder on the desktop, copy the template folder and file and rename it with today's date.
10. Add 10mL contraction force media to the bath on the contraction force tester.

LABVIEW:

There are two programs on the desktop, each calibrated to a specific force transducer. Use the **Old Pacing Test**

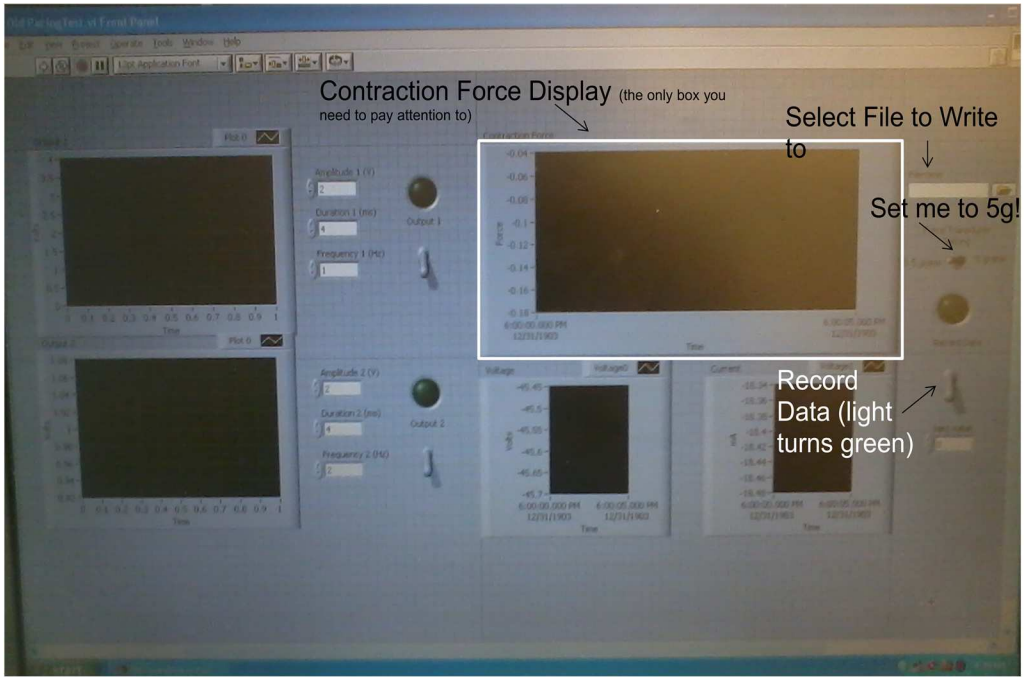

1. Select file to write to from your template folder
2. Set to 5g
3. Run program
4. Hit record when you want to record data. It will continually display output, but only records when you want it to.

Loading a Sample:

1. Once everything is set up and warmed up, remove a sample from its mandrel (I usually measure a representative width with calipers first).
2. Place sample over the fixed post.
3. Wait about 30s and see if you can observe any spontaneous contractions.
4. If yes, continue to step 7

5. If no, turn the S1 output on to 1 Hz and see again if you can see any contractions. If you do, continue to step 7
6. If not, ramp up the stimulator to a high frequency until you see hydrolysis (bubbles) from the electrodes near where the silver wire comes out of the bath.
    a. If you do not see bubbles, you hooked up something wrong. Troubleshoot and try again.
    b. If you do, the sample is probably a dud. Congratulations. Continue onto step 7 anyways because sometimes once you tension them they start to respond.
7. Make sure S1 is OFF and slide ring over force transducer probe, such that it goes around both the probe and the fixed post.
8. Adjust the stage until the sample is tensioned to 1g force (0.4V on this transducer)
9. Hit record! Be careful not to bump the incubator now….
10. Give it ~30s to 1 min for the stress relaxation to level off a bit. Then turn S1 back onto 0.5 or 1Hz.
11. Ramp up the output to ~15Hz and then quickly back down again
    a. We do this to try and get all the cells somewhat synchronized… sometimes they aren't and you will see secondary beats in the output
12. Wait about 5 beats or so and then record the max and min values of the twitch response
13. Repeat for increasing frequencies until the sample stops beating at the paced frequency (I call this the 'maximum capture rate' per Radisic et al.)
14. Turn the output off and observe for 1-2min to see if spontaneous beating returns.
15. Stop recording, return the sample to no tension and remove it from the bath.
16. Replace the contraction force media after each sample with fresh solution to avoid excess acidification of the media.

Picture Cheat Sheet:

Filter

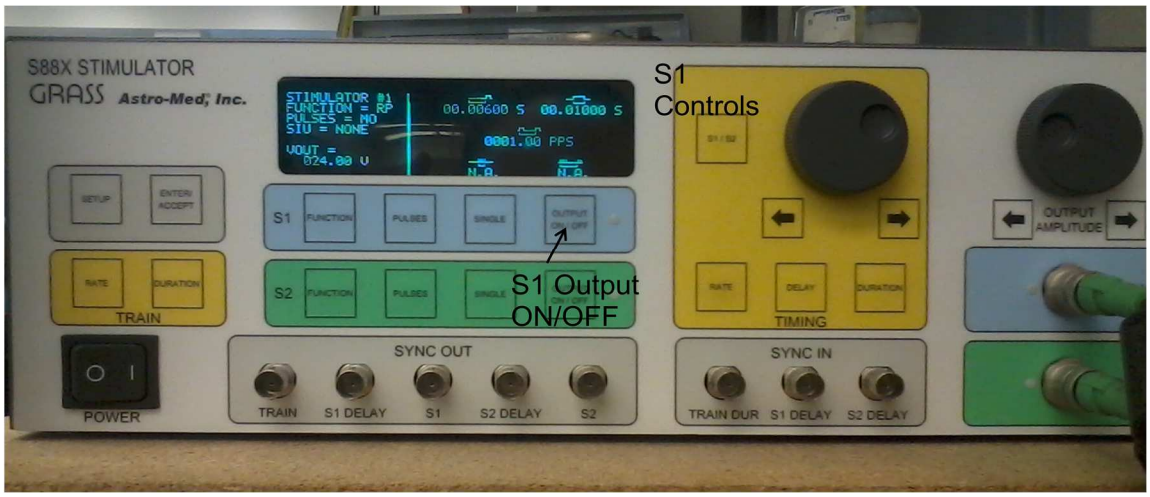

Stimulator

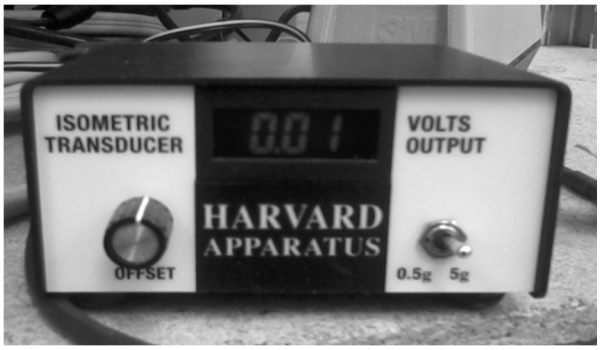

Force Transducer Display

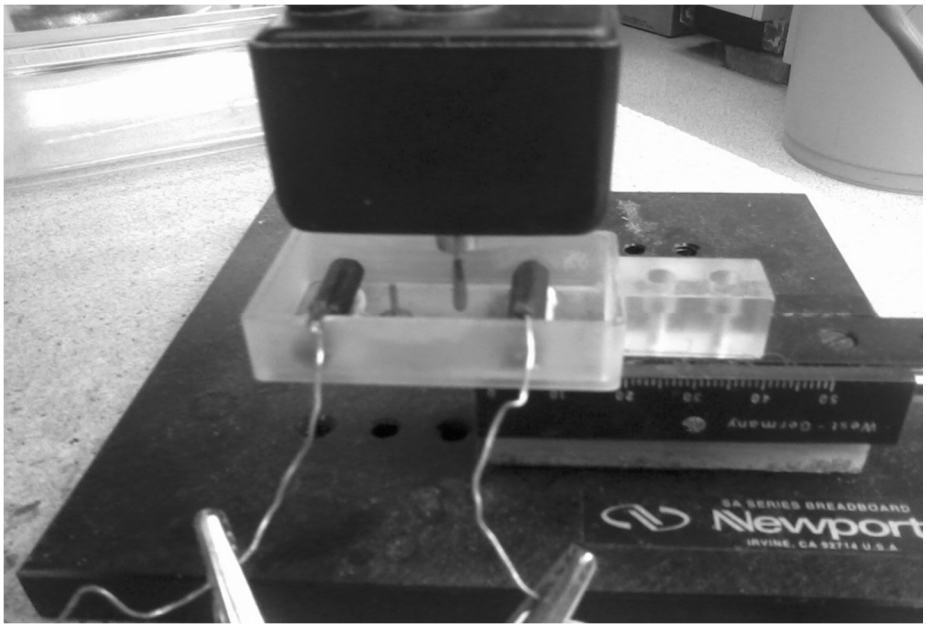

Contraction Force Tester

NEONATAL RAT CARDIAC CELL CULTURE (2D AND 3D)

Insulin: In aliquots in West side fridge if not in our fridge, 2mg/mL (1000x)

AA: In 0.5 and 1 mL aliquots in west side fridge (1000x)

If not already made for the day, 50 mg/mL in DD H20 and filter sterilized. AA is kept by the scale. Filter sterilizers are in the cabinet with the bottles.

MyoMedia: 5 mL FBS- frozen in aliquots in our freezer

5 mL Pen/Strep.- frozen in aliquots in west side freezer

50 mL Horse Serum – frozen in 45 and 5 mL aliquots in our freezer

5 mL 100x ACA – in our fridge

435 mL DMEM- in our fridge and/or cold room

Filter sterilize into 500 mL bottle

*keep all ingredients cold until feeding. Make media with cold DMEM, thaw serums –especially the FBS- in cold water then use immediately

Cardiac Fibroblast (CF) media:

75 mL FBS – frozen in 45 and 30mL aliquots

5 mL penn/strep

420 mL DMEM

Filter sterilize into 500 mL bottle

Feeding Patchess:

Aspirate off old media with a Pasteur pipet that has been heated in the bead sterilizer for > 10s

Remove pipette from vacuum line and gently pick aligned constructs, nudging them along the mandrel, making sure they are not sticking to the ends.

Replace media: 42 mL for small jars, 126 for large jars (21 mL/construct)

Supplement with insulin and AA (1000x = 1 ul for each mL media)

* Pre-aliquot media to be used for feeding and heat only as long as absolutely necessary. For the first feeding or two after an isolation, the media must be freshly made as well

Feeding plated non-CMs:

30 mL CF media for T175s, 10-15mL for T75s

Aspirate off old, replace with new media. Check for confluence first.

Thawing and Culture of hiPSC-CMs (From the Kamp Lab)

Culture Medias

EB20 (500mL):

910 µL β-mercaptoethanol (55mM stock)
5 mL non-essential amino acids
5mL Pennicillin/Streptomycin
100 mL FBS
389 mL DMEM/F12

EB2 (500mL):

910 µL β-mercaptoethanol (55mM stock)
5 mL non-essential amino acids
5mL Pennicillin/Streptomycin
10 mL FBS
479 mL DMEM/F12

Combine and sterile filter

Thawing iPSC-CMs (Jianhua Zhang/Kamp Lab)

1. Remove vial from liquid nitrogen and quickly place to 37^{o}C water bath for 1 minute. Using long forceps or floating rack to hold the vials, **avoid submerging the cap.**
2. Immediately remove vial from water bath, spray with 70% ethanol and wipe with Kimwipes. Place the vials in the cell culture hood.
3. Gently transfer thawed cells to a 15 ml conical tube using 1ml or 5ml pipette. If multiple vials of the same lot cells to thaw, use a 50 ml conical tube to combine cells.
4. **Slowly**, add 11 ml/vial room temperature EB20 medium **drop-wise** to cells in the 15 ml or 50 ml tube. While adding the medium, gently move the tube back and forth to mix the cells. This reduces osmotic shock to the cells. After adding the medium, cap the tube tightly and gently invert tube 2-3 times to mix the contents.
5. Centrifuge at 200x g for 5 minutes.
6. Aspirate the supernatant and resuspend in 4ml/vial EB20 medium.
7. Count the cells with Trypan Blue to determine the total viable cells and the viability.
8. Add 11 ml EB20 medium to fibronectin coated (2.5 µg/cm^2) T75 flask.

9. Add 4 ml cell solution to flask (total of 15 ml medium).
10. Change to the EB2 maintenance media 48 hours after the cells attached.
11. Harvest after 4 days.

Edits: Change EB20 media the day after thaw, harvest at or after 4 days.

Harvest of iPSC-CMs

1. Rinse 2x with 10 ml PBS.
2. Add 10 ml 0.25% Trypsin/EDTA with 200 µl chicken serum.
3. Put in incubator for 5 min. If cells are still attached, gentle tapping, or additional time in the incubator can be used (no more than 15 min total exposure to Trypsin).
4. Quench with 10 ml EB-20.
5. Spin at 200g for 5 min.
6. Resuspend in EB-20.

LACTATE PURIFICATION OF HIPSC-CM

Reagents Needed:
T75 flask
Fibronectin (Sigma F1141-5mg)
EB20 media
EB2 media
PBS

Lactate Media:

	Stock Conc.	Volume		Final Conc.	Cat#
L-Glutamine	200mM	2mL	50x	0.584g/L	Sigma G7513
Pennicillin/ Streptomycin	10k U/10k µg/mL	1mL	100x		
MEM NEAA		1mL	100x	0.1mM	Gibco 11140-050
Lactic Acid	1M	400uL	250x	4mM	Sigma 25476-100g
β-mercaptoethanol	55mM	182uL		0.1mM	Gibco 21985-023
DMEM no Glucose	-	96mL	-	-	Gibco 11966-025
		100mL			

Protocol:

Day 0: Thaw cells as per normal protocol into 1 T75 flask/vial coated with 2.5ug/cm2 fibronectin. Media: EB20, 15mL
Day 1: Media change: EB20, 15mL
Day 2: Media Change: EB2, 15mL
Day 3: Rinse flask twice with PBS then add 15mL Lactate Media
Day 4: -
Day 5: Rinse flask twice with PBS, add 15mL Lactate Media
Day 6: -
Day 7: Rinse flask twice with PBS, add 15mL EB2
Day 8: -
Day 9: -
Day 10: Harvest

Notes:

- Cells should start beating on day 4-6 of culture. Lactate media does not affect this timeline, you should see cell start to beat while in lactate media. If they aren't beating by day 10 of culture, you have a problem….
- 1M lactic acid: Dilute from stock into HEPES, aliquot and freeze immediately. For some reason, the lactic acid we use is stable indefinitely at high concentration in water, but when diluted into saline or HEPES, that lifetime gets cut to maybe a week
- Upon returning the cells to EB2, the CMs will expand to fill the empty space. Or maybe divide some too. We have not looked into it thoroughly, but a lot of the cell counts post-purification come close to the average yield (both overall and compared to side-by-side cultured unpurified cells) and ~95% CM. It could be that CMs like the lactate media and fewer of them die. Either way, if you see that, nothing went wrong. Stem cells are just weird.

HISTOLOGY: IMMUNOSTAINING OF SECTIONS AND CELL MONOLAYERS

Immunostaining: Sections/Cell Monolayers

Rinse 3x in PBS, 1st rinse incubate 5 min

- After 1st rinse, outline sections with water pen

Permeabilize in 0.1%TX100 (on shelf above Sonja's bench) in PBS at RT for 10 min

Rinse 3x, 5 min incubations in PBS

Block in 5% NDS in PBS for >30min at RT NDS in Ab freezer in 500ul aliquots (500ul NDS + 9.5mL PBS)

Add primary Ab at optimal dilution in NDS

Incubate overnight in coldroom or for 1h at RT (1h only for monolayers)

Rinse 3x in PBS with 5 min incubations

Add secondary Ab. RTT secondaries are diluted 1:200 in NDS (secondaries are diluted 1:1 in glycerol upon receipt and stored at -20)

*shield from light from this point on

Incubate at RT 1h or in cold room overnight

Rinse 3x PBS with 5min incubations

Incubate 10min in a 1:10000 dilution of DAPI @ RT

Rinse 3x5min in PBS

Coverslip when applicable with Dako mounting media (in fridge). Coverslips are in the long drawer on Sonja's bench or in the drawer at the end of Sandy's bench marked 'Cover Slips.'

Image

Whole Mount Immunostaining

Fix tissues as normal, leave them in PBS. No need to embed and freeze them.

Permeabilize in 0.1%TX100 (on shelf above bench) in PBS at RT on shaker for 1h

Rinse 3x by 3x, 5 min incubations in PBS

Block in 5% NDS in PBS for >1h at RT on shaker- NDS in Ab freezer

Add primary antibody, diluted in NDS

Incubate overnight in coldroom on shaker

Rinse 3x by 3x in PBS with 10 min-1h incubations

Add secondary antibody, diluted in NDS

Incubate a few hours-overnight in coldroom, shielded from light

Rinse 3x by 3x in PBS with 10min-1h incubations

Image. You can image on a typical upright microscope, but be aware only small parts of the surface may be in the focal plane at any given time. If the inverted scope doesn't work out and you want to image large areas at higher magnifications, use the confocal.

WESTERN BLOTTING: PROTEIN HARVEST FROM A CELL MONOLAYER (I.E. FLEXCELL PLATES)

Purpose: To harvest protein from the 24 well HTS Flexcell plates for Western Blotting

1. Put the plate on ice, all steps should be done @ 4C
2. Rinse the monolayer 2x with PBS to remove media.
3. Add 80-100uL Lysis Buffer to each well. Make sure the buffer covers the entire well.

    1x Lysis Buffer (for 10mL):

    5mL of 2x NP-40 lysis buffer
    50uL of $NaVO_3$, 200mM stock (sodium orthovanadate)
    5uL each of Aprotinin, Pepstatin, and Leupeptin, 1 mg/mL stock
    10uL of PMSF, 200mM stock in DMSO
    250uL Sodium Deoxycholate, 10% stock
    Fill to 10mL with ddH2O
4. Gently scrape the bottom of the wells with a spatula, rinsing the spatula between each well, to loosen adherent cells
5. Let sit for ~2-3min
6. Remove lysate from each well and place into 1.5mL eppendorf tubes.
7. Incubate lysate end-over-end in the cold room for 15min
8. Centrifuge lysate for 15min at top speed (13-14K RPM) at 4C in the Alford lab refrigerated centrifuge.
9. Move supernatant into new eppendorf tubes, label, and store at -80.

Notes and Future Protocol Development:

- Try switching to RIPA buffer and bought protease inhibitor cocktail in the future. It will make things a lot easier
- Sodium orthovanidate doesn't like to stay in solution, re- make frequently…

Western Blotting: Gel Running and Blotting Procedure

Cells (an example used for this protocol)**:** Lactate Purified (LA) iPS-CMs and unpurified (UN) iPS-CMs cultured statically for 10 days in a 24 well plate. Harvested on XX/XX/XX with the following protocol:

Cell Lysis:

1mL Lysis Buffer:
- 500uL of NP40 lysis buffer
- 25uL of 40x Sodium Deoxycholate
- 10uL 100x Sodium Orthovanadate (NaOV3)
- 1ul each of Aprotinin, Pepstatin, and Leupeptin
- Fill to 1mL with ddH2O

Place plate on ice, rinse cells in well with PBS
Add 100ul Lysis Buffer/well
Let sit 3min, scrape bottom of well to loosen cells from bottom of wells
Collect buffer from each well and place into a 1.6mL Eppendorf tube
Incubate 30min on the end over end incubator in the cold room
Spin down in refrigerated centrifuge (Alford lab) at 4C for 15min at 13k rpm
Remove supernatant and place in a new 1.6mL tube
Store in -80

BCA assay:

Follow the protocol on the box, all samples must be done in triplicate.

SDS-PAGE:

Running Buffer: Make 750 mL. 10x SDS/Tris/Glycine running buffer diluted in DI H2O.

Samples (for the 10 well/50uL gels): Protein diluted in ddH2O to 23 uL + 23 uL 2x Lamelli Sample Buffer with 100mM DTT (stock is 2M) in a labeled 1.6 mL eppendorf tube. An example is shown below:

Sample	UN1	UN2	UN3	UN4	LA1	LA2	LA3	LA4	LA5
uL protein for 10ug	16.89	18.9	21.23	16.25	14.5	14.18	15.6	16.77	18.19
uL ddH2O	6.11	4.1	1.77	6.75	8.5	8.82	7.4	6.23	4.81
uL 2x sample buffer + 100mM DTT	23	23	23	23	23	23	23	23	23
total	46	46	46	46	46	46	46	46	46

‘Boil’ samples for 5 min via a 95C heating block. Hold onto the caps when removing the tubes from the heating block.

Sample Gel Layout:

Gel	Lane 1	2	3	4	5	6	7	8	9	10
A	UN1	UN2	UN3	UN4	LA1	LA2	LA3	LA4	LA5	Ladder

Gently remove the comb form the gel and put gel into the cassette. If only running one gel, use the plastic plate for the other side of the cassette to create a seal. Remember to take the tape off of the bottom of the gel! Put the cassette in the gel running chamber.

Fill the inner part of the chamber with running buffer up to the top of the gels. Check for leaks. Then fill the outer part of the chamber with running buffer about halfway full, past the bottom of the gels at the very least.

Run gel at 200V for 1 hour. Keep track of the dye front, once it reaches the bottom you can stop the power supply or it will keep running off the gel.

Western Transfer:

1x CAPS buffer (80mL MeOH + 80mL 10X CAPS buffer + 640mL ddH2O).

Pre-wet sponges, filter paper, and nitrocellulose in CAPS buffer

For one gel, made a sandwich in the transfer cassette in the following order: Black side of cassette, sponge, filter paper, gel, nitrocellulose , filter paper, sponge, white side of cassette. The protein travels from (-) to (+) To remove the gel, use the crow bars at the arrows to crack open the casing.

Place transfer cassette in transfer box, black side facing black. Place transfer box and ice block in reservoir and fill with CAPS buffer. You won’t need all of the CAPS buffer.

Run at 75V for 1h on stir plate with a stir bar in the bottom of the reservoir.

Remove the nitrocellulose (gently with the flat tweezers) and place protein side up in a blotting dish with 5% milk + 0.1% Tween. Label with pencil along the edge OR, if you're not going to start blotting right away, rinse blot in TBS, wrap in saran wrap and store in the fridge until ready.

Transfer buffer has a waste container.
The gel, once done with it can go in the trash.
Running buffer can be poured down the sink.

Blotting

Milk solution:
5g milk (blocking powder)
100mL PBS
1 mL 10% Tween

Block in the cold room O/N on the shaker OR for >30min @ RT on shaker
Primary Ab: 1h @ RT on shaker or O/N in cold room on shaker
Rinse: 3x3x5min in TBS-T
Secondary Ab: 1h @ RT on shaker or O/N in cold room on shaker
Rinse 3x3x5min in TBS-T, last rinse being TBS (no T)

ECL: (shield from light at this time) 2mL Luminata Classico (in fridge) on benchtop (no shaker) @ RT for 3min

Developing:
Placed blot on plastic wrap, protein side (the side with pencil on it) down.
Wrapped in plastic wrap and taped in place (protein side up) in the developer case.
Exposed in developer room (while locked) for 10s, 30s, 1min, 5min. Notched film in one corner to mark orientation. Each film labeled with blot name, date, stain, exposure, initials, ladder markings.

Stripping:
1 rinse in TBS, 5 min on shaker @ RT
5min in Restore PLUS stripping buffer on shaker @RT
4x3x5min Rinses in TBS-T
Block >30min @ RT on shaker before adding next primary.

Appendix 4: Antibody Dilutions and Supply Information

Antibodies and Labels used for Immunohistochemistry

Primary antibody	Mfr.	Catalog #	Dilution	Dilution Conc.	Incub. Time	Incub. Temp
Cardiac Troponin T (cTnT)	Thermo Fisher Scientific	MS-295-P1	1:100	2 µg /mL	O/N	4C
Collagen I	Novus Biologics	NB 600-408	1:1000	1 µg /mL	O/N	4C
Collagen IV	Abcam	ab6586	1: 200	5 µg /mL	O/N	4C
Laminin	Abcam	ab11575	1:100	5 µg /mL	O/N	4C
Connexin 43 (CX43)	Santa Cruz	sc-9059	1:100	2 µg /mL	O/N	4C
HNA*	Millipore	MAB1281	1:200	-	O/N	4C
Ki67	Abcam	ab15580	1:400	2.5 µg /mL	O/N	4C
Cardiac Troponin I (cTnI)	Abcam	ab47003	1:100		O/N	4C
Myosin Heavy Chain α	Santa Cruz	Sc-32732	1:100	2 µg /mL	O/N	4C
Fibronectin	Abcam	Ab6584	1:200	5 µg /mL	O/N	4C

Secondary Antibodies						
Alexa Fluor® 594 AffiniPure Donkey Anti-Mouse IgG (H+L)	Jackson Immunoresearch	715-585-150	1:400	3.75 µg /mL	1h	RT
Alexa Fluor® 488 AffiniPure Donkey Anti-Mouse IgG (H+L)	Jackson Immunoresearch	715-545-150	1:400	3.75 µg /mL	1h	RT
Alexa Fluor® 647 AffiniPure Donkey Anti-Mouse IgG (H+L)	Jackson Immunoresearch	715-605-150	1:400	3.75 µg /mL	1h	RT

Alexa Fluor® 594 AffiniPure Donkey Anti-Rabbit IgG (H+L)	Jackson Immunoresearch	711-585-152	1:400	3.75 µg /mL	1h	RT
Alexa Fluor® 488 AffiniPure Donkey Anti-Rabbit IgG (H+L)	Jackson Immunoresearch	711-545-152	1:400	3.75 µg /mL	1h	RT
Alexa Fluor® 647 AffiniPure Donkey Anti-Rabbit IgG (H+L)	Jackson Immunoresearch	715-605-152	1:400	3.75 µg /mL	1h	RT
Other Labels and Reagents						
IB4 (Griffonia (Bandeiraea) Simplicifolia Lectin I, Isolectin B4 (fluorescein labeled))	Vector	FC-1201	1:50	20 µg /mL	10 min	RT
DAPI (Hoechst 33342)	LifeTech	H3570	1:10000	1 µg /mL	10min	RT
F-Actin (Phalloidin) Alexa Fluor 488	LifeTech	A12379	1:500	0.6 U/mL	1h	RT

Antibodies and Labels used for Western Blotting

Primary antibody	Mfr	Catalog #	Dilution	Dilution Conc.	Incub. Time	Incub. Temp
Myosin Heavy Chain α	Santa Cruz	sc-32732	1:1000	0.2 µg /mL	1h	RT
Myosin Heavy Chain β	Santa Cruz	sc-53089	1:1000	0.2 µg /mL	1h	RT
GAPDH	Santa Cruz	Sc-48167	1:2000	0.1 µg /mL	1h	RT
α-Sarcomeric Actinin	Sigma-Aldrich	A7811	1:2000		1h	RT
SERCA2A ATPase	Abcam	Ab2861	1:1000		1h	RT
Connexin 43 (CX43)	Santa Cruz	sc-9059	1:1000	0.2 µg /mL	1h	RT
Secondary Antibodies						
Amersham ECL Prime Mouse IgG, HRP-linked whole Ab	GE LifeSciences	715-585-150	1:2500	0.4 µg /mL	1h	RT
Peroxidase AffiniPure Donkey Anti-Goat IgG (H+L)	Jackson Immunoresearch	705-035-003	1:2500	0.32 µg /mL	1h	RT
Amersham ECL HRP Conjugated Antibody, Anti-Rabbit	GE LifeSciences	NA934-1mL	1:2500		1h	RT
Other Reagents						
Luminata Classico Western HRP substrate	Millipore	WBLUC0100	-	-	3 min	RT
Luminata Crescendo Western HRP Substrate	Millipore	WBLUR0100	-	-	3 min	RT

Other Supplies		
Blue Basic Autorad Film 5x7”	Bio-Rad	F-9023
4-20% Mini Protean TGX Gel, 10 well, 50uL	Bio-Rad	456-1094
BCA Protein Assay Kit	Thermo Fisher	PI23227
Blotting Grade Blocker	Bio-Rad	170-6404
Tris/Glycine/SDS running Buffer 10x	Bio-Rad	161-0732

Non-Standard Cell Culture Supplies:

Item	Mfr	Catalog #
2-mercaptoethanol, 50mL 55mM	Gibco	21985-023
Nonessential amino acids (100x)	Life Tech	11140-050
ε- aminocaproic acid	Acros Organics	103305000
Fibronectin	Sigma-Aldrich	F1141-5mg
Horse Serum	Hyclone	26050088
Lactic Acid	Sigma-Aldrich	252476-100g
Glucose-Free DMEM	Invitrogen	11966025